FIRAT UNIVERSITY
GRADUATE SCHOOL OF NATURAL AND APPLIED SCIENCES
TÜRKİYE

HYBRID IMAGE DENOISING IN MULTIRESOLUTION WAVELET DOMAIN

Ahmed Abdulmaged ISMAEL

Master's Thesis

DEPARTMENT OF SOFTWARE ENGINEERING

JUNE 2021

FIRAT UNIVERSITY
GRADUATE SCHOOL OF NATURAL AND APPLIED SCIENCES
TÜRKİYE

Department of Software Engineering

Master's Thesis

HYBRID IMAGE DENOISING IN MULTIRESOLUTION WAVELET DOMAIN

Author
Ahmed Abdulmaged ISMAEL

Supervisor
Dr. Öğr. Üyesi Muhammet BAYKARA

JUNE 2021
ELAZIG

FIRAT UNIVERSITY
GRADUATE SCHOOL OF NATURAL AND APPLIED SCIENCES
TÜRKİYE

Department of Software Engineering

Master's Thesis

Title:	Hybrid Image Denoising in Multiresolution Wavelet Domain
Author:	Ahmed Abdulmaged ISMAEL
Submission Date:	21 May 2021
Defense Date:	17 June 2021

THESIS APPROVAL

This thesis, which was prepared according to the thesis writing rules of the Graduate School of Natural and Applied Sciences, Fırat University, was evaluated by the committee members who have signed the following signatures and was unanimously approved after the defense exam made open to the academic audience.

		Signature
Supervisor:	Dr. Öğr. Üyesi Muhammet BAYKARA Firat University, Faculty of Technology	Approved
Chair:	Dr. Öğr. Üyesi Ahmet Arif AYDIN Inonu University, Faculty of Engineering	Approved
Member:	Prof. Dr. Resul DAŞ Firat University, Faculty of Technology	Approved

This thesis was approved by the Administrative Board of the Graduate School on

.... / .... / 20 ....

Signature

Assoc. Prof. Dr. Kürşat Esat ALYAMAÇ
Director of the Graduate School

DECLARATION

I hereby declare that I wrote this Master's Thesis titled "Hybrid Image Denoising in Multiresolution Wavelet Domain" in consistent with the thesis writing guide of the Graduate School of Natural and Applied Sciences, Firat University. I also declare that all information in it is correct, that I acted according to scientific ethics in producing and presenting the findings, cited all the references I used, express all institutions or organizations or persons who supported the thesis financially. I have never used the data and information I provide here in order to get a degree in any way.

17 June 2021

Ahmed Abdulmaged ISMAEL

PREFACE

This thesis introduces and implements a hybrid system of denoising degraded images that have been affected by AWGN to improve the quality of the image and enhance in terms of noise reduction by combining the concept of spatial domain filters with denoising method in the threshold-based wavelet transforms. To distinguish and remove the noise from the affected pixels. The advantage of adopting the hybrid method is to provide significant potential for edge extraction to improve the quality and properties of denoised images concerning noise elimination and structure preservation. The significant challenge facing the use of a denoising system is how to apply the noise removal system to remove as much noise as possible from digital images while trying to preserve the original data and image characteristics as much as possible.

First and foremost, I am very praised and thankful to God for giving me the power, health, and knowledge to accomplish the thesis finally. I would like to express my heartfelt gratitude and indebtedness to my supervisor, Dr. Muhammet BAYKARA, for his keen interest, close supervision, constant encouragement, and generous dedication of his time and advice which guided me throughout my studies and enabled me to complete my thesis. Finally, I'll be eternally grateful to my parents, wife, brothers, and all my friends for their tolerance and patience during this research, as well as to everyone who supported me in any way.

Ahmed Abdulmaged ISMAEL
ELAZIG, 2021

TABLE OF CONTENTS

Page

ABSTRACT

Hybrid Image Denoising in Multiresolution Wavelet Domain

Ahmed Abdulmaged ISMAEL

Master's Thesis

FIRAT UNIVERSITY
Graduate School of Natural and Applied Sciences

Department of Software Engineering

June 2021,   Page: xv + 114

Recently, with the explosion in the number of digital images captured every day in all life aspects, there is a growing demand for more detailed and visually attractive images. However, the images taken by current sensors are inevitably degraded due to the noise caused by the acquisition, transferring, compression, encoding, and storage processes, including retrieval process into the various fields, such as medical, astrophysics, weather forecasting, etc., which contributes to impaired visual image quality. Therefore, more work is needed to reduce noise by preserving the textural, information, and structural features of the digital image. So far, there are different techniques for reducing noise that various researchers have done. Each technique has its own advantages and disadvantages. In this work, and to denoise the blurred image caused by Additive White Gaussian Noise (AWGN) in the digital images field, a new approach is designed and implemented as a noise removal system aimed to study the application of spatial domain filters with working mechanisms based on the multiresolution wavelet domain threshold value. Various types of wavelet transform and threshold techniques have been tested to achieve improved results of the image noise reduction process by distinguishing and removing the noise from the affected pixel units, and the wavelet decomposition is applied with a three-levels of analysis. Hard and soft threshold techniques and spatial filters were applied for each of the high-frequency and low-frequency sub-images. Then, an inverse wavelet transform was applied to the denoised image. Finally, the performance metrics Peak Signal to Noise Ratio (PSNR) is calculated to estimate the evaluation of the suggested method. Experimental evaluation outcomes of the proposed method reveal a better improvement of image quality concerning minimizing noise and edge preservation than the results of the related works instead of using a threshold-based WT domain or spatial domain filters separately. Studying the application of a mechanism of image denoising as a hybrid system to applying it to the noisy image with a mixed type of noise can be considered future work.

Keywords: Digital Image Denoising, Hybrid Denoising, Multiresolution Wavelet Domain, Spatial Domain Filtering, Thresholding Techniques, PSNR.

ÖZET

Çoklu Çözünürlük Dalgacık Uzayında İmgelerden Hibrit Gürültü Temizleme

Ahmed Abdulmaged ISMAEL

Yüksek Lisans Tezi

FIRAT ÜNİVERSİTESİ
Fen Bilimleri Enstitüsü

Yazılım Mühendisliği Anabilim Dalı

Haziran 2021, Sayfa: xv + 114

Son zamanlarda yaşamın her alanında her gün elde edilen dijital görüntülerin sayısındaki artışla birlikte, daha detaylı ve görsel olarak çekici görüntülere olan talep de artıyor. Bununla birlikte, güncel sensörler tarafından alınan görüntüler, tıbbi, astrofizik, hava tahmini vb. gibi çeşitli alanlarda geri alma işlemi dahil olmak üzere edinme, aktarma, sıkıştırma, kodlama ve depolama işlemlerinin neden olduğu gürültü nedeniyle kaçınılmaz olarak bozulur. Bu nedenle, dijital görüntünün dokusal, bilgisel ve yapısal özelliklerini koruyarak gürültüyü azaltmak için daha fazla çalışmaya ihtiyaç vardır. Şimdiye kadar, gürültüyü azaltmak için çeşitli araştırmacıların yaptığı farklı teknikler bulunmaktadır. Her tekniğin kendi avantajları ve dezavantajları vardır. Bu çalışmada Eklemeli Beyaz Gauss Gürültüsünün (AWGN) neden olduğu bulanık görüntünün sayısal görüntü alanında ortadan kaldırılması için, mekansal alan filtrelerinin çalışma mekanizmalarına dayalı olarak uygulanmasını incelemeyi amaçlayan bir gürültü giderme sistemi olarak yeni bir yaklaşım tasarlanmış ve uygulanmıştır. Etkilenen piksel birimlerinden gürültüyü ayırt ederek ve kaldırarak görüntü paraziti azaltma işleminin daha iyi sonuçlarını elde etmek için çeşitli dalgacık dönüşümü ve eşik teknikleri test edilmiş ve dalgacık ayrıştırması üç seviyeli bir analiz ile uygulanmıştır. Yüksek frekanslı ve düşük frekanslı alt görüntülerin her biri için sert ve yumuşak eşik teknikleri ve uzamsal filtreler uygulanmıştır. Daha sonra gürültüden arındırılmış görüntüye ters dalgacık dönüşümü uygulanmıştır. Son olarak, önerilen yöntemin değerlendirmesini tahmin etmek için performans metriği olarak, Tepe Sinyal Gürültü Oranı (PSNR) hesaplanır. Önerilen yöntemin deneysel değerlendirme sonuçları, eşik tabanlı bir WT alanı veya uzamsal alan filtrelerini ayrı ayrı kullanmak yerine, gürültünün ve kenar korumanın en aza indirilmesiyle ilgili çalışmaların sonuçlarına göre görüntü kalitesinde daha iyi bir gelişme olduğunu ortaya koymaktadır. Karma bir gürültü türü ile gürültülü görüntüye uygulamak için bir karma sistem olarak görüntü temizleme mekanizmasının uygulanmasının incelenmesi gelecekteki çalışmalar için düşünülebilir.

Anahtar Kelimeler: Sayısal Görüntü Gürültü Giderme, Hibrit Gürültü Giderimi, Çok Çözünürlüklü Dalgacık Alanı, Mekansal Alan Filtreleme, Eşikleme Teknikleri, PSNR.

LIST OF FIGURES

LIST OF TABLES

Page

LIST OF APPENDICES

SYMBOLS AND ABBREVIATIONS

Abbreviations

1D-DWT	: One–Dimensional Discrete Wavelet Transform
2D-DWT	: Two–Dimensional Discrete Wavelet Transform
2D-DWT	: Two–Dimensional Discrete Wavelet Transform
AMF	: Adaptive Median Filter
AWGN	: Additive White Gaussian Noise
BF	: Bilateral Filter
BFO	: Bacterial Foraging Optimization
bior	: Biorthogonal
Coeff	: Coefficients
coif	: Coiflets
CORR	: Correlation
CT	: Computed Tomography
CWT	: Continue Wavelet Transform
db	: Daubechies
dmey	: Discrete Meyer
DTCWT	: Dual-Tree Complex Wavelet Transform
DWT	: Discrete Wavelet Transform
FIR	: Finite Impulse Response
FT	: Fourier Transform
fk	: Fejer-Korovkin
gaus	: Gaussian
GGD	: Generalized Gaussian Density
haar	: Haar
HH(D)	: High High (Diagonal Detail Band)
HL(H)	: High Low (Horizontal Detail Band)
IDWT	: Inverse Discrete Wavelet Transform
LH(V)	: Low High (Vertical Detail Band)
LL(A)	: Low Low (Approximation bundle Band)
LR	: Low Resolution
LTI	: Linear Time-Invariant
MAE	: Mean Absolute Error
mexh	: Mexican
MF	: Median Filter
MMSE	: Minimum Mean Square Error
morl	: Morlet
MRA	: Multiresolution Analysis
MSE	: Mean Square Error
PCC	: Pearson Correlation Coefficient
PDF	: Probability Density Function
PSNR	: Peak Signal-to-Noise Ratio
QI	: Quality Index
QMF	: Quadrature Mirror Filter
rbio	: Reverse Biorthogonal
RMF	: Relaxed Median Filter

RMSE	: Root Mean Square Error
SMF	: Standard Median Filter
SNR	: Signal to Noise Ratio
SSIM	: Structural Similarity Index Measure
STFT	: Short-Time Fourier Transform
SWT	: Stationary Wavelet Transform
sym	: Symlets
Th	: Threshold
WF	: WF
WHFC	: Weighted High pass Filtering Coefficients
WT	: Wavelet Transform

1. INTRODUCTION

Noise in digital images is any distortion that occurs within the digital image and may damage the contents of the image, it happens because of an introduction into the data through any system used for storage, transmission, and processing or may occur from noise sources in the vicinity of image capturing devices, defective memory location and other adverse conditions. A distorted image due to different forms of noise, such as salt and pepper noise, Gaussian noise, Speckle noise, Poisson noise, and many more are common types of noise for digital images [1,2].

Additive White Gaussian noise (AWGN) is one of these noises that occur through poor quality image accession, noisy surroundings, or internal noise in transmission mediums. In this study, the AWGN noise is added to the original image. It is useful to eliminate the AWGN noise in the noisy image until it becomes closer to the original image. Therefore, noise is among the principal restrictions in image precision and is regarded as one of the primary sources of information in various implementations. Image denoising aims to lessen the level of noise and extract relevant information from deteriorated and non-clear images. Hence, the main challenge is to retrieve the actual data from the noisy image as possible [3,4]. Denoising images are an essential pre-processing phase of the evaluation of images. Researchers are continuously focusing on it to obtain an enhanced quality of visual assurance [5].

Additive random noise can be eliminated without difficulty when using threshold procedures. The denoising of digital images degraded by noise via employing wavelet procedures is highly efficient due to its ability to capture a signal's energy in just a few energy transform values. In such varied areas as image denoising, image compression, signal processing, among others, both discrete and continuous wavelet transform tremendous, potentially producing small coefficients and a lesser significant coefficient [6]. The reason for employing the wavelet transform is that it is perfect for energy compression, as the small and large coefficients are generated due to noise and essential image elements. It is possible to threshold the low coefficients without affecting the image's significant features. Discrete wavelet transform is among the most utilized denoising procedures. This procedure isolates the noisy picture into various sub-band pictures, and then it associates the high-frequency wavelet coefficients as horizontal, vertical, and diagonal. The discrete wavelet transformation is commonly used in denoising images because of the sparse representation of the image, meaning that it has many coefficients close to zero [7]. In its most basic form, every coefficient is the threshold by contrasting against an estimate, called a threshold function. There are many threshold techniques investigated and used by researchers to compute a threshold value. In this study, a suggested method will be applied to mix the advantages of the denoising method in both domains, the multiresolution wavelet transform domain using threshold technics with spatial domain filtering to construct a hybrid denoising system. The noise will be

Additive White Gaussian Noise (AWGN). This hybrid denoising system will be used on several noisy images that are affected by the AWGN noise. The idea to merge the methods for the two domains will try to show and to use the advantages of these methods to improve the results. Moreover, four threshold techniques are selected to compute a threshold value: the hard threshold technique, the Visu shrink threshold technique, Bayes Shrink threshold technique, and the penalized threshold technique. Simple image denoising algorithms using DWT and SWT follow three steps, as shown in Figure 1.1 [8,9].

- Discrete and Stationary wavelet transformation (2D-DWT, 2D-SWT) are implemented to decompose the noisy image and to obtain wavelet coefficients.
- These wavelet coefficients are denoised through the wavelet threshold function.
- The inverse Discrete and Stationary wavelet transformation (2D-IDWT, 2D-ISWT) applied to the coefficients are modified to obtain the denoised image.

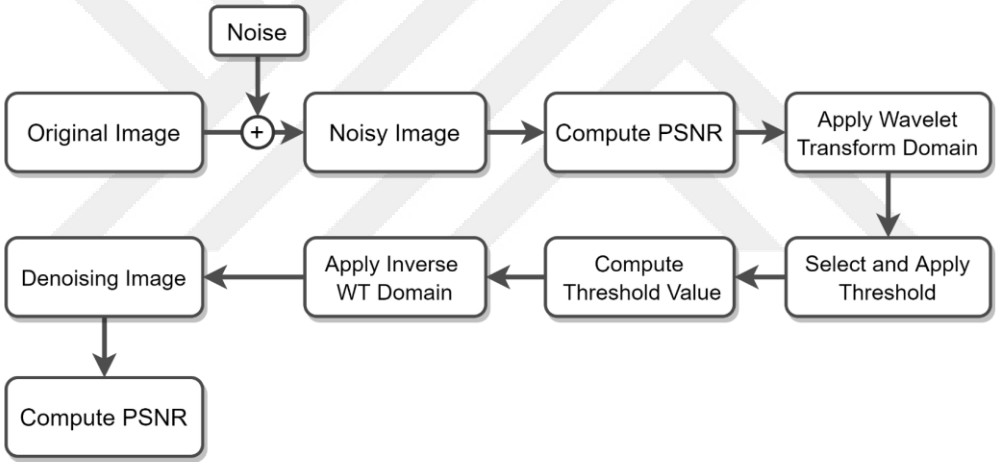

Figure 1.1. The Block diagram of Image denoising using 2D-Wavelet Transform [9].

In both DWT, SWT there are the wavelet families such as (Haar, Daubechies, Biorthogonal, Symlet, Coiflets, Mexican hat, Meyer, etc.) used to analyze wavelet, while the selection of wavelet filter depends on the properties of the analysis and synthesis wavelet [10,11].

All types of the wavelet family’s filters have been applied in this study by using many techniques during the three decomposing levels of the 2D-DWT and 2D-SWT to obtain the best result depending on peak signal-to-noise ratio (PSNR) values. Finally, the performance of all denoising algorithms in the suggested hybrid denoising system is analyzed quantitatively by the PSNR index with the original images.

1.1. Problem Statement

Digital images are exposed to various types of noise and its effects through many applications and activities that deal with it, such as photo-capture devices, medical devices, stereoscopic scanning mechanisms, information compression applications, and transferring through transmission communication networks, etc., where the images resulting from such applications contain noise or some additional information that is not related to the original image and present a challenge in the aspect of image quality. These noises appear in different forms in images, which are usually random information added or multiplied by the main image. The noise in digital images makes the interpretation of images more difficult, and the digital image quality is degraded by many sources of noise such as imperfect instruments, interference from natural phenomena, data acquisition, and transmission errors. The presence of noise in digital images is one of the critical obstacles in the various fields that depend on the quality of the images being dealt with, so there is an ongoing need to find ways to increase this quality by trying to remove the noise effect as much as possible from these images. Additionally, and for the critical role that Wavelet Transformation Mechanism plays in dividing the image into bands by frequency (with the ability to apply threshold techniques for each band), these noise removal techniques based on the work in the Wavelet domain are among the effective methods in the noise reduction field due to its sparsity and multiresolution properties. Spatial filtering techniques have also proven to work for purifying the digital image from noise when applied to the noisy image in the spatial domain.

1.2. Objectives of the Study

This study aims to image denoising from the degraded digital image and restore original content using a combination of the threshold-based multiresolution wavelet transform domain with spatial filter techniques (hybrid method). To reduce the noise value in the digital image as much as possible while preserving the value of the original data within the image. Also, remove non-significant parts and improve visual quality. The objectives of the thesis are as follows:

- Design and implement a hybrid filter system for reducing the noise inside the noisy images; the noise will be Additive White Gaussian Noise (AWGN).
- Study the performance of all filters that belong to the wavelet filter families by measuring their effectiveness in applying the noise removal system to improve results.
- Study the performance of using many types of filters in one system and discover the effectiveness of select the locations where the filters have been added inside the denoising system.

- Measure the denoising system performance by using the threshold technics inside the wavelet domain.
- Study and measure the role that will be played by using multiresolution wavelet analysis.

1.3. Motivation

The wavelet transforms and the work to remove the noise in its domain has become one of the distinct and promising methods of giving results, as it has an efficient ability to divide the points depending on the frequency, and thus restricting the noise that is of high frequencies is confined to a specific beam range to be dealt with in a more advanced way on spatial domain filters. The significant challenge that facing the use of a denoising system is how to apply the noise removal system in a way that removes as much noise as possible from digital images while trying to preserve the original data and image characteristics as much as possible. The motivation for using digital image denoising methods is to facilitate the extraction of image properties and reduce the impact of noise as much as possible and in a manner that can be utilized in many applications that have a significant impact on human life.

1.4. Significance of the Study

This approach will introduce and implement a hybrid system of denoising blurred images (degraded) that has been affected by AWGN to improve the quality of the image, enhance in terms of noise reduction, and compare the 24 cases as one system rather than using each part solo. The proposed method is realized by using the concept of spatial domain filters, and the denoising method in the threshold-based wavelet transforms with multiresolution analysis. To distinguish and remove the noise from the affected pixels. The advantage of adopting the hybrid method is to provide significant potential for edge extraction to improve the quality of denoised images concerning noise elimination and structure preservation. The presented work will be carried out from several methods so that they work together in the form of one system in which the positive characteristics of each method will participate in this system (hybrid method) and works with the other methods as an integrated system. Also provide essential material for researchers, especially the new entrants in the field of image denoising.

1.5. Research Questions

1) Which types of wavelet transform domain and families (Filters) more appropriate for the project?
2) Which types and number of thresholding function techniques should be applied in the wavelet transform domain to eliminate the noise of the degraded image?
3) How many levels of wavelet decomposition applied to decompose the degraded image?
4) Which spatial domain filters to be implicitly formed with the wavelet transform to make an efficient algorithm?
5) Which type of images should be used, and which noise (type and ratio) added to the image will be dealt with in this project?

1.6. Thesis Structure

The events of this thesis or work are listed in six chapters as follows:

- Chapter one is concerned with the introduction of the thesis study, and it presents the overview, aims/objectives, problem statement, motivation, research questions, and the structure of the thesis.
- Chapter two focuses on the literature and related work to the thesis topic; the contribution of other academics on the subject matter is discussed.
- While chapter three expounded on the conceptual part of the thesis which consists of digital image processing, noise, filters, digital image denoising, threshold techniques, wavelet transform, wavelet filter families, and measurement parameters (PSNR), with an explanation of each of these topics separately.
- Chapter four outlines the general structure of the proposed system continues to introduce the proposed algorithm, followed by all steps and cases proposed methods that have been used in this work in detail.
- Chapter five presents the performance and implementation of the proposed method contain results, discussion, evaluation, comparison. While the final chapter, which is chapter six, contains conclusions derived from the study with discussions and suggestions for future works.

2. LITERATURE REVIEW

The area of digital image denoising is still considered a hot area of research, especially for preserving edges and all fine details to get better visual quality from noisy images (degraded) while preserving the essential signal features as much as possible. The following are some resources that summarized the concept of several different works that have been done in this field.

A new image denoising approach that applies the 2D-discrete wavelet transform (2D-DWT) on the noisy image was proposed by Ismael et al., which is the recommended procedure for image analysis as it can split the image to decomposed into four sub-bands, one low-frequency sub-band (LL), the other three high-frequency sub-bands (LH, HL, and HH) and function separately on each sub-band frequency. The noise ratio in the noisy image was estimated and measured by a Robust Median Estimator parameter. Furthermore, to assess the performance of the whole process, two measurement parameters were used to calculate the noise in the image, namely (MSE, PSNR). Based on their experimental findings, they achieved an improved MSE (mean square error) and PSNR (Peak signal-to-noise ratio) for denoised images by adopting different filters of wavelet transform filters [12].

Three experiments were conducted by Golilarz and Demirel for image denoising in the wavelet domain depending on the soft-threshold function. The first experiment applied the 2D-discrete wavelet transform (2D-DWT) along with the soft and hard thresholding values to remove the noise from the degraded image, while the second one used the un-decimated wavelet (UWT) with the hard threshold value on the image. In the last experiment, they used image denoising based on UWT using the soft threshold value. The comparative findings observed the outperforming of the proposed technique in terms of achieving higher PSNR value and improved visual quality while using Lena and Barbara grayscale images (512 x 512 pixels) in and the different contrasts of AWGN noise in addition to retaining most of the image details while eliminating the noise [13].

Koranga et al. focused on wavelet transform using wavelet shrinkage function in their study. Where the wavelet transform has been used to decompose a degraded image to get two groups of image wavelet coefficients, the first one was a wide range of wavelet coefficients that included the features of the image, while the second group of the wavelet coefficients was contained a narrow range of coefficients that included the features of the noise. The soft threshold function (Visu shrink) was then applied to remove some insignificant wavelet coefficients regarding some boundary values. Finally, by reconstruction of inverse decomposition coefficients for each sub-band, the denoised image was obtained. Two measurement parameters were used to calculate the noise in the image, which are (PSNR, RMSE) for various wavelet filters as Db1, Bior1.5, Sym1, and coif1. The results presented an improved performance in eliminating the Gaussian noise from the degraded image and achieved better visual quality [3].

In another scenario investigated by Jianhui and Li introduced an improved denoising algorithm based on a new threshold adjusted by a coefficient considering noise variance. They observed that the current wavelet transform has some limitations and tried to address them by applying the new proposed threshold, for instance, the fixed threshold formula does not follow the changes of the decomposition scale, the hard threshold technique is not continuous at the threshold point, the constant deviation between the original image wavelet coefficients and their estimates always exists in soft threshold technique, and so on. To enhance the denoising effect of the wavelet transform, this paper first layered a new formula for estimating the threshold and a new threshold function calculation method of noisy images with wavelet transform functions. Then, the threshold was calculated with the new threshold formula, and the noise was removed through the new threshold function. Finally, reconstruct the processed wavelet coefficients to obtain the denoised image. Simulation outcomes showed that the denoising result was better than that of traditional wavelet threshold denoising in terms of (MSE, PSNR) value to calculate the denoised image [14].

In the medical field, Mittal et al. presented a new methodology to improve and remove the high noise of the medical image using the stationary wavelet transform (SWT) method. In their study, an effective and simple technique for adaptive noise removal was used, the SWT 2D denoising method on the medical image that is polluted by noise. The structure-constrained low-rank approximation (SLR) method was applied as a pre-processing to calculate the input images to denoise and recover sharp edges and detail structures. The experimental results demonstrated that the suggested method not only achieved more accurate performance in denoising of medical images in terms of entropy and standard deviation but also improved the image quality, which helped in accurate disease detection [15].

A new method to image denoising by using the local wiener filter was introduced by Zhang. In his method, he made use of the advantages of the non-subsampled shearlet transform (NSST), Stein’s unbiased risk estimate (SURE), and linear expansion of thresholds (LET) approach in the process of denoising. The procedure involved in his work was first used NSST in the decomposed noisy image because of the NSST effectiveness as a multi-scale and a multi-directional analysis tool concerning digital image processing. The denoising of high-frequency NSST coefficients was then followed by applying shrinkage functions founded on the local wiener filter. Shrinkage function with the method noise of local wiener filter was adopted efficiently by SURE-LET strategy. In the final step of the procedure, the NSST inverse was made to get the denoised image. Findings made from the method used in the study illustrated that the suggested approach was more efficient and higher-performing than existing methods such as Shear-Wiener, UWT SURE-LET, and SURE-NeighShrink. At the same time, it presented better results compared with some other wavelet-based approaches [16].

Arazm et al. investigated the improved pixel-wise adaptive wiener filter to eliminate additive white gaussian noise (AWGN) of the scanning electron microscope image (SEM). In their work, the adaptive weight function (AWF) has been discussed in detail, especially for the wiener filter estimation of the local spatial statistics as well as an estimate of the needed noise variance while using the method of linear regression (LR). The suggested filter was eventually compared to the Wiener filter and adaptive noise wiener (ANW) to denoise SEM images based on the PSNR value. For various noise variances, the experimental outcomes showed that the suggested filter had improved performance because of the use of adaptive weighted local statistics, which perform better noise removal near sharp edges and a most accurate estimate of noise variance comparison with other mentioned filters [17].

The work of Devi and Sujatha introduced an efficient fingerprint enhancement compared with the existing techniques using the wiener filter. The work was preprocessed in several steps, starting with converting the input fingerprint gray image into the Binary image by applying Otsu thresholding. Then, brighten the binary image using histogram equalization followed by denoising and blurring the equalized binary image and filtering the denoised and blurred image by employing the Wiener filter and ended with enhancing the filtered fingerprint morphological operations through contrast, sharpening, and thinning were performed for more clarity. The image quality was improved, and the proposed methodology was effective since it creates a PSNR value that is better in comparison with common methods [18].

Metri and Asha engaged in a study in which a unique image denoising method was proposed. The approach presented in the investigation was performance limits analysis in denoising of images. Using patches that rely on redundancy in patches for image denoising, a wiener filter framework was established. Then, Lena image based on 512X512 resolution was used to examine the proposed algorithm in denoising to evaluate different images that had varying noises. The findings illustrate that the various parameters can be estimated by the input of the noisy image. The statistical base of the denoising algorithm is credible and is deliberated in detail. The outcomes indicated that the unique denoising algorithm performed was effective on different images and noise models [19].

A new technique for denoising via a modified adaptive median filter (AMF) was proposed by Zhang et al. The proposed procedure to restoring the degraded image was included in two-phase, first detecting the noise and then eliminating the noise. When detecting the noise in the images, the MSD (minimum set difference) was specified to represent the correlation between pixel-values into the non-pollution group for the determination of high-frequency signal and noise components. In the next phase of the procedure, the noise pixels were replaced with the median value. The findings showed the superiority of the suggested approach compared to the existing techniques as SMF (standard median filter) and AMF in terms of high-noise detection rate, impulse noise reduction effect, as well as keep the details right, particularly under the density of high-noise [20].

Tang et al. introduced a new technique for structured light image denoising by the improved (AMF). The goal of the study was to improve an AMF approach to overcome the limitations associated with standard and adaptive median filter (SMF, AMF) approaches employed in reducing structured light images. The AMF used in the study to seeks and achieved better outcomes and involved the following steps. First, they began to detect the actual noise point and local noise density in the noisy image by performing the procedure twice. Second, the filtering window was adjusted in size adaptively based on the density of discovered noise points. Finally, discovered images were filtered from four available directions. The simulation results showed that the suggested technique could effectively preserve the image details while removing noise, as well as achieved better filtering performance compared to SMF and AMF techniques [21].

A new adaptive non-linear filter to remove noise based on the right median filter (rm) was developed by Erkan U. et al. A distinct approach was applied to eliminate salt and pepper noise using the adaptive right median filter (ARMF) in their experiment. In the beginning, they defined a unique median method (rm – right median) and a distinct adaptive non-linear filter (ARMF) generated with the right median. Then, the ARMF filter results were compared with some known filters by using two image quality metrics (PSNR, SSIM) on the 12 image tests. The results illustrated that ARMF performs better in removing salt and pepper noise than other NAFSMF, MDBUTMF, and DBA methods. However, while it outperforms those other methods at various densities, ARMF failed to achieve that same impressive performance when the noise density is at 80 or 90 percent in the mean percentage. The researchers asserted the variation in performance to be a development linked with the Centre pixel. When the noise density is high, the distance between the regular entries (in the windows that have high size) and the Centre pixel seems to be large. As such, a drawback is observed in ARMF when the noise densities exceed 80 percent [22].

Lyakhov et al. investigated a practical approach to impulse noise removal using AMF. The best process to eliminate impulse noise is through the median filter, which replaces pixel units for the corrupted image with the similar median values of some neighborhood points. However, the median filter contributes to the image blurring and becomes primarily noticeable while processing images degraded by high-intensity impulse noise. In their work, an approach focused on the AMF has been suggested to minimize the negative effect resulting from conventional procedures by adopting iterative image processing with small masks and pre-processing of the median filter outcomes and improved the efficiency of the processing. The numerical assessment of simulation results by PSNR and SSIM concluded that the suggested approach achieved better clear images from low-intensity and high-intensity impulse noise via an intensity of (90-99) percent, and it helps solve the impulse noise problem more efficiently [23].

Mridula et al. presented a new algorithm, which combines spatial domain filtering with frequency-domain methods to remove speckle noise form found in synthetic aperture radar images (SAR). The Wiener filter (WF) was used as a pre-processing phase in the spatial domain by the algorithm proposed. Then, by taking the logarithm of the filtered image from the wiener filter, the multiplicative noise model for the speckled image was transformed into an additive one. In the second phase, a decomposition of the wavelet transform was performed with Meyer wavelets, and adaptive soft thresholding was implemented to detail coefficients only (LH, HL, HH). Lastly, to obtain a denoised image, the inverse discrete wavelet transformation (IDWT) was calculated by combined the approximation and threshold detail coefficients for the reconstructed image. Then results were quantitatively analyzed by (PSNR) and (SSIM) metrics. Compared to the other algorithm, the simulation outcomes showed that the presented algorithm effectively eliminated speckle noise from the degraded image [24].

A new method to eliminate the noise from computed tomography (CT) images using a combination of locally adaptive wiener filtering with a threshold-based wavelet domain was presented by Diwakar and Kumar. In their proposed methodology, the 2D-discrete wavelet transform (2D-DWT) was performed on the input CT medical image to decompose into low and high-frequency subbands. The detail wavelet coefficient (high frequency) was adjusted by applying local wiener filtering. The first-intermediate outcome was achieved by implementing the IDWT. As a second step, the first-intermediate was subtracted from the input CT medical image and processed through threshold-based wavelet coefficients for improved edge preservation, thus generating a second-intermediate result. Finally, both-intermediates output was combined to obtain the last outcome of the CT medical image. To estimate and evaluate the performance of the suggested method, the performance metrics (PSNR, SSIM) were used. The experimental result of the presented process indicates improved CT medical image with relation to noise suppression and structure conservation [25].

In another scenario, Santhanam and Chithra suggested a hybrid denoising filter to eliminate additive noise in the field of medical images (CT) by combining the absolute difference and mean filter (ADMF) with a modified median wiener filter (MMWF). The authors focused on reducing the Gaussian noise from computer tomography (CT) degraded images to enhance the medical image quality to increase the ability to diagnose disease by merging the complementary qualities and abilities for each of Median and Wiener spatial filter together with the ADMF filter also. The simulation results showed that the algorithm produces higher (PSNR) and lower (MSE) values. The average (MSE) values for new hybrid filtering techniques compared with similar approaches (TDBF, DWTTV, EPHF, MMWF, and ADMF) have been calculated. The new hybrid method showed a decrease of 73.76% MSE value and an increase of 26.24% concerning the PSNR value. The indicated outcomes that the suggested approach in their study was more suitable for eliminating Gaussian noise in the field of medical images (CT) than other algorithms [26].

A new technique to eliminate image noise by adopting a median filter (MF) in the wavelet domain was suggested and tested by Ramadhan et al. They examined various types of wavelet transformation filters by coupling with a median filter to test the proposed approach and achieve better results for the process of image noise removing. After the test has been done, a suitable filter was chosen for their work. The algorithm showed that the quality of the image produced through the technique suggested of corrupted images involving Gaussian noise compared to the PSNR value achieves better results than traditional methods for wavelet-based thresholding and Median filter each alone. The experimental results appeared the higher levels of PSNR for the denoised images, providing clear images and improve the visual quality [27].

A research was suggested by Longkumer and Gupta about a new technique that used wavelet transform on the input noised image with thresholding function and Weiner Filter. In their proposed method, an investigation into several research papers on image denoising was done and their performance analyzed. A new approach based on the Daubechies wavelet family (db4) was applied which uses a Weiner filter with approximation coefficients (LL) sub-band and soft thresholding with the detail coefficients (HH, HL, LH) sub-bands after adding Gaussian, salt and pepper noise to the image. Then reconstructed the denoised image by inverse wavelet transform. The performance of the suggested algorithm assessed in terms of measurement criteria (MSE, PSNR), competitive performance compared to existing techniques has been observed in removing noise for images contaminated with AWGN noise and salt and pepper noise. The method showed the effectiveness of the proposed algorithm [28].

Aghabalaei et al. suggested a new procedure that combines a Kalman filter with the wavelet transformation to eliminate speckle-noise from synthetic aperture radar (SAR) images. In their study, the dataset was collected from different paths and periods during their capture. Therefore, the single look complex (SLC) data was initially then co-registered into the image of the first path, and then a re-sampling of the images was performed process on a similar scale in both directions (range, azimuth). The first image was de-speckled as the second step by applying the B-spline wavelet combined with the Birgé-Massart strategy to obtain denoising thresholds. Lastly, to get the de-speckled time-series (SAR) image, the recursive Kalman filter was used on other images. They used each of the quantitative and qualitative tests, including the two criteria (ENL, EEI) for evaluation. The performance results of the suggested method were better in terms of preserving the major edge structures and details compared to other current filters such as Lee-Sigma and Frost filters in eliminating speckle-noise from (SAR) images. Furthermore, it is computationally effective in maintaining spatial accuracy and reducing remote sensing processing [29].

As regards the objective and subjective performance of the conventional filtering, a combination algorithm applied by Choi and Jeong showed a better performance to eliminate speckle noise of SAR image and retaining edge details by applying speckle-reducing anisotropic diffusion filter (SRAD) with the threshold-based wavelet transform and guided filter. The SRAD filter was adopted as a pre-processing filter to retain useful information and enhance the SAR image quality. A logarithmic transformation (log) function was then used to further eliminate the multiplicative noise residual in the prefiltered image by transforming speckle noise to additive one. As a penultimate step, the resulting image was decomposed to a multiresolution process by a soft threshold-based discrete wavelet transform (DWT) and guided filter for the four decomposed subband images (LL, LH, HL, HH). Finally, the inverse wavelet transformation (IDWT) and an exponential function were implemented to the reconstructed image to get a denoised image [30].

Dass suggested a new approach to speckle-noise reduction of ultrasound images by applying bacterial foraging optimization (BFO) cascaded with wavelet transformation and Wiener filter. In his technique, the Wiener filter was adopted as a pre-processing filter to eliminate speckle noise from the degraded image. To further eliminate the noise residual in the prefiltered image, a wavelet packet was used with the adaptive soft thresholding function to detect and remove noise from the affected pixels. Then inverse wavelet transformation (IDWT) and an exponential transform function were implemented to reconstruct the prefiltered image to get a denoised image. Lastly, the BFO algorithm reduces the error percentage between both the speckled-image and the de-speckled output-image of the homomorphic framework after pre-processing, maintaining the finer details, as well as the error percentage. The technique presented superior results compared to other techniques based on two measurement criteria (MAE, PSNR). The results displayed that the merger of DWT with the Wiener filter performs better outcomes in preserving the image by eliminating noise from images. Simultaneously, the combined BFO and AMF achieve improvement in the visual and statistical results [31].

Moving to the medical images field, Tayade and Bhosale presented a modified technique that works on improving the low-resolution (LR) medical image by using the dual-tree complex-based wavelet transform (DTCWT) along with image interpolation and wiener filter. In their procedure, the cascaded structure of DTCWT was employed to produce various frequency bands for the evaluation and analysis of their algorithm due to the properties of shift-invariance and good directional selectivity. While the denoising approach of their proposed has been based on the Wiener filter and dual-tree complex. The LR of the input image was decomposed into multiple frequency sub-bands by using six-level of decomposition to the production of various frequency sub-bands for analysis. Simultaneously, numerous quality standard criteria such as PSNR, MSE, and SSIM were employed to assess the technique of resolution enhancement and quality of the denoised medical image. The findings indicated that the suggested process has a better smoothness and higher accuracy balance of image compared to the discrete wavelet transform (DWT) as well as less redundant than the stationary wavelet transform (SWT) [32].

Researchers were also interested in enhancing computed tomography (CT) Luo et al. investigated a new denoising algorithm of CT images by applying a double-density dual-tree complex based-wavelet transform (DDCWT) with a modified thresholding technique. The method starts with decomposing the noisy CT medical image into low and high-frequency wavelet coefficients, then adopting a modified threshold function to enhance the performance and preserve effective wavelet coefficients for all sub-bands. The thresholding value was determined depended on the modified threshold function. In the end, the denoised image was obtained by reconstructing inverse decomposition coefficients for each sub-band (low and high frequency) of DDCWT. The evaluation of the method included two measurement parameters computed visual quality between the input image and the out image, namely (MSE, PSNR). The experimental results indicated that the denoising image algorithm based on DDCWT performs better and maintains more rich details in CT images than the classical DTCWT algorithm [33].

Qian proposed a new algorithm that combined the improved threshold-based wavelet decomposition with the median filter to degraded image denoising. In his research, the improved threshold function has been employed on wavelet detail coefficients (high frequency) mixed by noise which was denoised of each level after two-level decomposition of wavelet was performed on the noisy image, then reconstructed the restored image by wavelet approximation, and the denoised wavelet details of each level. Eventually, the Median filtering was twice performed for the reconstructed images to obtain the denoised image. The findings of the new method showed that the denoising effect of the improved threshold technique was better from soft and hard thresholding techniques in eliminating Gaussian noise and Median filter in eliminating salt and pepper noise based on measurement parameters (PSNR). Therefore, the presented algorithm can effectively eliminate the multiple random noises into the degraded image and be implemented in engineering image field denoising because of strong adaptability and a more stable noise reduction effect [34].

A year after, Qian presented another combined algorithm for image denoising that consists of AMF with an improved threshold-based wavelet transform (WT). In the first step, the upper limit of the template was set in his algorithm, the salt and pepper noise was removed by employed an AMF filter within the limit. In the second step, a two-level decomposition of the wavelet was performed on the degraded image. The coefficients of high-frequency were denoised by applying an improved threshold technique, then reconstructed the restored image by coefficients of low-frequency. MATLAB simulation outcomes showed that the investigated approach (AMF-WT) was superior to the AMF filter, reducing salt and pepper noise. The improved threshold function development had a better denoising effect compared to the soft and hard threshold functions [35].

Nishu et al. suggested combining the speckle reducing anisotropic diffusion filter (SRAD) with Bayesian threshold-based wavelet transform to eliminate speckle noise effectively and enhance image visual quality. In their work, the uncompressed noisy image has been processed by applying an SRAD filter, and then the logarithmic transformation converted the speckle noise into additive noise. Finally, the DWT employing a soft thresholding function (Bayesian) has been done on the log compressed image to get a denoised image. The results showed that the performance of the suggested technique, compared to several other different techniques, provides an improved visual quality based on the measurement parameters like RMSE, PSNR, SSIM, and computational time (s) metrics [36].

Fan et al. investigated two different methods to remove Gaussian white noise from the image with a threshold-based wavelet and Wiener filter. In the first method, the DWT was made on a grayscale image to decomposed into approximation and detail coefficients. Then wavelet coefficients were adjusted using wavelet thresholding by eliminating the noisy-affected coefficients from the image. While in the second method, the image was analyzed using a wiener filter in the wavelet domain. Finally, after noisy coefficients are removed from both methods (first, second), the denoised image was reconstructed by inverse DWT. By comparing the performance of both methods, they observed that the second method (wiener filter in the wavelet domain) was better to remove Gaussian noise from the image [37].

A new procedure for image denoising affected by additive white gaussian noise (AWGN) using threshold-based discrete wavelet transformation with wiener filter by Ferzo and Mustafa was adopted. They employed multiresolution wavelet transform to reduce the noise from pixel units of the damaged image by relying on four thresholding functions into all wavelet filters. Then, the inverse discrete wavelet transform (2D-IDWT) was implemented to the reconstructed image to get a denoised image. Simultaneously, the Wiener filter was used before/after also to remove noise and complete the denoising procedure. The Peak Signal to Noise Ratio (PSNR) was chosen to measure the performance efficiency that led to an improvement of about 17.5 percent compared to other existing work, as well as to the improved quality and edge preservation of the image [38].

3. BACKGROUND THEORY

This chapter illustrates the main concept of image processing, especially in the denoising image field, including types of noise, sources of noise, and various forms of noise that have been explained. Then it illustrates filters in general, filter techniques, types of filters including Mean filter, Median filter, and Wiener filter with explaining of two main processes, convolution, and correlation, while one of the most used types of correlation that has been illustrated which is PCC. Also, this chapter explaining digital image denoising and threshold techniques with its main two types (Hard threshold, Soft threshold) were mentioned and explained some types of soft threshold techniques. The Wavelet transform is also addressed in this chapter and compared with FT. Furthermore, the advantages of wavelet, types of WT approach, and multiresolution analysis are mentioned, 2D-DWT and 2D-SWT will be addressed in detail, and how this approach can be performed to denoise an image. The main filter families for WT will be mentioned in this chapter. Finally, measurement parameters such as PSNR are explained, which were used with the evaluation for the proposed method.

3.1. Digital Image Processing

Digital image processing is a continually interesting field as it provides enhanced pictorial particulars for human clarification and processing of image data in machine display respecting memory, transmission, and representation. While Image Processing is a technology used by multiple apps to improve the expected raw pictures from life to get an enhanced image to extract some useful information. The main purpose of image processing is to introduce an image through image retrieval tools to evaluate and modify a picture to output a report which can be dependent on image analysis. In recent periods, this field of image processing has been expressively improved in quality and extended by progress in scientific and technological areas. Image processing deals with image acquisition, image improvement, image categorization, image segmentation, and features extraction. In an image processing procedure, the input is an image, and its output is an enhanced image of high quality [39].

Image selection, image improvement, image recovery, color image processing, wavelet and multiresolution processing, data compression, character recognition, and identity checking are fundamental measures in digital image processing [39].

The description of an image is, two-dimensional function f (x, y), with x and y being spatial coordinates, and the amplitude of the function f is known as the intensity or gray level of the image at that point at every pair of coordinates (x, y). The image is represented as a digital image if (x, y) and density estimate of f are all restricted distinct amounts. The digital image processing sector relates to digital image handling in a digital computer. The digital picture consists of a limited range of values, elements (components), and specific locality. These components are termed as image components, pixels, and image elements. A pixel is a word most commonly exploited to describe digital image elements [40]. The model of digital image degradation and restoration process shows in Equation 3.1 and Figure 3.1.

$$g\ (x, y) = h(x, y) * f(x, y)\ \ +\ n(x, y) \tag{3.1}$$

Where, f (x, y) is the pixel value of the original image, n (x, y) indicates the additive noise, the degradation function refers to h (x, y), and g (x, y) is the resulting noise image (degraded) [41].

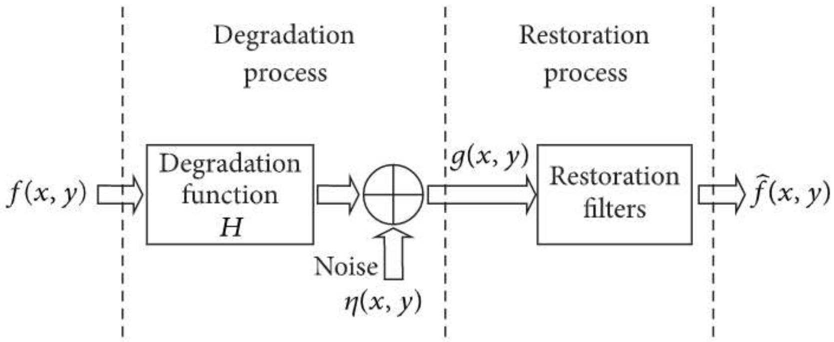

Figure 3.1. Image Degradation and Restoration Model process [41].

3.2. The Noise

Noise in digital images can be defined as any unwanted data that spread on the digital image domain and acts to damage or distort the image. It is, therefore, essential to remove the noise until the degraded image is closer to the actual image. The quality of the image is lowered due to the existence of noise and other characteristics severely affected, such as border sharpness and pattern recognition [42]. Noise occurs because of the exposure of digital images to many types of noise and their effects through many applications and activities that deal with them, such as image capture devices, CT medical devices, information compression applications, and transmission through transmission and communications networks. The images generated by these applications contain noise or some additional information not related to the original image. Various kinds of noise exist in the digital image (Salt and pepper noise, Gaussian noise, Shot noise, and Speckle noise), and there are varieties of noise. The choice of noise removal algorithms depends on the application, but noise removal is vital for image applications in order to obtain invisible data details and improve the image quality [43,44].

Noise implies the pixels in the image have different values of intensity instead of the correct values of pixels. The noise is defined as a process (n) that affects the image (f) that was acquired and that is not part of the scene (initial signal-s) [44].

3.2.1. Sources of Noise

Image is a powerful medium to convey visual information. In Digital Image Processing, the removal of noise is a highly demanded area of research. Digital images are often corrupted by different types of noise for the following reasons, Digital Image Acquisition Process, in this status, the optical image is transformed into a series of electronic signals during the acquisition process. In this phase, unwanted signals can be inserted into the original series of the electronic signal. There are also certain other unforeseen conditions such as a mechanical problem, focus blurring, movement, and the light level and sensor temperature are also major factors affecting the amount of noise in the resulting image. Image Transmission Process: The noise in this status is added particularly when transferring, including scanning the image via scanner device, convert one type of format to another type of format, etc. In this process, errors due to the measurement process and the noisy channel (interference errors) will contribute to the introduction of unwanted signals into the data stream that results in a noisy image. The sensitivity of Image Sensors: The image sensors in this status are sensitive towards motion and cause noise during capturing since the pixel elements in the camera sensors are malfunctioning, faulty memory locations, digitization process defects over time [45,46].

3.3. The Noise Models

The noise in the signals may have occurred as an additive or multiplicative form, and this classification will be illustrated in the following sections.

3.3.1. Additive Noise Model

The additive noise can occur on the signals through the adding process which will add the noise into the original signal and according to Equation 3.2 below:

$$f\,(x,y) \;=\; s(x,y) \;+\; n(x,y) \tag{3.2}$$

Where, s(x, y) is the intensity of the original image, and n(x, y) indicates the noise introduced to produce the noisy signal f(x, y) at (x, y) pixel location [47,48].

3.3.2. Multiplicative Noise Model

The original signal in this model multiplies the input signal. The multiplicative noise occurs according to the process illustrated by Equation 3.3 below:

$$f\ (x, y) = s(x, y) * n(x, y) \tag{3.3}$$

Where, s(x, y) is the intensity of the original image, and n(x, y) indicates the noise introduced to produce the noisy signal f(x, y) at (x, y) pixel location [47,48].

3.4. Types of Noise

Various types of noise have their own characteristics and are inherent in images in different ways. The common types of noise are:

3.4.1. Salt and Pepper Noise

Sometimes, salt and pepper noise is called impulse noise or spike noise. This type of noise comes due to the errors of the data transmission policy. This noise occurs within the picture due to sharp and abrupt image signal changes. However, some values of the pixel will be changing due to this type of noise. Therefore the image is not completely corrupted by salt and pepper noise, and there is a possibility that some neighbors will not change [49]. If the total of bits is 8 for transmission, the noisy pixels may only carry the maximum and the minimum values in the image quality; 0 refers to the standard value of pepper noise while 255 refers to salt noise. In a picture with impulsive noise, dark pixels are found in bright and bright pixels in dark areas. The noise caused by salt and pepper is usually due to pixel element failure in camera sensors, poor memory positions, or timing errors in the digitization process [50].

The following Equation 3.4 and next Figure 3.2 represent and show a PDF of impulse noise [48,50].

$$p(z) = \begin{cases} p_a & for\ z = a \\ p_b & for\ z = b \\ 0 & otherwise \end{cases} \tag{3.4}$$

Where:

z: gray level.

a: minimum gray level region.

b: maximum gray level region. If b > a, b: is a light dot (salt), and a: is a dark dot (pepper) in the image.

It is salt and pepper noise when Pa, Pb is zero.

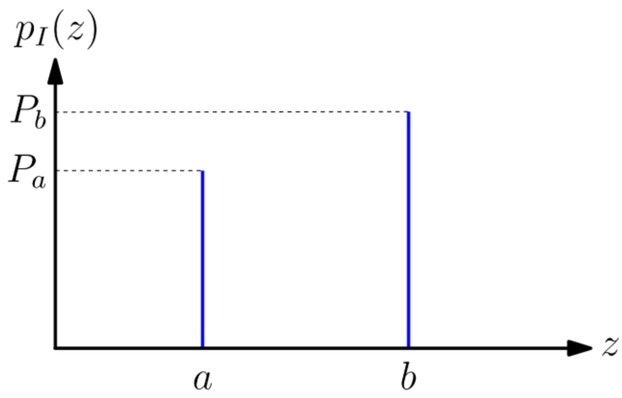

Figure 3.2. PDF of Salt and pepper Noise [50].

3.4.2. Poisson Noise

Poisson or photon shot noise is the noise caused if the photons detected by the sensor are not sufficient to supply statistically measurable data. Shot noise occurs due to the motion of individual packets which are consisted of a mechanism such as light and electrical current. The root mean square (RMS) of this noise is proportional to the image's square root intensity. The photon and other sensor noises corrupt the signal at various levels. The magnitude of this noise increases with the current average or light intensity. The following Equation 3.5 and Figure 3.3 represent and show the PDF of Poisson Noise [45,46].

$$p(x) = (e^{\lambda}\,\lambda^{x})/x! \quad for\ \lambda > 0\ \ and\ \ x = 0,1,2 \tag{3.5}$$

Where:

λ: is the expected number of occurrences that occur during a given interval.

x: is the number of occurrences of an event.

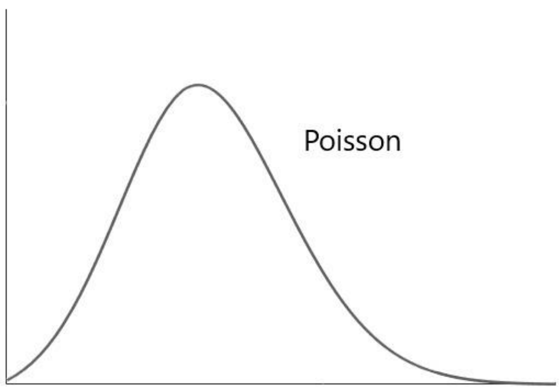

Figure 3.3. PDF of Poisson Noise [46].

3.4.3. Speckle Noise

As opposed to Gaussian and salt and pepper noise, speckle noise is known as multiplicative noise. This noise can be modeled by multiplying random values with the picture pixels which is expressed as Equation 3.6 [47].

$$P = I + n * I \tag{3.6}$$

Where:

P: is speckle noise distribution image.

I: is the input image.

n: is uniform noise image with mean o and variance v.

It is a granular noise that reduces the image quality obtained from active camera sensors or from other causes. This noise is usually caused by a random signal to ups and downs from an item that is smaller than an image processing component. It is also caused due to the consistent processing of backscattered signals which is come from the number of distributed targets. In general, this noise is usually observed in a coherent imaging system such as radar sensing technology, laser, acoustics, etc. [51]. In image denoising the effect of this noise is like Gaussian noise, and it has a probability density function that follows a gamma distribution. The following Equation 3.7 expresses this type of noise [45,50].

$$p(z) = \frac{z^{\alpha-1} e^{\frac{-z}{\sigma}}}{\sigma-1\,!\,\sigma^{\alpha}} \tag{3.7}$$

Where:

Where:

z: gray level.

σ: standard deviation.

σ2: variance of the noise.

3.4.4. Gaussian Noise

Gaussian noise is distributed equally across the signal. This type of noise is also named Gaussian distribution. So, each pixel in the noisy picture is therefore summarizing the true pixel value and a random distributed Gaussian noise value [46]. Natural sources such as thermal vibration of atoms as well as the discrete character of radiation of warm entities lead to Gaussian noise, such as sensor noise due to poor light, extreme temperatures, or transmitting Gaussian noise [50]. In the noisy image, the noise at each point depends on the pixel intensity. During the acquisition of digital images, the principal sources of Gaussian noise emerge. In a normal distribution, this type of noise has a PDF. The PDF of Gaussian Noise describes and is shown in the following Equation 3.8 and Figure 3.4 [52].

$$p(z) = \frac{1}{\sqrt{2\pi\sigma}} e^{\frac{-(z-\bar{z})^2}{2\sigma^2}} \tag{3.8}$$

Where:

z: gray level.

$\bar{z}$: mean or average of the function.

σ: standard deviation.

σ2: variance of the noise.

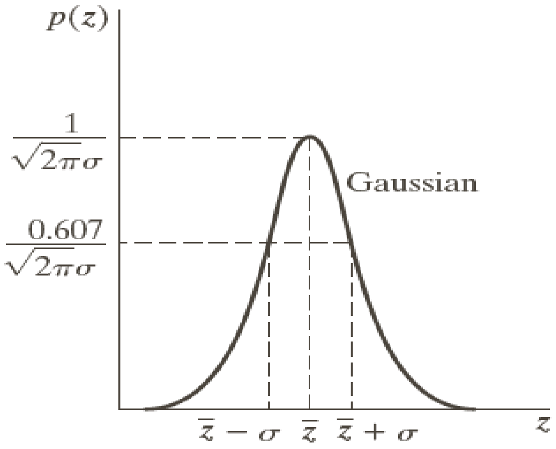

Figure 3.4. PDF of Gaussian noise [52].

A special case is white Gaussian noise, in which the values at any pair of times are identically distributed and statistically independent [45].

3.4.5. Additive White Gaussian Noise

Additive white Gaussian noise is a fundamental noise model used in the theory of data to replicate the impact of various random executions occurring in nature. The modifiers indicate features. **Additive** because it adds to any noise inherent to the information structure. **White** entails the notion that the information system has constant frequency band power. It is like the white color with uniform discharges in the perceptible spectrum at all frequencies. **Gaussian** due to possession of a standard time-domain value of zero consists of ordinary distribution in time domain allocation [50,53].

The process of denoising images tries to decrease or eliminate noise. It is a challenging job to denoise an image damaged by additive white Gaussian noise (AWGN). Additive Gaussian noise is studied in the image data as the main undesired source of interference. The AWGN is mathematically represented by Equation 3.9 [54].

$$\eta\, NAWGN(t) \;=\; \eta G(t)\sigma\, fAWGN \;=\; f(x,y) \;+\; \eta G(x,y) \tag{3.9}$$

Where:

ηG (t): is a random variable that has a Gaussian probability distribution.

σ: is additive noise.

ηG: is represented as a sum of the original uncorrupted image and the Gaussian distributed random noise (the variance of the random noise ηG is very low).

ηG (x, y): is zero or very close to zero at many pixel locations.

fAWGN: is a noisy image that is the same or very close to the original image f (x, y) at many pixel locations (x, y).

3.5. Digital Image Denoising

Denoising images relate to the method in which the unidentified signal from the loud sample is accessed and evaluated. The most important benefit of using image denoising is that while eliminating additive noise from the signal, it maintains the signal characteristics of the original picture as far as feasible. Recovering the actual data from the noisy data is the biggest challenge in denoising, while data recovered by denoising ought to be closer to the actual data. The primary purpose of image denoising is to eliminate haphazard noise and conserve the image details from being degraded from the noisy environment. It is contemplated to be the most important issue as it distorts the picture due to blurring, movement, camera misfocus, etc. [55].

The denoising technique is used to reduce or, if possible, to eliminate noise and maintain detail in digital image processing. There exist various procedures of denoising by using a spatial filter, Gaussian noise can be decreased, blurring of fine-scaled image edges and data while smoothing an image is possible for, they correspond to the high frequencies blocked by the process. Most of the standard algorithms used to denoise are filtered individually. The outcome reduces the noise, but owing to high-frequency losses, the picture is fuzzy or smoothed at corners and lines [55].

WT is one of the most conventional approaches used in denoising. This procedure fragments the noisy image into various sub-band images. By using the Donoho threshold theory the horizontal, vertical, and diagonal high-frequency wavelet coefficients are correlated and manipulated minus action changes in low-frequency coefficients. The denoised image was subsequently obtained using the threshold procedure and reverse wavelet transformation [56]. The image denoising technique is used to extract the noise from the degraded image, which in turn enhances the image quality.

Many techniques that are used to denoise the image have been implemented in the past. One of the most widely utilized procedures in picture denoising is a wavelet transformation that closes many coefficients to zero during sparse image representation [57]. Earlier transformation of Fourier was used to denoising images, while the signal was only present in the frequency domain; thus, the wavelet transformation technique was employed, representing the frequency and the time domain of the signal inclusively. Transforming Wavelet has great compaction of energy. The wavelet transform is introduced to the degraded image, and the technique of soft or hard threshold is used. The inverse wavelet transformation is finally implemented to achieve a reconstructed image [58].

3.6. Spatial Filtering Techniques

There are two filtering techniques approaches to remove noise from the degraded image, namely linear filtering and nonlinear filtering [59].

Linear Filtering: For the reduction of such forms of noise, linear filters are used. These filters eliminate noise by convolving the original picture with the help of a mask that indicates a low-pass filter or smoothing process. According to the sum of two inputs, the output of a linear process is the same as that of the actual process on the inputs and the summary of the results. These types of filters often blur the sharp edges, killing the lines and other accurate information on the picture. Linear approaches are simple, but the picture data are not preserved [57,60].

Non-Linear Filtering: Non- Linear filter is a filter that does not have a linear input function of its output data. Filters that are not linear maintain the picture information. Non-linear filters have many implementations, in particular the elimination of some noise forms which is not additive. The use and configuration of non-linear filters is far more complex than linear filters [57,60].

3.6.1. Mean Filter

The mean filter is a simple spatial filter and is also called an averaging filter. It provides a smooth picture by reducing the amplitude differences of the neighboring pixels. This filter a basic sliding-window spatial filter in the window or kernel, it replaces the middle value in a window with the average mean of all the neighboring pixel values and adds a mask in the signal over each pixel; therefore, every pixel component falling under a mask is an average filter to produce a single pixel. The main drawback is that the average filter has weak edge preservation requirements. Typically, the sliding window spatial filter is usually quadratic but can take any other form [61].

3.6.2. Median Filter

The Median filter is a simple and effective nonlinear filter that can, to some extent, distinguish out-of-range isolated noise from valid image features such as edges and lines, also known as a filter, centered on the order statistics, whose response is dependent on the filter area rating of pixel values. Smoothing degraded images can be easily performed through this filter. Median filters are made in the first phase; the median value is calculated by sorting in numerical order for all pixel values from the nearby area, after which each entry pixel value is easily replaced by the median intensity point in the pixel neighborhood. It's replacing a pixel value by the median, instead of the average value, of all values pixel in a neighborhood w. If the neighboring pixel of the image contains an even number of pixels, the replacement of the typical two mid-pixel values is applied [45,49,54]. Median filters are used for smooth processing and time series processing of pictures. It has the benefit that it is much less sensitive to extreme values than the mean (called outliers). Thus, these outliers can be eliminated without the sharpness of the degraded image. This type of filter considers most suitable to effectively remove salt and pepper noises and maintain sharp edges [62]. The Median filter of a function y [m, n] is illustrated in Equation 3.10 as follows [63]:

$$y[m,n] = median\{x[i,j],[i,j] \in w\} \tag{3.10}$$

Where:

w: denotes a neighborhood defined by the user, centered around location [m, n] in the image.

3.6.3. Wiener Filter

In 1940 Norbert Wiener proposed the Wiener filter and published it in 1949; this method has based on statistics [62]. This technique is applied according to comparison the approximation of the optimal noiseless signal with the amount of noise existing in an image to reduce the amount of the noisy image. When a recognized low-pass filter blurs the picture, it is possible to inverse the image, so one of the important features in denoising it is inverse filtering which is very sensitive to noise, especially in additive noise. Therefore, this filter allows the perfect combination of noise smoothing and inverse filtering [64]. It eliminates the additional noise and reverses the blurring effect. The Wiener filter minimizes the mean square error between the estimated process and the desired process. It minimizes the overall mean square error in the process of inverse filtering and noise smoothing. The Wiener filtering is a linear estimation of the original image [65,66]. The important objective of using the Wiener filter is to calculate a statistical value of an unidentified wave via a connected wave as input and by filtering this wave to generate the forecast as an output. For instance, the familiar signal may be containing an unknown signal of interest distorted by additive noise. To furnish the value of the basic signal of interest, the Wiener filter is employed to remove the noise from the distorted wave [67]. Wiener filters are characterized by some important features such as [61,66,68]:

- Assumption: Signal and additive noise (additive white Gaussian noise) are stationary linear with known spectral characteristics or known autocorrelation and cross-correlation.
- Requirement: the filter must be physically realizable/ causal (this requirement can be dropped, resulting in a non-causal solution).
- Performance criterion minimum mean-square error (MMSE). This filter is frequently used in the process of deconvolution.

Wiener filter is widely used due to its high flexibility and speed. It is considered effective since linear equations are used to determine an optimum range of filter weights, which reduces the noise level of a signal obtained. One other feature of this filter is estimated cross-correlation and regression coefficients matrices of noise signals and calculated to measure these weights and accurately estimate the non-fixed deterministic signal under Gaussian noise. This filter dependent on the power of noise (i.e., noise variance in a noisy image). The filter smoothed the image little when the variance is high, and it smoothed more when the variance is small [69]. Despite all these important characteristics of this filter, it does not mean that this strategy is the best. Therefore, applying the Wiener filter techniques on the image achieved satisfying outcomes, while the execution is limited since these procedures are executed in the wavelet area. This is due to the failure of the traditional two-dimensional wavelet transformation to execute with multi-dimensional data like an image that is generally controlled by anisotropic characteristics such as edges [70].

The objection function between degraded image f^(x, y) and original image f (x, y) shows in Equation 3.11 [64].

$$e^2 = E\left[(f(x,y) - \hat{f}\ (x,y))^2\right] \tag{3.11}$$

Where, E = The expectation of both the original signal and the reconstructed signal. While the next formulas show the Wiener filter Equations 3.12 [64].

$$\hat{F}\ (u,v) = W(u,v)\ G(u,v)$$

$$W\ (u,v) = \frac{H^*(u,v)}{|H(u,v)|^2 + K(u,v)} \tag{3.12}$$

$$\hat{F}\ (u,v) = \frac{H^*(u,v)}{|H(u,v)|^2 + K(u,v)}\ G(u,v)$$

Where:

K (u, v) = Sη (u, v) / Sf (u, v).

Sf (u, v) = |F (u, v) |2 power spectral density of f (x, y).

Sη (u, v) = |N (u, v) |2 power spectral density of η (x, y).

If K = 0 then $W\ (u, v) = 1\ /\ H\ (u, v)$, it is an inverse filter.

If K > |H (u, v) | for large u, v the high frequencies are attenuated.

|F (u, v) | and |N (u, v) | are often known approximately.

K: is set to a constant scalar which is determined empirically.

3.7. Wavelet Transform (WT)

Wavelet transformation is described by several authors as a mathematical technique that analyzes (or synthesizes) a signal in the time domain using various editions of an enlarged and translated base function named the wavelet prototype or the mother wavelet. Besides, the wavelet transformation is a method that subsumes time and frequency fields and is exactly known as a non-stationary signal's time-frequency representation. In wavelet transform, the signal in the time domain is disintegrated (decomposed) to create two separate parts by carrying it via a high pass filter and low pass filter (low pass (L) and high pass (H) versions) [11]. Wavelet transform can be demonstrated by Equation 3.13 as follows [71]:

$$X_{a,b} = \int_{-\infty}^{\infty} x(t)\ \psi_{a,b}\ (t)dt \tag{3.13}$$

Where:

x: is indicate to the real signal.

ψ: is an arbitrary mother wavelet.

a: is denote the scale, while b is the translation (X is the processed signal).

3.8. Fourier Transform (FT)

The Fourier transform is a mathematical function that takes as input a time-based pattern and determines the overall offset cycle, rotational strength, and speed in the given pattern for each possible cycle. The transformation of Fourier is added to waveforms that are basically a function of space, time, or another parameter. FT breaks down a waveform into a sinusoid, thus providing another way of representing a waveform. The Fourier transform is, therefore, an operation that transforms data from the domain of time (or space) into the domain of frequencies. The Fourier transform of a function f(x) is illustrated in Equation 3.14 as follows [72,73]:

$$f(x) \equiv \int_{-\infty}^{\infty} F(s)\ e^{2\pi isx}\ ds\ ,\ \ F(s) \equiv \int_{-\infty}^{\infty} f(x)\ e^{-2\pi isx}\ dx \tag{3.14}$$

Where:

F(s) can be obtained using the forward and inverse Fourier transform.

3.9. Comparing Wavelet Transform and Fourier Transform

Compared to wavelet transform, Fourier transforms just offer frequency data, while wavelet transform enables localization in each of these time domains through mother wavelet conversion and dilation of the frequency domain. In addition to supporting multiresolution design, the wavelet transform model has the benefit of sparsity and compaction of energy [74].

The wavelet transform can be contrasted to the Fourier transform with a totally explicit merit function. Fourier transform decomposes the wave into sines and cosines, i.e., the functions located in Fourier space; on the other hand, the wavelet transform uses functions located for both real and Fourier space. Generally, the Wavelet transformation is an infinite disposition of various transforms relying on the function of merit employed to compute it. The wavelet transform is more efficient than the Fourier transform because at any given interval time it gives frequency representation of the signal, while Fourier transforms only provide the frequency amplitude representation of the signal while the time information is lost. This is the primary reason why in very distinct situations and apps, the word "wavelet transform" can be heard. The fundamental comparison linking FT and WT is shown in Table 3.1 [74,75].

Table 3.1. The basic contrast linking Wavelet Transform and Fourier Transform

Wavelet Transform (WT)	Fourier transform (FT)
The mathematical expression for Wavelet transform is $\boldsymbol{W_c f(s,t) = \int_{-\infty}^{\infty} x(t), s^{-\frac{1}{2}\psi(\tau-\frac{t}{s})}\ dt}$ With s being the scale and Tao, the translation variable x(t) is an original signal.	The mathematical expression for Fourier transform is $X(f) = \int_{-\infty}^{\infty} x(t).e^{-iwt}\ dt$ With s being the scale and Tao, the translation variable x(t) is an original signal.
Suitable for both the stationary signal and the nonstationary signal.	Suitable for the stationary signal.
WT supplies a detailed three-dimensional in relation to any signal, i.e., the various frequency components present in any signal and their separate amplitudes, including a time axis where these various frequency elements subsist.	FT converts the wave from a time domain to a frequency domain signal and issues two-dimensional details in relation to any signal about the various frequency elements available in a signal with their separate amplitudes.
WT consists of not only a high time resolution with a high-frequency resolution but also time and frequency resolution, subject to changes	FT consists of zero-time resolution with a very high-frequency resolution.
In wavelet transform, the wave is changed into a scaled and transferred kind of mother wavelets.	In Fourier analysis, a signal is translated as sine and cosine waves into different amplitudes and frequencies.

WT has suitability in studies related to the local behavior of the wave, for example, discontinuity or spikes.	FT lacks suitability in studies related to the local conduct of a wave.
In WT the admission and production can be an actual or complicated function.	In FT, the input can be a real or complex function, but its output is always complex.

3.10. The Theory of Wavelets

Several researchers describe the transform wavelet as a mathematical method, when a certain signal is analyzed or synthesized in a time domain, through using multiple versions of contracted and shifted the base structure named a wavelet model or a wavelet mother. But the development of the wavelet has known its meaning and has emerged from various disciplines. In 1989, Mallat stated that this technique is a new method that can not only be used by mathematicians working in harmonic analysis and can also be used in all fields of engineering and application, such as image processing. Harr, a German mathematician at the beginning of the 20th century, invented the first wavelet transformation named after him, and the Haar foundation provides a flexible service and an integer component [76].

In the development of the wavelet theory, different works were conducted in different fields. The great achievements, as stated by Mallat, Meyer, and Daubechies research have allowed a various and wide range of wavelet-based applications to emerge in the field of signal processing. Indeed, guided by Mallat's research on the connections between the QMF filters, the algorithms of the pyramids, and the orthonormal wavelet. The first non-trivial wavelets were developed by Meyer in 1990. Ingrid Daubechies, therefore, performed the most important work. Daubechies managed to build a series of orthonormal waves-dependent functions that became the foundation of many applications based on Mallat's research. A few years later, Daubechies proposed a series of biorthogonal dependent wavelets which were later implemented in various applications, especially in image processing [71].

A wavelet is useful in image compression and digital signal processing as a mathematical function. Using wavelets for these purposes is a new development, whereas the theory is not new. The concepts are similar to those of the analysis of Fourier that was first evolved in the early 19th century. There are various modern wavelet theory applications for the propagation of waves, such as pattern recognition, signal processing, computer graphics, image processing, and data compression. Moreover, it also includes general functions at various scales and positions in terms of simpler building blocks. The basic concept under the wavelet transformation is analyzing it by scale [77].

The sinusoids employed in Fourier analysis are huge waves, but a wavelet implies a tiny wave; to sum it, a wavelet is a rapidly declining oscillation. Wavelet's equivalent mathematical circumstances are shown in Equations 3.15 and 3.16 [78]:

$$\int_{-\infty}^{\infty} |\ \psi(t)\ |^2 dt < \infty \qquad (3.15)$$

$$\int_{-\infty}^{\infty} |\ \psi(t)\ |\ dt = 0 \qquad (3.16)$$

3.10.1. The Relevance of Wavelets

Wavelets entail a strong statistical instrument that is utilized in a broad variety of apps, namely [74]:

- Signal processing.
- Data compression.
- Computer graphics.
- Smoothing and image denoising.
- Fingerprint verification.
- Protein analysis.
- DNA analysis.
- Speech recognition and multifractal analysis.

3.10.2. Advantages of Wavelet Theory

Some of the base wavelet theory advantages are [74]:

- Wavelets give a time and frequency domain concurrent localization.
- The rapid transformation of the wavelet is computationally quick.
- The fantastic advantage of wavelets is that they can split the interesting details in a message.
- Using very small wavelets, interesting details can be identified in a signal, while coarse details can be identified by very big wavelets.
- The signal can be decomposed into wavelets of components by using the wavelet transform. Without significant degradation, it can often compress or denoise signal (wave).

3.11. Continuous Wavelet Transform

Continuous Wavelet Transformation (CWT) employs internal inventions to estimate the distinction linking a signal, analyzes function, and contrasts the signal to a wavelet transferred and condensed or stretched into varieties, as well as a time-frequency depiction of a wave that provides frequency localization and excellent time. CWT is used as a method to determine if the signal is stationary or not. Also, CWT is an execution of the wavelet transform employing arbitrary scales and almost arbitrary wavelets. Therefore, the wavelets are not orthogonal and are extremely associated with the data obtained through this transform [79].

3.12. Multiresolution Analysis

Mallat 1989 and Meyer 1990 were the first to introduce and present the multiresolution method, which can be known as the subbing signal processing operational analytical method, widely used and extended to issues in technologies such as engineering [80]. It clearly defines the relations between the QMF, pyramid implementations, and orthonormal wave bases. It can decompose a signal into simpler and clearer information depending on its power. Especially in the field of time-frequency or time scale analysis, multiresolution allows the description of the signal. Through a bank of corresponding filters, the smart relation between an orthonormal wavelet decomposition of a signal and its filtering contributes to an axiomatic formalization of principle and corresponding equivalence. This led to a new wide-ranging research direction for designing and developing new technical bases and filter banks [71].

3.13. 2D Discrete Wavelet Transform

The discrete wavelet transform (DWT) is an application that employs a distinct set of wavelet scales and conversions in accordance with certain specified regulations. Similarly, this transform fragments the signal into a mutually orthogonal positioning of wavelets, which is the main uniqueness in comparison to continuous wavelet transform, or its implementation for the discrete-time series are occasionally named the continuous discrete-time wavelet transformation [81]. A discrete wavelet transform provides techniques such as clipping, thresholding, and decreasing coefficients amplitude to extract the noise from the data. DWT is efficient, particularly when it comes to nonlinear filtering [82,83].

The Discrete Wavelet Transform (DWT) is used to extract the data through the signal processing technique by using different scales. It is based on sub-coding and symbolizes the data through a set of details and coarse values. In many practical apps, DWT is repeatedly used, for instance, image compression, image denoising, audio analysis, and video encoding. Discrete Wavelet Transform is used in the image field to analyze different resolutions of signal possessing at various frequency bands by decomposing the signal into two stages (level), including coarse approximation and detailed information [84]. There are two sets of functions for Discrete Wavelet Transform; by Low-pass filter the scaling operations are implemented, and by High-pass filter the wavelet operation is implemented as illustrated in Figure 3.5.

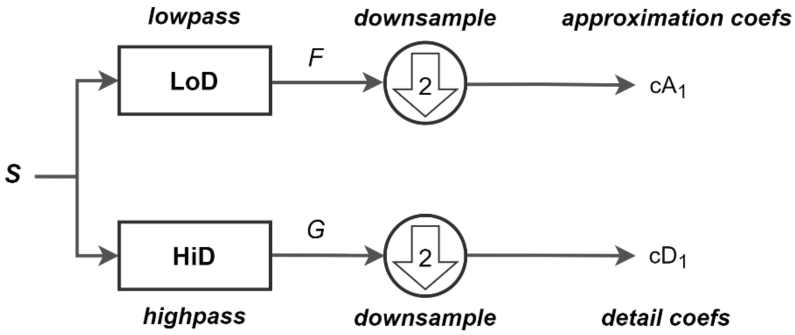

Figure 3.5. 1-D level of Discrete Wavelet Transforms [11].

The Discrete Wavelet Transform (DWT) naturally is a one-dimensional transform but forms a two-dimensional transform by applying it in the vertical and horizontal directions. DWT method can be performed several times and via dyadic decomposition, as it is called, at level j the 2D-DWT decomposes one approximation coefficient into four components at altitude j+1. The approximation coefficient cAj+1, and information coefficients at three inclinations: horizontal cDh j+1, vertical cDv j+1, and diagonal cDd j+1 [85].

DWT applies the concept of decomposition of the wavelet and can decompose in the multi-level environment defined as multiresolution [86]. In signal or image processing, DWT considers as a powerful tool for its multiresolution capabilities. Wavelets have superior picture denoising performance due to properties like multiresolution structure [83].

The 2D-DWT is one of the most employed transform approaches in image processing. The scaled and translated basis elements of two-dimensional DWT of an image f (x, y) is given as following Equation 3.17 [86]:

$$\begin{aligned} &\varphi(x,y) = \varphi(x)\varphi(y) = LL \\ &\psi\text{^}H\ (x,y) = \psi(x)\varphi(y) = LH \\ &\psi\text{^}V\ (x,y) = \varphi(x)\psi(y) = HL \\ &\psi^D(x,y) = \psi(x)\psi(y) = HH \end{aligned} \tag{3.17}$$

Where:

H, V, and D: are superscripts that refer to the vertical, horizontal, and diagonal of the decomposition direction of the WT. Two-dimensional wavelets are employed as a part of image manipulation. The multiresolution representation of scaling and WT functions for the 2-D is shown in Equations 3.18 and 3.19:

$$\varphi_{j,m,n}(x,y) = 2^{j/2}\, \varphi(2^j x - m, 2^j y - n) \tag{3.18}$$

$$\psi^i{}_{j,m,n}(x,y) = 2^{j/2}\, \psi^i(2^j x - m, 2^j y - n) \tag{3.19}$$

Where:

i: is the represent of H, V, and D.

In image pixels and according to filter bank the 2D-DWT is calculated by utilizing low-pass and high-pass filtering.

A hybrid of a high pass filter and a low pass filter is known as the filter bank, which is accompanied by two elements [87]. Therefore, decomposition from the digital signal processing principle is limited to two key operations which are filtering and a down-sampling. Identical phases leading to a multiresolution analysis are cascaded to enable further decomposition. This technique is known as the structure for sub-band coding when g represents the high pass filtering, and h represents the low pass [88]. The three levels of the decomposition of the 2D-DWT were demonstrated as a layout in Figure 3.6 which is normally used to apply the algorithm of Mallat [71,85].

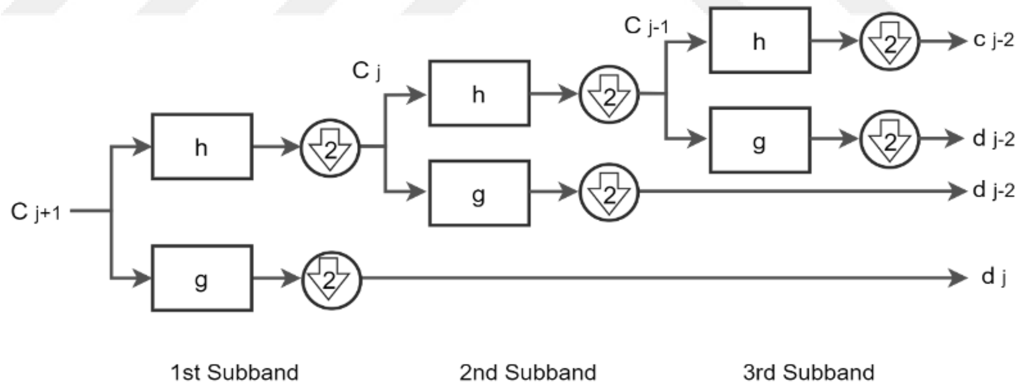

Figure 3.6. A three-stage analysis sub-band of an image using filter bank [89].

The high-pass filter produces description image pixels ’detail’ information in each level, whereas with the low-pass filter generating the coarse estimates of the input image at each level. The outputs are down-sampled by two (↓2) at the terminate of every low-pass and high-pass filtering; the two 1D-DWT can be given one 2D-DWT; this means 2D-DWT can be separated from two 1D-DWT. Likewise, a 2D-DWT can be achieved by executing a 1D-DWT of the image on every row, known as horizontal filtering, while called vertical filtering by executing a 1D-DWT on every column. A reversed model of the review filter bank is required to recover the initial signal from the previously evaluated one. There are two fundamental operations that must be applying to achieve which are filtering and an up-sampling or interpolating process. For multiple digital signal processing, the up-sampling occurs through inserting a zero sample for two successive samples. Therefore, can be got two output samples for each input sample. A three-stage synthesis sub-band coding is illustrated in Figure 3.7 [89].

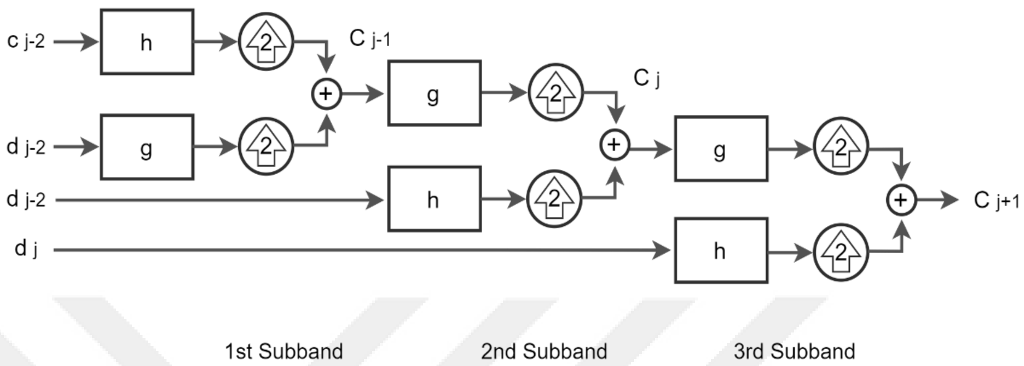

Figure 3.7. A three-stage synthesis sub-band of an image using filter bank [89].

2D-DWT fragments a picture into four wavelet coefficients (sub-bands) A, H, V, D (LL (Low Low), LH (Low High), HL (High Low), HH (High High)) [86]. In these, the estimation coefficient (A) carries the most significant details of the data, while detail coefficients (H, V, D) contain the edges of the image that are equated to a particular threshold estimate to be utilized to reduce the noise [58,84]. The first phase of decomposition of 2D-DWT application on a resolution (image) is shown in Figure 3.8. At this level, the initial resolution is fragmented into four sub-bands carrying both the horizontal and vertical frequency information. The low pass filter was used and applied in the horizontal direction, and the high pass filter was used and applied in the vertical direction to generate the LL sub-band. The LL sub-band provides additional details and is beneficial for extracting processing [89]. The algorithm is implemented iteratively to the LL sub-band to create various levels of decomposition. The second and third levels of fragmentation and the design of the different bands are shown in Figure 3.9.

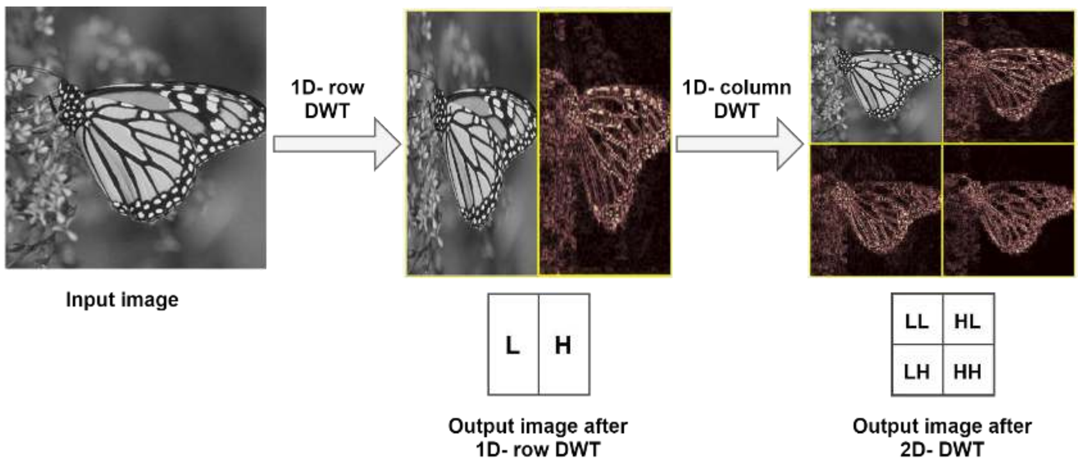

Figure 3.8. First decomposition level of 2D-DWT implementation on an image [90].

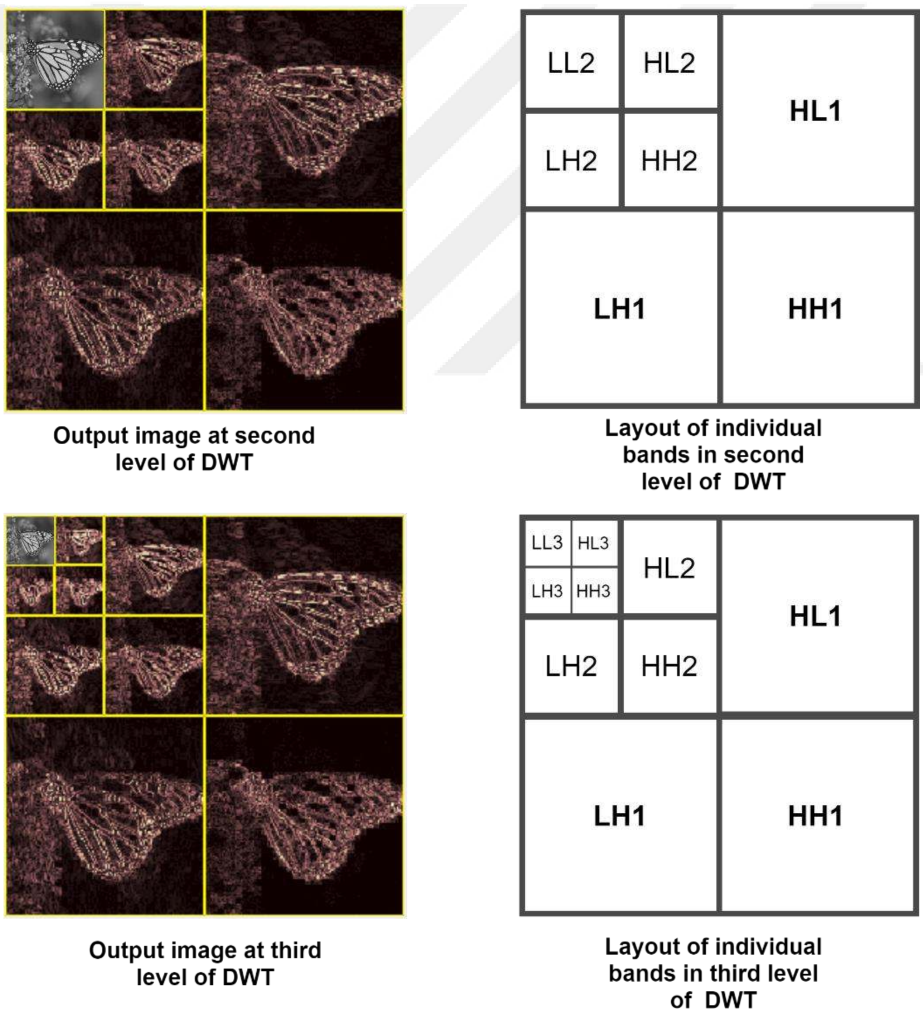

Figure 3.9. Second and third decomposition level of 2D-DWT implementation on an image [90].

In general, the level j in 2D-DWT decomposition stages built using three filter banks which is represented in Figure 3.10 depending on Mallat's analysis.

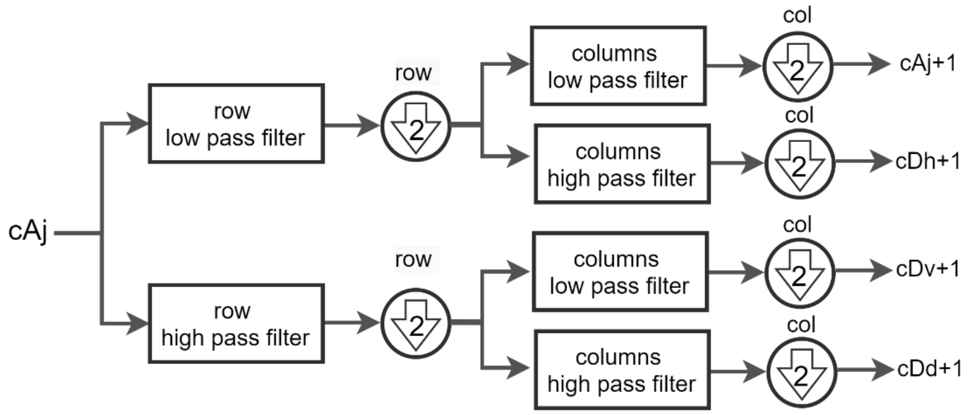

Figure 3.10. 2D-DWT implementation for level j Mallat's analysis [71].

Figure 3.11 below illustrates the operation of the 2D inverse discrete wavelet transform (A reconstruction step).

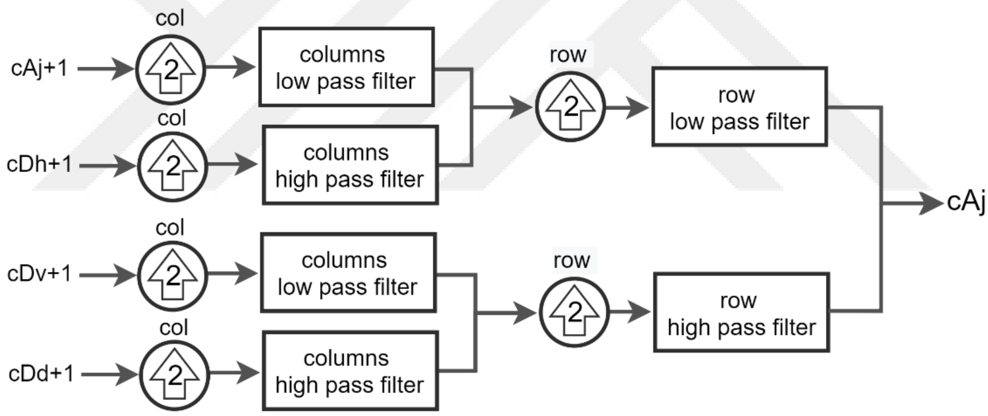

Figure 3.11. 2D inverse discrete wavelet transform (Mallat's synthesis) [71].

3.14. 2D Stationary Wavelet Transform

Wavelet is a time-frequency analysis commonly used in image processing, such as denoising, compression, and segmentation, and is one of the many multi-scale signal processing techniques available. Wavelet-based denoising allows for multi-scale noise treatment, sub-band image down-sampling during decomposition, and threshold-wavelet coefficients may cause distort the edge and artifact in the reconstructed free-noise image [91]. So, a multi-layer stationary wavelet transform (SWT) has been applied to overcome the conventional wavelet transform limitation.

The SWT presents effective numerical solutions for signal processing applications. Several researchers independently developed it and under various names, e.g., the undecimated wavelet transform (UWT), the invariant wavelet transforms (IWT), and the redundant wavelet transforms (RWT)[92].

SWT performs a multi-level stationary wavelet decomposition using either a specific orthogonal wavelet or specific orthogonal wavelet decomposition filters. The SWT has almost similar tree-structured implementation to DWT where the high pass and lowpass filters are applied to the input signal with equal length wavelet coefficients at each level, but the principal point of SWT is that it returns a better approximation result compared to DWT, due to the output signal is not decimated (without down-sampling). Instead, at each level, the filters are up-sampled, and hence a better edge detection, denoising, and data fusion can be performed. The DWT cannot provide this feature [93,94]. The two-dimensional SWT of an image f (x, y) is given as following Equation 3.20 [95]:

$$\begin{aligned} LL_{j+1}(a,b) &= \sum_x \sum_y l_x^j\, l_y^j\, LL_j(a+x, b+y) \\ LH_{j+1}(a,b) &= \sum_x \sum_y l_x^j\, h_y^j\, LL_j(a+x, b+y) \\ HL_{j+1}(a,b) &= \sum_x \sum_y h_x^j\, l_y^j\, LL_j(a+x, b+y) \\ HH_{j+1}(a,b) &= \sum_x \sum_y h_x^j\, h_y^j\, LL_j(a+x, b+y) \end{aligned} \tag{3.20}$$

Where:

a=1, 2, ..., M, and b= 1, 2, ..., N

h and l: are denotes to the High-pass and Low-pass filters.

In each two-dimensional SWT sub-band various information of the image is retained. The LL sub-band is represented the overall image approximate (a), while LH, HL, and HH have image information horizontal (h), vertical (v), and diagonal (d) sub-bands, respectively. As shown in Figure 3.12. The resulting decomposition of two-dimensional SWT has the same size as the input image (original), which results in four times the number of coefficients than the original image (input)[93,95].

Figure 3.13. below illustrates the operation of the 2D inverse stationary wavelet transform (A reconstruction step).

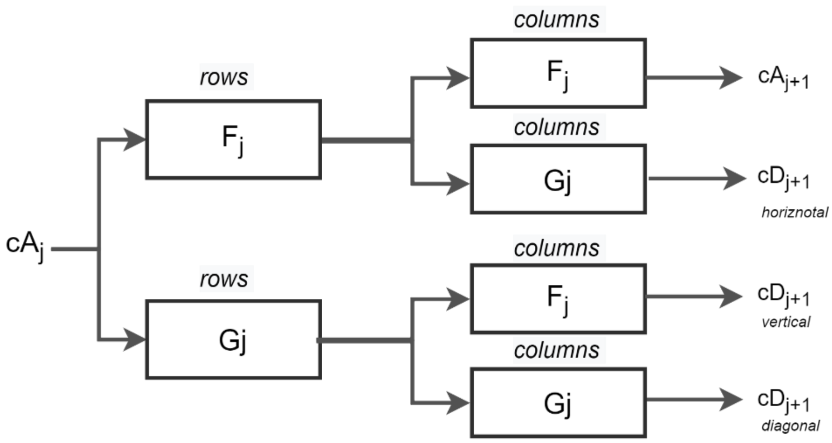

Figure 3.12. 2D-SWT implementation for level j analysis stages [95].

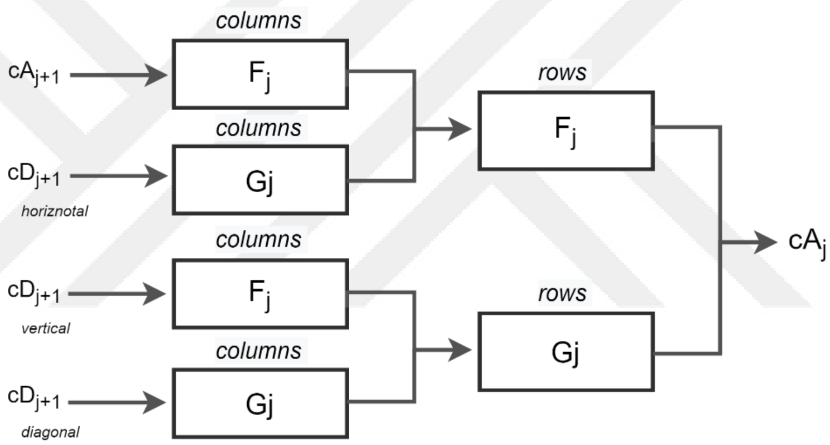

Figure 3.13. 2D inverse stationary wavelet transform (synthesis) [95].

3.15. Wavelet Thresholding Techniques

The thresholding technique is a simple non-linear method used to denoise wavelets. In this technique, the threshold value that is decomposed into three main steps is compared to each wavelet coefficient. The first one is to calculate the wavelet transform coefficients, which is a linear operation, while the second one consists of these coefficients being in the threshold. In the last step, the threshold values are reversed by implementing the reverse wavelet transform, resulting in a denoised signal. If all the values of the coefficients are lower in comparison to the value of the threshold, it is assigned to zero; else, all the values of the coefficients will be set as it is or shrinks. In the wavelet thresholding denoising, the first step must select a threshold and process the wavelet transform components of the noisy signal. A high denoising image would be provided by the best choice of threshold values. Selecting the threshold procedure is an important variable in determining which pixel values in a sub-band are to be retained or removed. There are two types of thresholding procedures, namely soft thresholding and hard thresholding [96,97].

3.15.1. Selection of Threshold Function

The threshold function determines the various strategies and different estimation techniques for the wavelet coefficients. Hard threshold function and soft threshold function are two frequently utilized threshold functions. Suppose that Wj i is the Wavelet transform of the image hold noise, while the inverse wavelet transform of the noisy image is represented by Ŵj i, and T is the threshold value, these two types of threshold functions can be expressed as hard threshold and soft threshold [97,98]. Hard thresholding is ideally suited where either a signal or a noise coefficient is a coefficient of information wavelets. On the other side, soft thresholds function best when both signal and noise are present in a Detail wavelet coefficient [99].

3.15.2. Hard Thresholding

The absolute estimate of the wavelet coefficients is compared to a threshold estimate, and if the wavelet coefficients are smaller than the threshold value, it is set to zeros; otherwise, it remains as it is (the hard threshold signal is Wj i if Wj i ≥ T and is 0 if Wj i < T). The following Equation 3.21 describes the hard threshold [100,101].

$$\widehat{W}_{j\,i} = \begin{cases} W_{ji} & When \quad |W_{j\,i}| \geq T \\ 0 & When \quad |W_{j\,i}| < T \end{cases} \tag{3.21}$$

Where:

W j i: are noisy wavelet coefficients.

Ŵ j i: are denoised wavelet coefficients.

j: is decomposition level.

i: is the location of the detail component.

T: is the representative of the threshold value.

The hard threshold technique can maintain the image's local characteristics, such as edges of images, etc. In mathematical therapy, this is not simple to accomplish because its systolic function is not continuous. Simultaneously, many artificial noise points are generated at image edges resulting in image distortion, such as ringing impact or pseudo-Gibbs impact [98,101].

3.15.3. Soft Thresholding

Soft threshold shrinks the values of the wavelet towards zero; for this reason, it is sometimes known as wavelet shrinkage function. Soft thresholding creates an image that is visually pleasant than hard thresholding [102]. The wavelet coefficients in the wavelet domain are smoother after soft thresholding, and the recreated picture also appears lesser when contrasted with the hard thresholding approach. Soft thresholding is described in Equation 3.22 below [101].

$$\widehat{W}_{j\,i} = \begin{cases} W_{ji} + T, & if\ |W_{ji}| \geq T \\ W_{ji} - T, & if\ |W_{ji}| \geq T \\ 0, & if\ |W_{ji}| < T \end{cases} \tag{3.22}$$

Where:

W j i: are noisy wavelet coefficients.

Ŵ j i: are denoised wavelet coefficients.

j: is decomposition level.

i: is the location of the detail component.

T: is the represent of threshold value.

The soft threshold algorithm allows shrinkage therapy to decrease the wavelet coefficients whose estimates are higher compared to the threshold (soft threshold is an expansion of the hard thresholding), initially if absolute values are lesser in comparison to a threshold value, they are assigned a zero, and then the non-zero coefficients are shrinking to 0. If $Wj\ i \geq$ T, the soft threshold wave is ($Wj\ i$ + T) [101]. Because the soft threshold is a continuous function, the weaknesses in the hard threshold algorithm can be well overcome. Thus, the findings handled are comparatively clean with the wavelet coefficients having big absolute values. However, if reduced, it will result in some high-frequency data losses. There are many wavelet threshold denoising techniques for estimating the threshold function in image denoising [100].

3.16. Threshold Estimation Methods

There are several methods to estimate threshold values. The three following threshold techniques are used in the proposed algorithms.

3.16.1. Sure Shrink

Donoho and Johnstone proposed a threshold chooser based on Stein's Unbiased Risk Estimator (SURE), who referred to it as the "Sure Shrink" which is the product of combining the universal and SURE thresholds [97]. This method specifies a value of threshold tj for each resolution level j in the wavelet transformation referred to as the level-dependent threshold [103]. Sure Shrink aims to reduce the Mean Squared Error described as 3.23:

$$MSE = \frac{1}{n^2}\sum_{x,y=1}^{n}(z(x,y) - s(x,y))^2 \quad (3.23)$$

Where:

z (x, y): is the estimate of the signal.

s (x, y): is the original signal without noise, and n is the size of the signal.

Sure Shrink suppresses noise through thresholding the empirical wavelet coefficients [103]. The Sure Shrink threshold t* is denoted as:

$$t^* = min(t, \sigma\sqrt{2\ log\ n}\ ) \quad (3.24)$$

Where:

t: is denotes the value that reduces SURE,

σ: is the noise variance computed from Equation 3.24, and n is the size of the image.

Sure Shrink is following the rule of soft thresholding. The threshold employed is adaptive, i.e., a threshold level is set for each dyadic resolution level through reducing SURE for threshold estimates. It means that if the unknown function contains sudden changes or limits in the image, so does the reconstructed image [98].

3.16.2. Bayesian shrinkage

Bayesian has been proposed by Chang et al. (2000) as an adaptive data-driven image denoising threshold via wavelet soft thresholding, which is based on a threshold estimate based on the hypothesis that the wavelet coefficients of the natural non-noise image are in the GGD. This method's objective is to predict a threshold estimate that reduces the possibility of Bayesian. It employs soft thresholding and is sub-band dependent, meaning thresholding is performed in the wavelet decomposition at each resolution band. The Bayes threshold is estimated as shown by Equation 3.25 [102,103]:

$$\lambda_{Bayes} = \hat{\sigma}_n^2 / \hat{\sigma}_x \quad (3.25)$$

Where:

$\boldsymbol{\hat{\sigma}_n}$ is calculated by Equation 3.25, and $\boldsymbol{\hat{\sigma}_x}$ is estimated by using the wavelet coefficients in each sub-band.

$\boldsymbol{\hat{\sigma}_x}$ can be obtained by Equation 3.26 and Equation 3.27 as shown below:

$$\hat{\sigma}_x = max\sqrt{\hat{\sigma}_y^2 - \hat{\sigma}_n^2, 0)} \qquad (3.26)$$

$$\sigma_y = \frac{1}{n^2}\sum_{j,k=1}^{n} w^2 \ j,k \qquad (3.27)$$

Where: $\boldsymbol{n^2}$ is the size of the subband under consideration.

3.16.3. Penalized Threshold

This threshold procedure was presented by Birge and Massart in 1997. It utilizes level-dependent thresholds gotten from the subsequent selection rules for wavelet coefficients. This procedure could arrange the detail coefficients in declining sequence then accordingly, the subsequent Equation threshold λ could be calculated as shown by Equation 3.28 [6,104]:

$$\lambda = arg_t^{min}\left[-\sum_{k=1}^{t} d_k^2 + 2\sigma^2\, t(\alpha + ln\frac{n}{t})\right]; t = 1, \ldots\ldots, n \qquad (3.28)$$

Where: $\alpha > 1$ is the sparsity parameter.

3.17. Wavelet Transformation Filters Families

For each continuous, discrete, and stationary investigations (analysis), the wavelet can be used as a method for wavelet analysis, consists of orthogonal wavelets (Daubechies least asymmetric wavelets and extremal phase) and B-spline biorthogonal wavelets, while the wavelet is inclusive of Morlet, Meyer, the derivative of Gaussian, and Paul wavelets for continuous analysis. The selection of wavelets depends on many variables, such as image features and implementation features (characteristics of the investigation and synthesis wavelet) [105].

The wavelets can be classified into two categories:

- Orthogonal (the low pass and high pass filters have similar lengths).
- Bi-Orthogonal (the low pass and high pass filters contain different lengths).

Concerning implementation, it is possible to select and use either of the above two classifications. The selection of the wavelet, therefore, relies on the sort of implementation in question. In general, several wavelet functions are utilized in the data analysis for both stationary and discrete wavelet transformation that has been applied to an image, such as

Haar wavelet, Daubechies wavelet, Biorthogonal wavelet, Mortlet, Symlet, Mexican hat, Shannon wavelet, Coiflets, among others [105,106]. Table 3.2 shows the abbreviations name for the filters of the wavelet transformation filter families.

Table 3.2. The abbreviations name for the filters of the wavelet transformation filter families used in the proposed system

Wavelet Family Name	Wavelet Family Short Name
Haar wavelet	'haar'
Daubechies wavelets	'db'
Symlets	'sym'
Coiflets	'coif'
Biorthogonal wavelets	'bior'
Reverse biorthogonal wavelets	'rbio'
Discrete approximation of Meyer wavelet	'dmey'
Fejer-Korovkin wavelets	'fk'

Wavelet families are distinct regarding various significant characteristics. Examples include [105]:

- The time and frequency support of the wavelet and decomposition rate.
- Wavelet symmetry or antisymmetric: a linear phase accompanies the perfect reconstruction filters.
- The frequency of disappearance (vanishing moments): the wavelets with a growing number of times of vanishing outcomes in scarce representations for a large signal category.
- Wavelet regularity: smoother wavelets provide sharper frequency resolution. The iterative algorithms for wavelet formation coverage are quicker.
- Presence of a scaling variable, φ.

3.17.1. Haar Wavelet

In 1909 the Haar wavelet was a sequence of rescaled functions that together form a wavelet family or basis suggested by Alfred Haar. The Haar wave is the first and simplest wavelet form and is also an orthogonal wavelet with linear phase and one of the oldest wavelet types. It has been employed for a long period in image analysis as a Haar Transform [107]. A drawback of the Haar wave is that it is discontinuous and therefore not differentiable. Transitions can, however, be an advantage to the analysis of discrete signals with sudden transitions due to the Haar wavelet is a step function with values (+1, -1). And a close resemblance to the Walsh basic. The transfer function of the Haar wavelet transformation filter family is shown in Figure 3.14 and properties: asymmetric, orthogonal, biorthogonal [105].

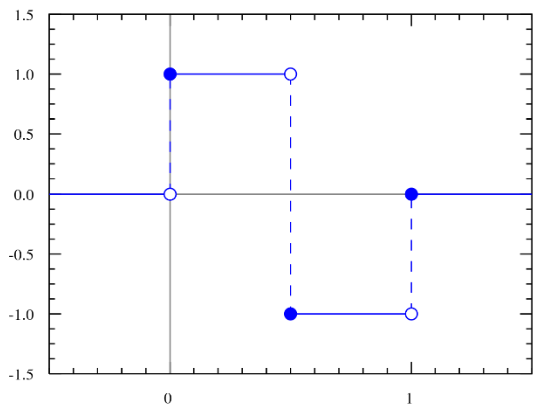

Figure 3.14. The transfer function of the Haar wavelet transformation filter family[108].

3.17.2. Daubechies wavelets (dbN)

Daubechies wavelets are distinguished by the maximal number of vanishing moments for specified support. The identities of the Daubechies family wavelets are indicated as dbN, with N being the order and db the "surname" of the wavelet. The db1 wavelet is like a Haar wavelet. Daubechies orthogonal wavelets from D2-d20 are usually utilized, although D4, D6, D8 are more frequent. The index number is the quantity of moments N. The quantity of vanishing moments is equivalent to half of the number of coefficients. For instance, D2 has a single vanishing moment (Haar wavelet), and D4 possesses two vanishing moments. Properties: asymmetric, orthogonal, biorthogonal. The transfer functions of the Daubechies wavelet transformation filter family are shown in Figure 3.15 [105].

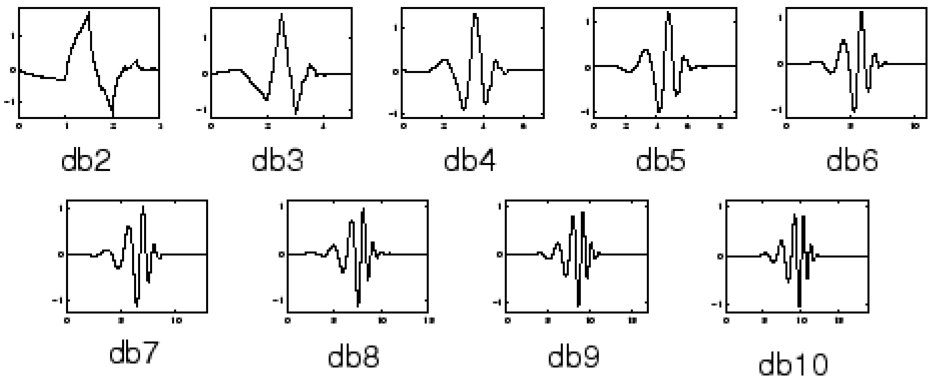

Figure 3.15. The transfer function of the Daubechies wavelet transformation filter family [108].

3.17.3. Symlet Wavelets (symN)

Similarly known as the least-asymmetric wavelets of Daubechies, the symN wavelets are supported very compactly. The symlets are more symmetrical than the wavelets of the extreme phase, which means building symlets like the wavelets of Daubechies is possible, but their symmetry is powerful. In symN, N stands for the quantity of vanishing moments. These filters are sometimes known as the number of filter taps, symbolized as 2N. The transfer function of the Symlet wavelet transformation filter family is shown in Figure 3.16 and properties: near symmetric, orthogonal, biorthogonal [105].

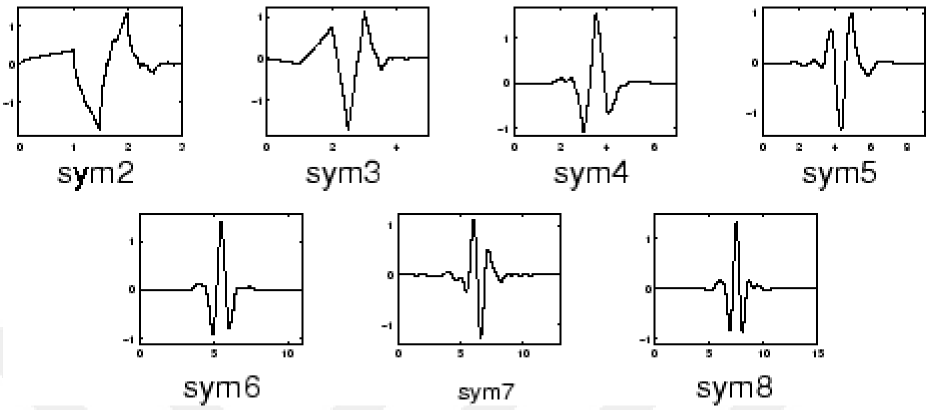

Figure 3.16. The transfer function of the Symlet wavelet transformation filter family [108].

3.17.4. Coiflet Wavelets (coifN)

Coiflet scaling functions are exhibited in vanishing moments and were designed by Ingrid Daubechies and Ronald Coiffman. This family filter is more symmetrical than the mother wavelet of the Daubechies. In coifN, for both wavelet and scaling functions, N stands for the quantity of vanishing moments. Figure 3.17 shows the transfer function of the Coiflet wavelet transformation filter family and properties: near symmetric, orthogonal, biorthogonal [109].

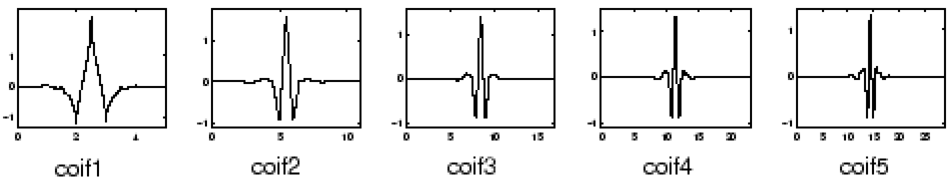

Figure 3.17. The transfer function of the Coiflet wavelet transformation filter family [108].

3.17.5. Biorthogonal Wavelet Pairs (bior Nr.Nd)

The Biorthogonal wavelet attribute has a set of advantages that are linked with scaling filters inclusive of scaling functions. Additionally, it has a set of wavelets and connected wavelet filters, one for analysis and another for synthesis, and there are various quantities of vanishing moments and regularity attributes that existed in analysis and synthesis wavelets, so many vanishing moments are used by wavelet for analysis because of sparse representation. Similarly, the smoother wavelet is used by the wavelet for reconstruction. Biorthogonal systems also allow extra degrees of freedom compared to orthogonal wavelets. These wavelets are a compact wavelet that offers symmetrical wavelet functions. The transfer function of the Biorthogonal wavelet transformation filter family is shown in Figure 3.18 below and properties: symmetric, not orthogonal, biorthogonal [110,111].

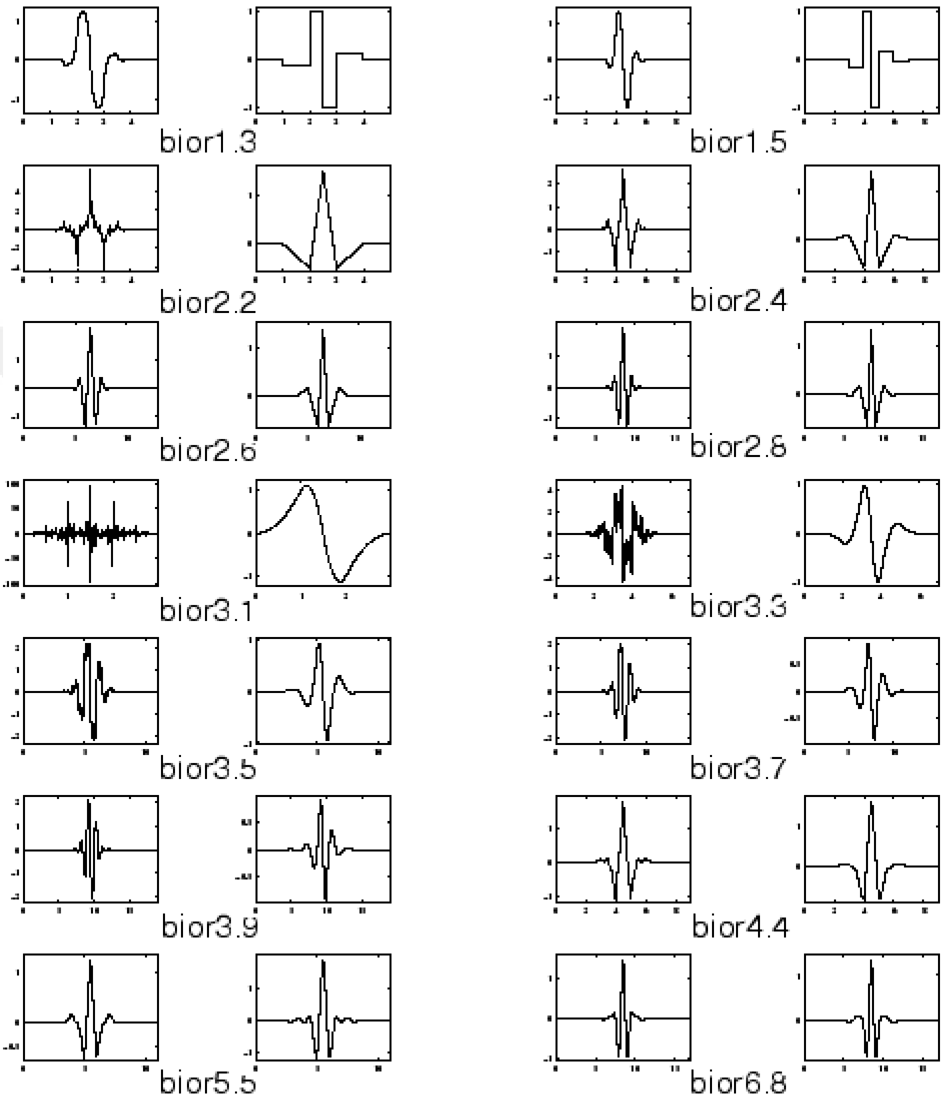

Figure 3.18. The transfer function of the Biorthogonal wavelet transformation filter family [108].

3.17.6. Reverse Biorthogonal Wavelet Pairs (rbioNr.Nd)

This family is acquired by biorthogonal wavelet sets as earlier explained and properties: symmetric, not orthogonal, biorthogonal [110,111].

rbio1.1, rbio1.3, rbio1.5, rbio2.2, rbio2.4, rbio2.6, rbio2.8, rbio3.1, rbio3.3, rbio3.5, rbio3.7, rbio3.9, rbio4.4, rbio5.5, and rbio8.8.

3.18. Metric

The mean-square error (MSE) and the peak signal-to-noise ratio (PSNR) are employed to compare the quality of the picture compression. The MSE represents the cumulative squared error connecting the compressed and the actual picture, while PSNR symbolizes an estimate of the peak error. The error becomes less if the MSE estimate is low. PSNR relies on MSE to calculate the PSNR. The initial block computes the mean-squared error by utilizing Equation 3.29 [112,113].

$$MSE = \frac{1 \sum_{x=1}^{M} \sum_{y=1}^{N} [g(x,y) - f(x,y)]^2}{M\,N} \tag{3.29}$$

Where:

M is the quantity of rows in the input image.

N is the quantity of columns in the input image.

g is an input image (noise picture).

f is an output image (denoising picture).

While the next block computes the PSNR by using Equation 3.30 as below:

$$PSNR = 10\, log_{10}(\frac{R^2}{MSE}) \tag{3.30}$$

R is the greatest fluctuation in the input image data type. The input image contains an 8-bit unsigned integer data type, so R is 255 [114].

4. METHODOLOGY OF PROPOSED SYSTEM

This chapter presents the structure of two-dimensional wavelet transform (WT) with the spatial domain filtering technique, and the proposed method has been explained in seven steps about the denoising image as process steps. Also, all cases of this technique are mentioned in detail (24 cases) and how these cases work, and their applications to denoising the noisy images. At the end of this chapter, the applications and all software tools applied in the proposed method are mentioned. The block diagram of the proposed method is describing the image denoising process which has been shown in Figure 4.1. The additive white Gaussian noise is inserted into all the input images (original images). The proposed method is executing in Twenty-four cases with adding three noise ratios $\sigma = 10$, $\sigma = 15$, and $\sigma = 25$. This type of noisy image implementation undergoes the 2D-WT process with three levels. At the end of the proposed algorithm process, the denoised image was compared with the original image depending on PSNR values. Additionally, filter families in the wavelet domain are applied to know the most frequent family in all cases. According to the proposed algorithm, there are fifteen images in each case at a noise ratio ($\sigma = 10$, $\sigma = 15$, and $\sigma = 25$). The phases of the denoising process are started by selecting an image each time and then selecting one of the three ratios of noise. The three levels of both 2D-DWT and 2D-SWT have been used to generate the nine detail bands (High frequencies bands) and three approximation bands (Low frequencies bands) and select the threshold method to be applied on all the detail bands. After using the threshold technique with the detail bands, modified bands are generated, and these are called the denoised detail bands which will be used with approximation bands to reconstruct the denoised image.

4.1. Process Steps of Proposed Algorithm

In the performed algorithm structure, there are seven crucial steps and five gray images of the same size will take into consideration as an original image named (Cameraman, Lena, Butterfly, Peppers, and Fruits) is shown in Figure 4.2 applied for all cases for the experimentation, the steps are explained in detail as follow:

Step 1: Select any one of the original images as an input image.
Step 2: Three noise ratios (σ=10, σ=15, and σ=25) are added to the original image (input).
Step 3: In this step, there are several processes of the denoising image explained in the proposed algorithm diagrams.

The first process is to apply the spatial filters as a spatial domain technique to eliminate noise from the noisy image (degraded), compute the PSNR value of the denoised image (output), and compare it to the PSNR value of the original image (input). Figure 4.3 explains the process of using the spatial filtering domain to denoising the image only.

The second process is to apply the threshold-based two-dimensional wavelet transform (2D-WT) as a transform domain method to eliminate noise from the noisy image (degraded), compute the PSNR value of the denoised image, and compare it to the PSNR value of the original image. Figure 4.4 explains the process of using the 2D-WT with a select threshold value to denoising the image only.

The third process is to apply the spatial filters as a spatial domain technique before/after performing the threshold-based two-dimensional WT to eliminate noise from the noisy image (degraded), compute the PSNR value of the denoised image, and compare it to the PSNR value of the original image. Figure 4.5, Figure 4.6, Figure 4.7, and Figure 4.8 explain the process of using a combination of the spatial filters with 2D-WT to denoising the image (hybrid method).

The last process is to apply the threshold-based two-dimensional WT as a transform domain method between two spatial filters to eliminate noise from the noisy image (degraded), compute the PSNR value of the denoised image, and compare it to the PSNR value of the original image. Figure 4.9 to Figure 4.11 explains the process of using a combination of the spatial filters twice (before and after) simultaneously applying 2D-WT to denoising the image (hybrid method).

Step 4: Different wavelet transformation filter families such as haar, db, sym, coif, and rbio, among others, are applied to these noisy images (degraded) to decompose them.

Step 5: Three levels of decomposition are performed to this noisy image (which has been mentioned previously).

Step 6: Hard and Soft thresholding techniques (Hard Threshold, Sure Shrink Threshold, Bayesian shrinkage, and Penalized Threshold) performed at each decomposition level of an image for different wavelet transforms. At each level, the value of the threshold is varied.

Step 7: Finally, inverse wavelet transforms (IWT) was performed to obtain a denoised image (output image). The performance of different WT has been compared depending on the PSNR metric.

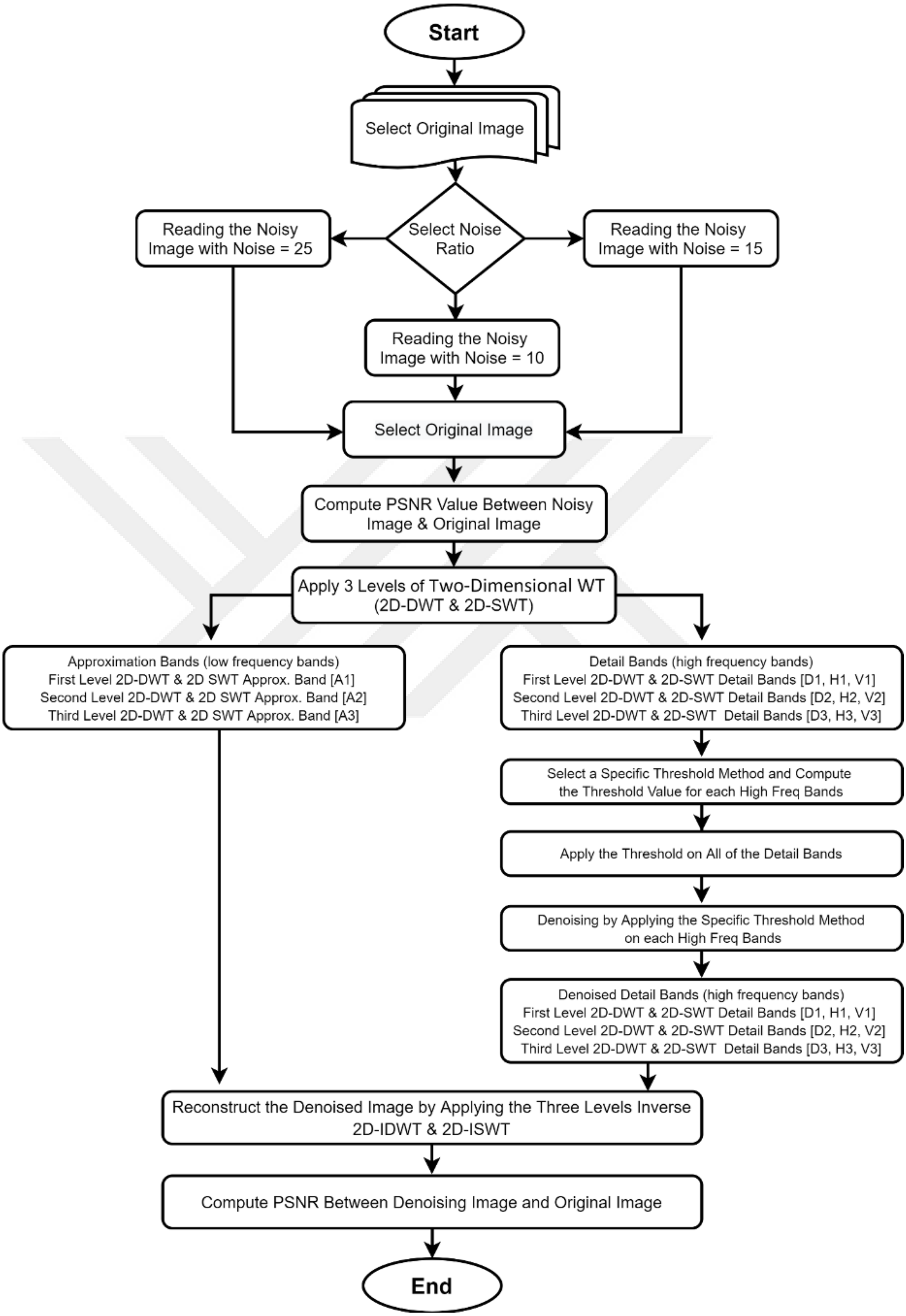

Figure 4.1. The flowchart for Three-level 2D-DWT and 2D-SWT analysis image denoising by the threshold techniques.

The 2D-WT and the spatial domain techniques are applied in image denoising. During the implementation stage, apply WT using all family filters for all the five experimental images with sizes 256 * 256 that is shown in Figure 4.2 (I, II, III, IV, V). The noise type (AWGN) adds to the original experimental images with zero mean (m = 0), with noise ratios σ=10, σ=15, and σ=25.

I. Cameraman II. Lena

III. Butterfly IV. Peppers V. Fruits

Figure 4.2. The test original images used in proposed algorithms.

4.1.1. Proposed Method Cases

In the proposed system, 24 cases have been applied to cover the steps and the sequence for using the threshold-based two-dimensional WT (2D-DWT, 2D-SWT) as a transform domain method through selecting a threshold technique (Hard Threshold, Sure Shrink Threshold, Bayesian shrinkage, and Penalized Threshold) at each threshold process with applied the spatial filters (Wiener filter, Median filter) as a spatial domain filters technique to eliminate noise from the noisy image (degraded). The cases are explained as follow:

Applying spatial domain filtering: In these two cases, both Wiener and Median filters are used separately as a spatial domain filtering technique to eliminate noise from the noisy image (degraded). Figure 4.3 illustrates the process of using only the spatial domain filtering to denoise the image.

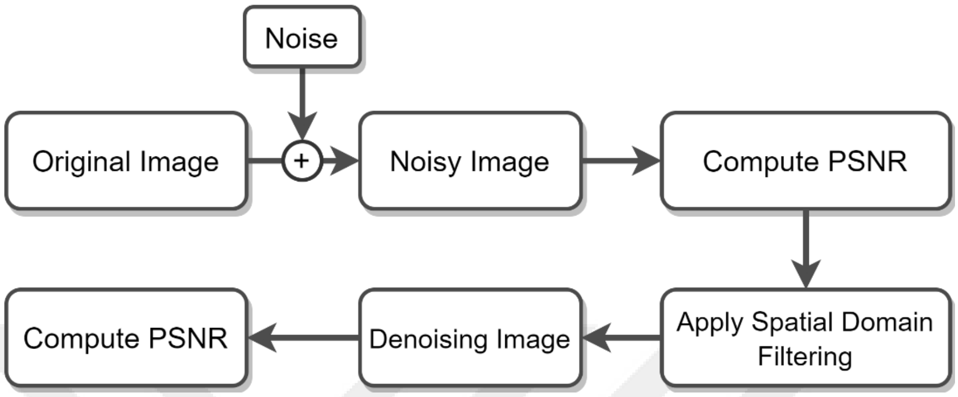

Figure 4.3. Block diagram of spatial domain filtering to denoise the image.

Applying 2D-WT based on threshold technique: Threshold-based WT used for these two cases, both 2D-DWT and 2D-SWT are applied each separately as a wavelet transform domain method with select a threshold technique to eliminate noise from the noisy image (degraded) and then reconstruct denoised image (output) by IWT2 from the approximation and detail coefficients. Figure 4.4 illustrates the process of using the WT domain to denoise the image only.

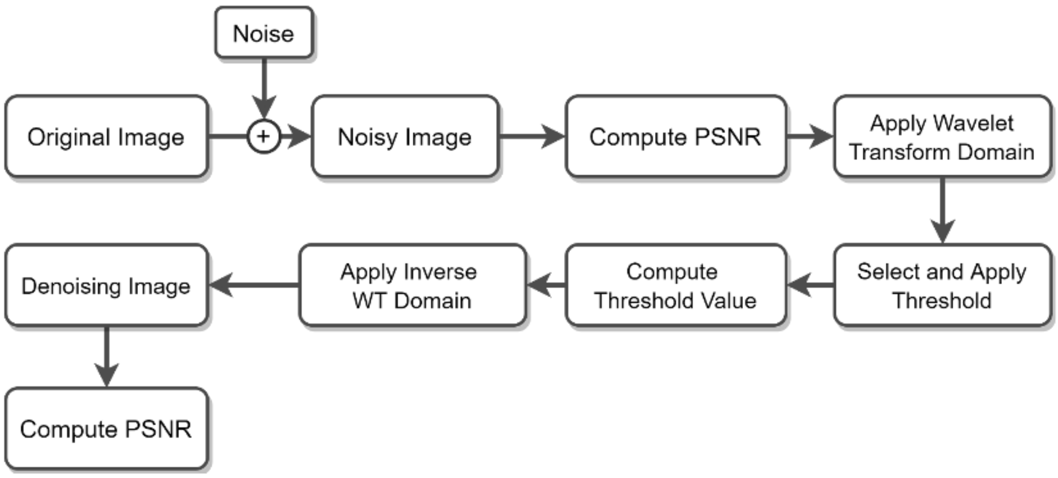

Figure 4.4. Block diagram of WT domain to denoise the image.

Wiener filter before using 2D-WT based on threshold technique: To implement these two cases of the proposed method. The Wiener filter at first applied as a spatial domain technique to the noisy image, and after that, both 2D-DWT and 2D-SWT separately depending on select a threshold technique at each threshold process to eliminate noise from the noisy image (degraded) and the denoised image (output) reconstruct by IWT2 from the approximation and detail coefficients. Figure 4.5 illustrates the process of using the spatial domain with the WT domain to denoise the image (hybrid method).

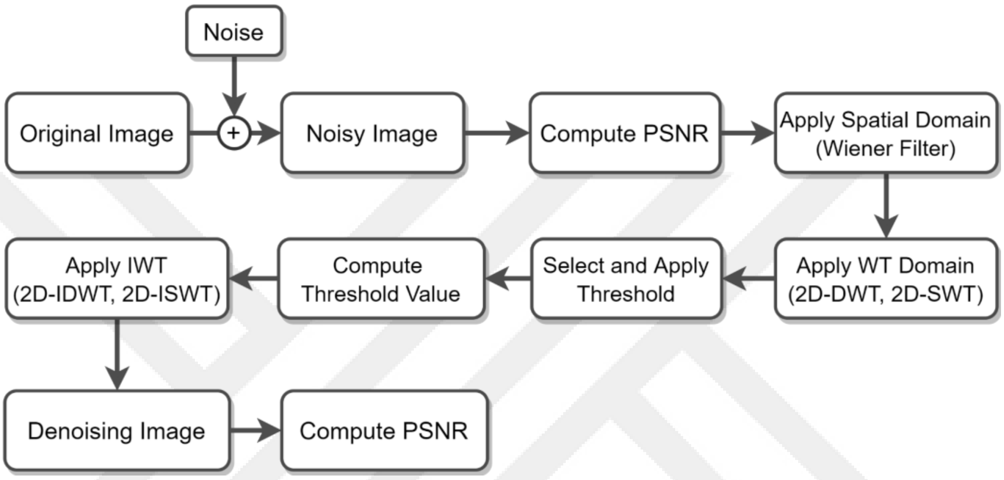

Figure 4.5. Block diagram of the Wiener filter processes before WT domain to denoise the image.

Applying Wiener filter after using 2D-WT based on threshold technique: Through these two cases, both 2D-DWT and 2D-SWT are applied separately as a pre-processing wavelet transform domain method with select a threshold technique at each threshold process to eliminate noise from the noisy image (degraded) and then reconstruct denoised image through IWT2 from the approximation and detail coefficients. Subsequently, the process continued by applying the Wiener filter as a spatial domain technique. Figure 4.6 illustrates the process of using the WT domain with the spatial domain to denoise the image (hybrid method).

Applying Median filter before using 2D-WT based on threshold technique: To obtain a denoising image from the noisy images (degraded) in these two cases. The Median filter is applied as a spatial domain technique to the noisy image before using both 2D-DWT and 2D-SWT each separately as a WT domain method depending on select a threshold technique (Hard Threshold, Sure Shrink Threshold, Bayesian shrinkage, and Penalized Threshold) at each threshold process, and then reconstruct output image by IWT2 from the approximation and detail coefficients. Figure 4.7 illustrates the process of using the spatial domain with the WT domain to denoise the image (hybrid method).

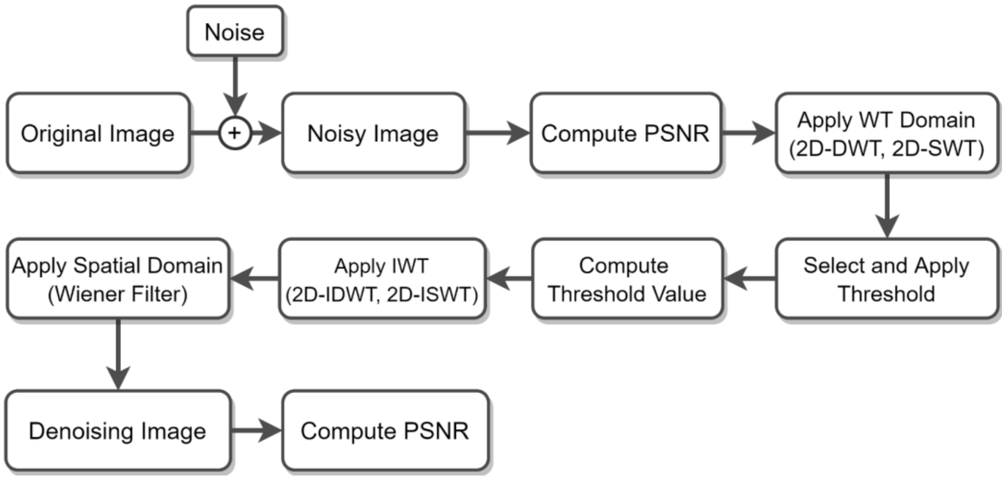

Figure 4.6. Block diagram of the Wiener filter processes after WT domain to denoise the image.

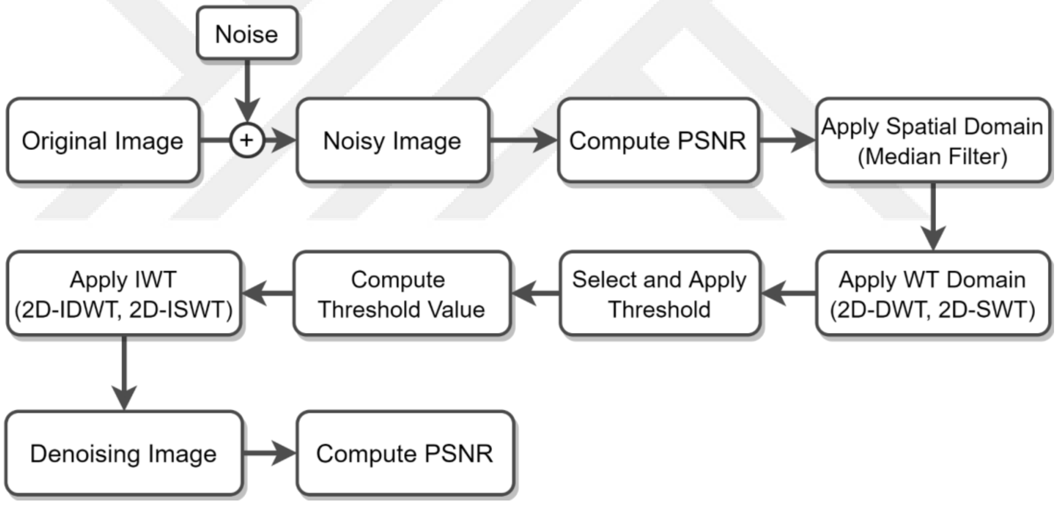

Figure 4.7. Block diagram of the Median filter processes before WT domain to denoise the image.

Applying Median filter after using 2D-WT based on threshold technique: The noisy image is processed in a couple of phases during these two cases. As a first process, the 2D-DWT and 2D-SWT both are applied separately as a pre-processing WT domain method with select a threshold technique (Hard Threshold, Sure Shrink Threshold, Bayesian shrinkage, and Penalized Threshold) at each threshold process to eliminate noise from the degraded image and then reconstruct output image (denoised) through IWT2 from the approximation and detail coefficients. As a second and final process, the Median filter is applied as a spatial domain technique. Figure 4.8 illustrates the process of using the WT domain with the spatial domain to denoise the image (hybrid method).

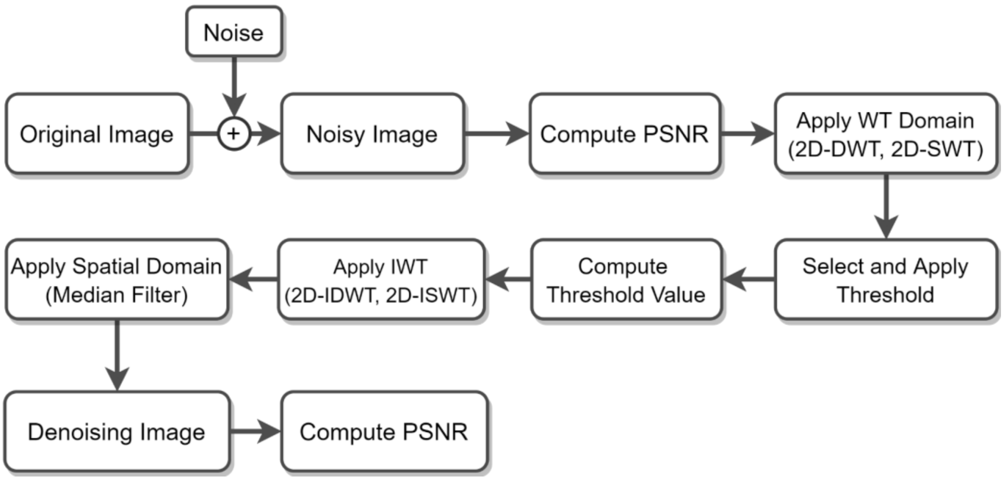

Figure 4.8. Block diagram of the Median filter processes after WT domain to denoise the image.

Applying spatial filters (WF, MF) before using 2D-WT Based on Threshold Technique: To obtain an improved visual quality from the degraded image in these two cases. Both the Wiener filter and then the Median filter as pre-processing spatial domain filters are applied in sequence and together to eliminate noise from the noisy image. Thereafter, the 2D-DWT and 2D-SWT both are applied separately as a WT domain method depending on select a threshold technique at each threshold process, and then reconstruct output image via IWT2 from the approximation and detail coefficients. Figure 4.9 illustrates the process of using the spatial domain with the WT domain to denoise the image (hybrid method).

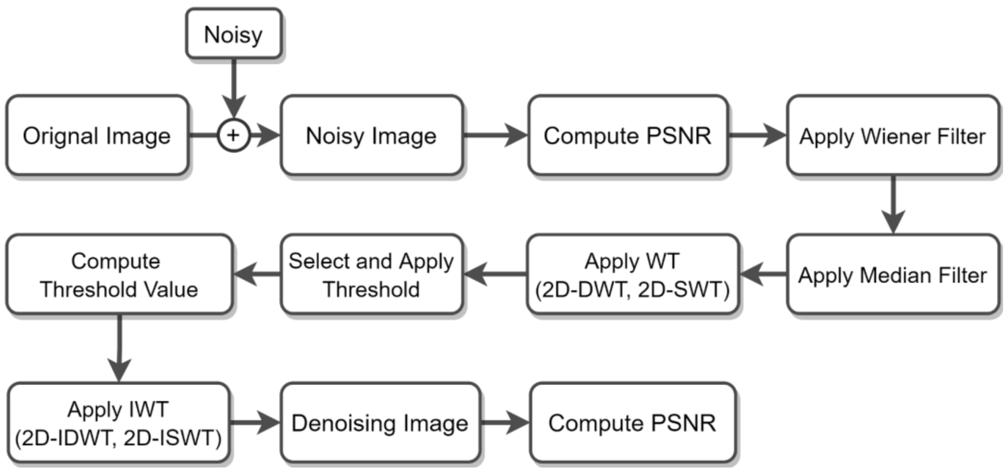

Figure 4.9. Block diagram of the spatial filters (WF, MF) processes before WT domain to denoise the image.

Applying spatial filters (WF, MF) after using 2D-WT Based on Threshold Technique: To perform these two cases, in the first step of the procedure, both 2D-DWT and 2D-SWT are applied each separately as a WT domain method with select a threshold technique at each threshold process, and then reconstruct denoised image by IWT2 from the approximation and detail coefficients. In the second step, the Wiener filter and then the Median filter as spatial filters are applied in sequence and together to eliminate noise from the noisy image (degraded). Figure 4.10 illustrates the process of using the WT domain with spatial domain filtering to denoise the image (hybrid method).

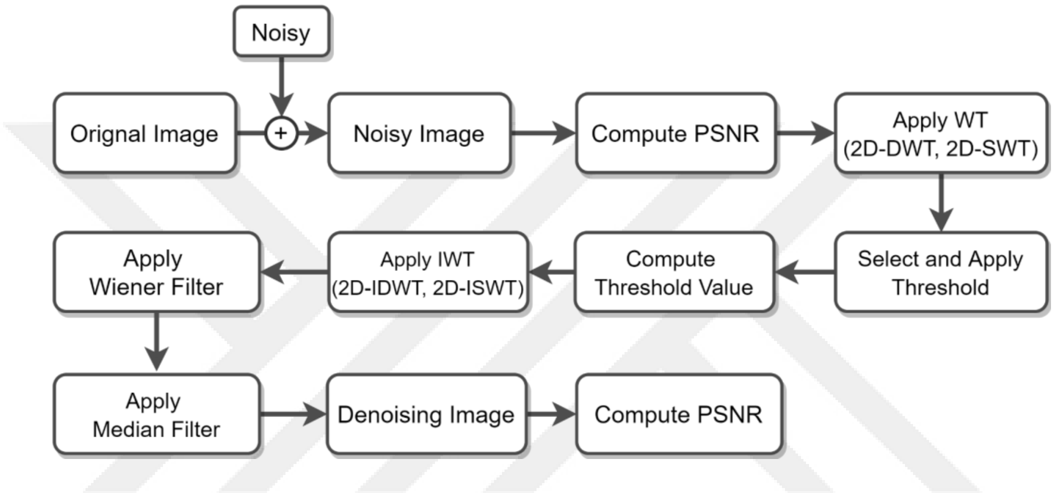

Figure 4.10. Block diagram of the spatial filters (WF, MF) processes after WT domain to denoise the image.

Applying spatial filters (MF, WF) before using 2D-WT Based on Threshold Technique: In these two cases, the Median filter and then the Wiener filter as pre-processing spatial domain filters are applied in sequence and together to eliminate noise from the noisy image to obtain an improved visual quality from the degraded image. Following that, to reconstruct the denoised image by IWT2 from the approximation and detail coefficients, both 2D-DWT and 2D-SWT are applied separately as a WT domain method with select a threshold technique (Hard Threshold, Sure Shrink Threshold, Bayesian shrinkage, and Penalized Threshold) at each threshold process. Figure 4.11 illustrates the process of using the spatial domain with the WT domain to denoise the image (hybrid method).

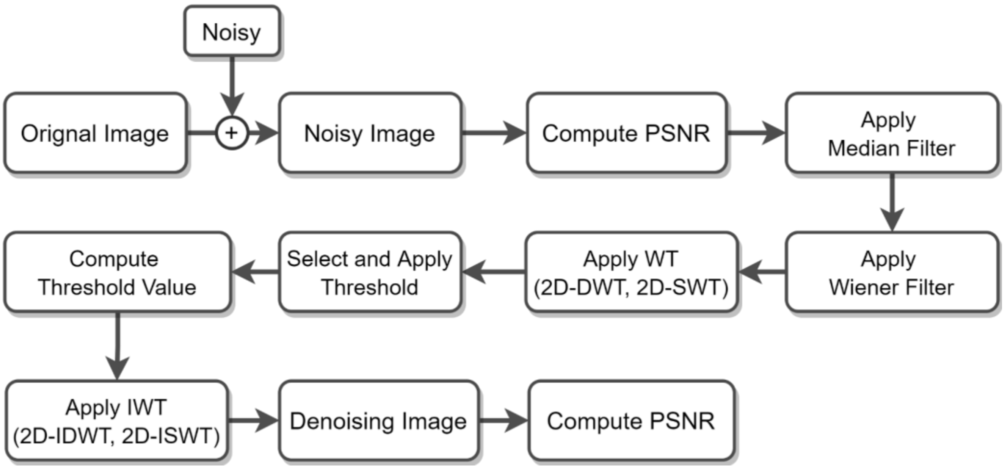

Figure 4.11. Block diagram of the spatial filters (MF, WF) processes before WT domain to denoise the image.

Applying spatial filters (MF, WF) after using 2D-WT Based on Threshold Technique: To achieve these two cases of the proposed method in the first step of the procedure, to reconstruct the denoised image by IWT2 from the approximation and detail coefficients. Both 2D-DWT and 2D-SWT are applied separately as a WT domain method with select a threshold technique (Hard Threshold, Sure Shrink Threshold, Bayesian shrinkage, and Penalized Threshold) at each threshold process. In the second step, the Median filter and then the Wiener filter as spatial filters are applied in sequence and together to eliminate noise from the noisy image (degraded). Figure 4.12 illustrates the process of using the WT domain with spatial domain filtering to denoise the image (hybrid method).

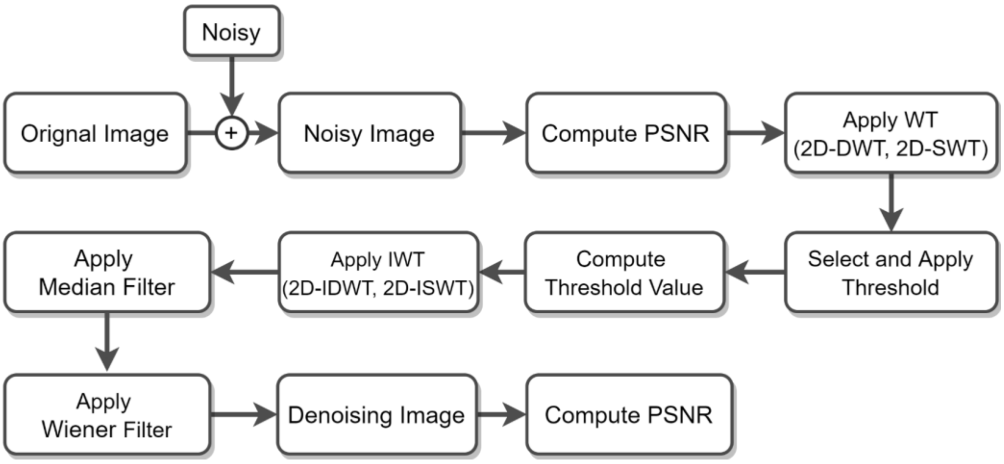

Figure 4.12. Block diagram of the spatial filters (MF, WF) processes after WT domain to denoise the image.

Applying 2D-WT based on threshold technique between using two spatial domain filters (WF and MF): The noise removal stages of the degraded images will pass through three sequential processes in these two cases. The first process is to apply the Wiener filter as a spatial domain technique, while the second process used both threshold-based 2D-DWT and 2D-SWT separately as a transform domain method with select a threshold technique (Hard Threshold, Sure Shrink Threshold, Bayesian shrinkage, and Penalized Threshold) at each threshold process. Then the Median filter is applied as the final process. Figure 4.13 illustrates the process of using the WT domain between two spatial domain filters to denoise the image (hybrid method).

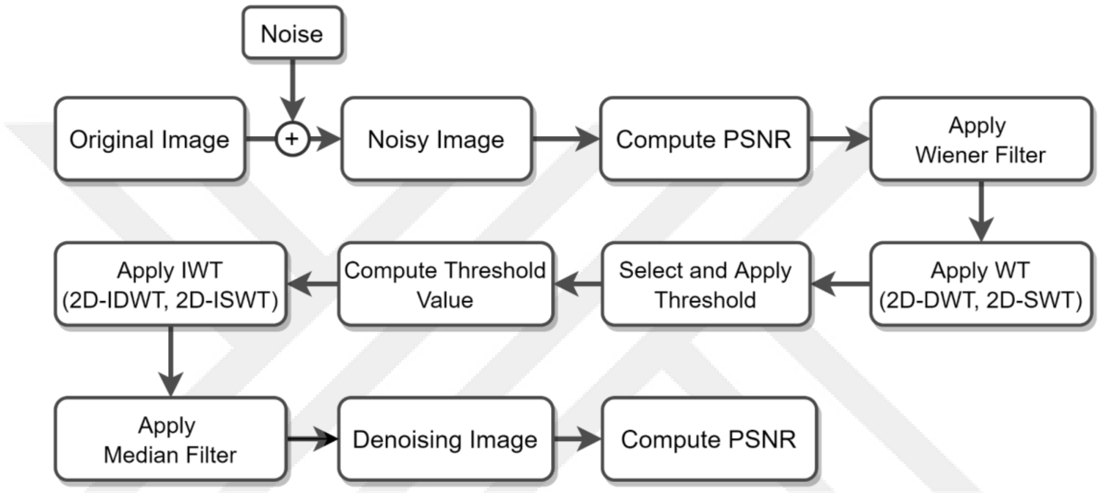

Figure 4.13. Block diagram of the threshold-based 2D-WT between processes two spatial domain filters (WF and MF) to denoise the image.

Applying 2D-WT based on threshold technique between using two spatial domain filters (MF and WF): The last two cases of the proposed method, also like the above case, but the difference is in the change location of the spatial filters when addressing the noisy image. The Median filter is used as a pre-processing technique. Then both threshold-based 2D-DWT and 2D-DWT are applied separately as a WT domain method depending on select a threshold technique. Finally, as a spatial domain technique to eliminate noise from the noisy image (degraded) and to obtain the denoised image, the Wiener filter is applied. Figure 4.14 illustrates the process of using the WT domain between two spatial domain filters to denoise the image (hybrid method).

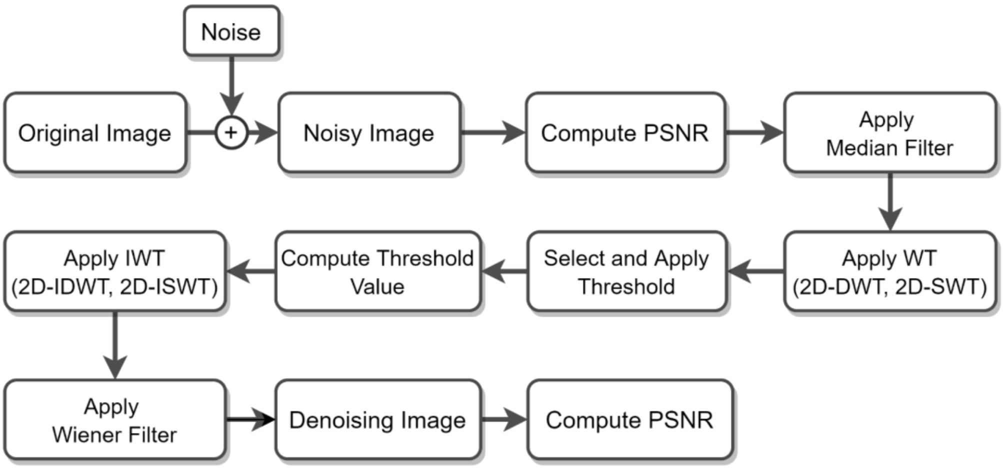

Figure 4.14. Block diagram of the threshold-based 2D-WT between processes two spatial domain filters (WF and MF) to denoise the image.

There are 126 types of WT family filters that were used and stored for each case, depending on PSNR value as shown in APPENDICES. For all cases, the PNSR value of the denoising image was computed and compared with the PSNR value of the noisy image and stored. The whole process of all cases mentioned before is explained in Table 4.1.

To evaluate the performance of the proposed image denoising algorithm, a Matlab technical programming language version R2020a was used for writing an image denoising program with the help of the application Microsoft Excel version 2019. The 24 cases that have been applied to the program depend on the seven previous steps, while the results have been saved as a list of figures and tabulated as tables and depicted in charts.

Table 4.1. All Cases Applied in the Proposed System

No	Case	Description (Domain)
1	Wiener Filter (WF)	Spatial domain
2	Median Filter (MF)	Spatial domain
3	2D-DWT	2D wavelet transform domain
4	2D-SWT	2D stationary transform domain
5	WF_2D-DWT	Wiener Filter with 2D-DWT domain
6	WF_2D-SWT	Wiener Filter with 2D-SWT domain
7	2D-DWT_WF	2D-DWT domain with Wiener Filter
8	2D-SWT_WF	2D-SWT domain with Wiener Filter
9	MF_2D-DWT	Median Filter with 2D-DWT domain
10	MF_2D-SWT	Median Filter with 2D-SWT domain
11	2D-DWT_MF	2D-DWT domain with Median Filter
12	2D-SWT_MF	2D-SWT domain with Median Filter
13	WF_MF_2D-DWT	Wiener and Median Filter with 2D-DWT domain
14	WF_MF_2D-SWT	Wiener and Median Filter with 2D-SWT domain
15	2D-DWT_WF_MF	2D-DWT domain with Wiener and Median Filter
16	2D-SWT_WF_MF	2D-SWT domain with Wiener and Median Filter
17	MF_WF_2D-DWT	Median and Wiener Filter with 2D-DWT domain
18	MF_WF_2D-SWT	Median and Wiener Filter with 2D-SWT domain
19	2D-DWT_MF_WF	2D-DWT domain with Median and Wiener Filter
20	2D-SWT_MF_WF	2D-SWT domain with Median and Wiener Filter
21	WF_2D-DWT_MF	Wiener Filter with 2D-DWT domain and Median
22	WF_2D-SWT_MF	Wiener Filter with 2D-SWT domain and Median
23	MF_2D-DWT_WF	Median Filter with 2D-DWT domain and Wiener
24	MF_2D-SWT_WF	Median Filter with 2D-SWT domain and Wiener

5. IMPLEMENTATIONS AND RESULTS OF PROPOSED METHOD

This chapter presents the implementation of an image denoising system that attempts to solve the problem of additive noise in digital images. Following that, the chapter presents the implementation and discusses the experiential results of applying the Spatial domain filters (Wiener filter and Median filter) as a level of image denoising system while applying 2D- WT (DWT and SWT) by using several various types of threshold techniques (hard and soft) for five different images. Moreover, the evaluation of the method and comparison with previous works also are presented in this chapter.

5.1. Implementations and Results Analysis of Proposed Algorithm Method

The performance analysis of proposed algorithm structures that have been generated in chapter four will be implemented in this chapter through determining and analyzing the output results. There are five gray images of the same size with three ratios of noise (σ=10, σ=15, and σ=25) were applied to the proposed method which is implementing, analyzing, and evaluating individually.

5.1.1. Implementation and Results Analysis of Cameraman Image

After implementing the process steps of the proposed algorithm methods on the Cameraman image, the experimental performance results are shown in Table 5.1. The three levels of noise ratios (σ=10, σ=15, and σ=25) were added to the original image (input), at σ=10 PSNR value of noisy image = 28.8721, PSNR value with Median filter = 25.3431, and PSNR value outcome with Wiener filter = 28.2313. While at σ=15, the result of the PSNR value of noisy image = 24.5420, PSNR value with Median filter = 24.7423, and PSNR value with Wiener filter = 27.2401. Finally, at σ=25 PSNR value outcome of noisy image = 20.0792, PSNR value with Median filter = 23.4400, and PSNR value with Wiener filter = 25.2783.

Table 5.1. The best PSNR values of the Cameraman image for image denoising process steps with all the used threshold cases, for noise ratios σ = 10, σ = 15 and = 25.

Noise Ratio	Threshold Cases	PSNR	2D-WT	W-WT-M	M-WT-W	W-M-WT	M-W-WT	WT-W-M	WT-M-W	W-WT	M-WT	WT-W	WT-M
σ=10	Hard	2D-SWT	29.2974	24.7765	24.4518	24.7765	24.4511	24.7822	24.4582	28.2314	25.3472	28.2363	25.3565
		2D-DWT	28.9104	24.7765	24.4517	24.7765	24.4511	24.7815	24.4561	28.2314	25.3434	28.2347	25.3531
σ=10	Sure Shrink	2D-SWT	**31.6320**	24.8246	24.4048	24.7804	24.4569	24.8240	24.5398	28.2666	25.4089	27.8765	25.6384
		2D-DWT	29.9968	24.5744	24.0901	24.5708	24.2574	24.3697	24.0730	27.8115	25.0787	27.0977	25.0539
σ=10	Bayes Shrink	2D-SWT	30.1508	24.7765	24.4511	24.7765	24.4511	24.8260	24.4998	28.2314	25.3589	28.2340	25.5290
		2D-DWT	29.8089	24.7765	24.4513	24.7767	24.4513	24.7611	24.4352	28.2316	25.3497	28.1988	25.3956
σ=10	Penalized	2D-SWT	29.7640	25.6180	27.5037	29.7640	29.7640	24.7847	24.4917	29.7640	29.7640	27.5062	25.6180
		2D-DWT	29.7640	25.6180	27.5037	29.7640	29.7640	24.7847	24.4917	29.7640	29.7640	27.5062	25.6180
σ=15	Hard	2D-SWT	25.9470	24.4643	24.1668	24.4637	24.1628	24.4816	24.1777	27.2410	24.7720	27.2847	24.8118
		2D-DWT	24.8652	24.4636	24.1641	24.4636	24.1628	24.4795	24.1751	27.2401	24.7448	27.2609	24.8183
σ=15	Sure Shrink	2D-SWT	**28.6777**	24.5273	24.1159	24.4657	24.1691	24.5338	24.2520	27.3610	24.9251	26.9608	25.1718
		2D-DWT	27.4317	24.2761	23.7831	24.2462	23.9737	23.9338	23.6531	26.9608	24.6222	25.9966	24.5694
σ=15	Bayes Shrink	2D-SWT	27.5992	24.4636	24.1639	24.4636	24.1628	24.5574	24.2514	27.2404	24.7844	27.3247	25.1288
		2D-DWT	26.7897	24.4637	24.1584	24.4638	24.1629	24.4733	24.1697	27.2402	24.7844	27.2570	24.9681
σ=15	Penalized	2D-SWT	26.6720	25.0527	26.1786	26.6720	26.6720	24.4153	24.1581	26.6720	26.6720	26.1828	25.0527
		2D-DWT	26.6720	25.0527	26.1786	26.6720	26.6720	24.4153	24.1581	26.6720	26.6720	26.1828	25.0527
σ=25	Hard	2D-SWT	22.9093	23.7510	23.5989	23.7476	23.5949	23.8132	23.6439	25.2800	23.5425	25.4381	23.8040
		2D-DWT	21.2831	23.7476	23.5977	23.7475	23.5948	23.7858	23.6249	25.2785	23.4497	25.3628	23.7074
σ=25	Sure Shrink	2D-SWT	**25.7784**	23.8318	23.5575	23.7543	23.6139	23.8935	23.6963	25.5369	23.9978	25.2599	24.2467
		2D-DWT	24.8839	23.5265	23.1741	23.4606	23.3592	23.2394	23.0208	25.0784	23.7205	24.4025	23.6220
σ=25	Bayes Shrink	2D-SWT	24.4595	23.7509	23.6062	23.7479	23.5951	23.9391	23.7519	25.2880	23.5538	25.6226	24.1312
		2D-DWT	23.8250	23.7501	23.5991	23.7481	23.5987	23.8410	23.6320	25.2894	23.5867	25.4673	24.0097
σ=25	Penalized	2D-SWT	23.6640	23.8848	24.5706	23.6640	23.6640	23.6997	23.5377	23.6640	23.6640	24.5832	23.8848
		2D-DWT	23.6640	23.8848	24.5706	23.6640	23.6640	23.6997	23.5367	23.6640	23.6640	24.5832	23.8848

The best process steps result of the cameraman image is detected when applying 2D-SWT based on the Sure Shrink threshold technique referred to in the Figure 4.4 scheme of chapter four (Methodology of Proposed System) with selected Haar, Biorthogonal, and Reverse biorthogonal Wavelet Filters Families (db1, bior1.1, and rbio1.1), which has a better PSNR value compared to the other cases (process steps) at the noise ratio σ=10. However, by using noise ratio σ=15, the best result of this image is determined in the Figure 4.4 scheme also by applying 2D-SWT based on the Sure Shrink threshold technique with selected Haar, Biorthogonal, and Reverse biorthogonal Wavelet Families (db1, bior1.1, and rbio1.1).

While the more accurate and efficient result value of PSNR is indicated in comparison with other cases with noise ratio σ = 25 when applying 2D-SWT based on the Sure Shrink threshold technique referred to in the Figure 4.4 diagram with selected Haar, Biorthogonal, and Reverse biorthogonal Wavelet Families (db1, bior1.1, and rbio1.1).

The charts in Figures 5.1, 5.2, and 5.3 show the comparison of all cases (process steps) between the PSNR value of the noisy image and the denoising image of each threshold technique function and noise ratio separately based on Table 5.1. While Figures 5.4, 5.5, and 5.6 show outcome images for each case.

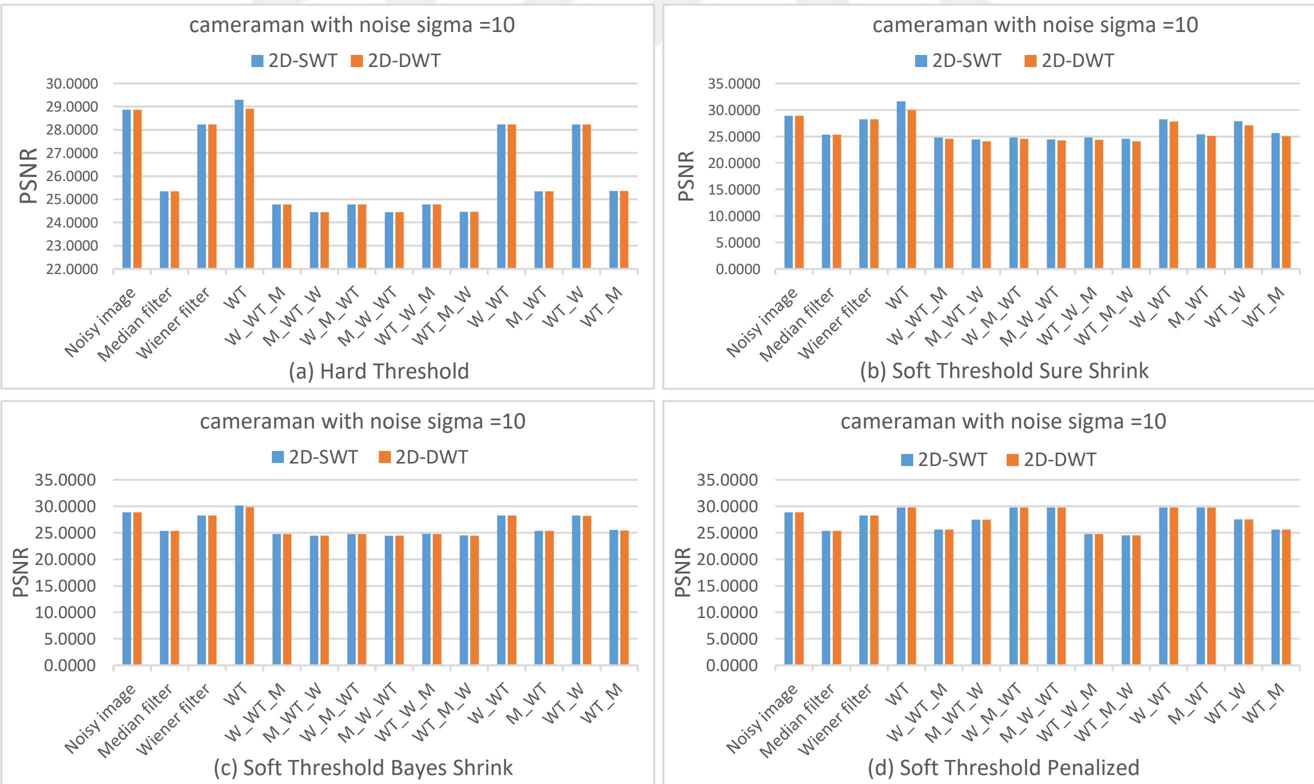

Figure 5.1. PSNR values of the comparison between process steps with (a) Hard, (b) Sure Shrink, (c) Bayes Shrink, and (d) Penalized threshold technics used, for Cameraman image, with noise σ=10.

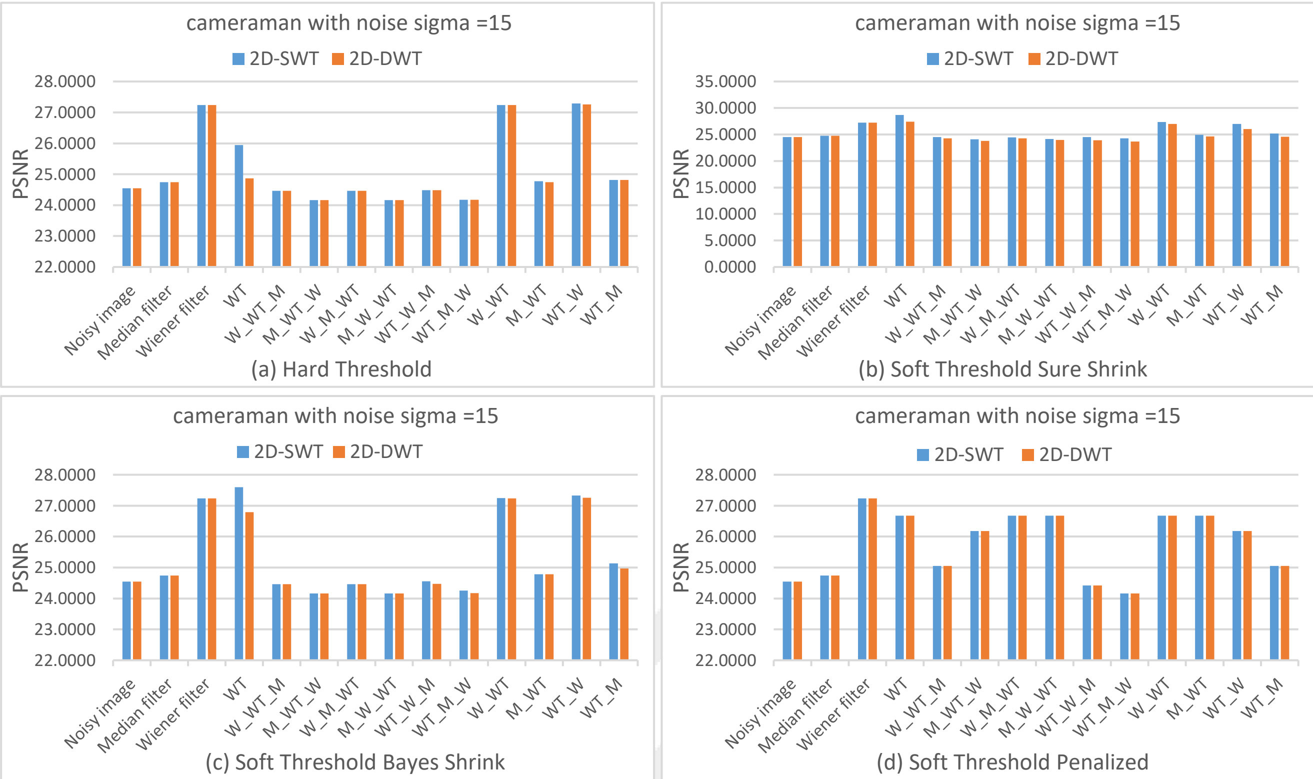

Figure 5.2. PSNR values of the comparison between process steps with (a) Hard, (b) Sure Shrink, (c) Bayes Shrink, and (d) Penalized threshold technics used, for Cameraman image, with noise σ=15.

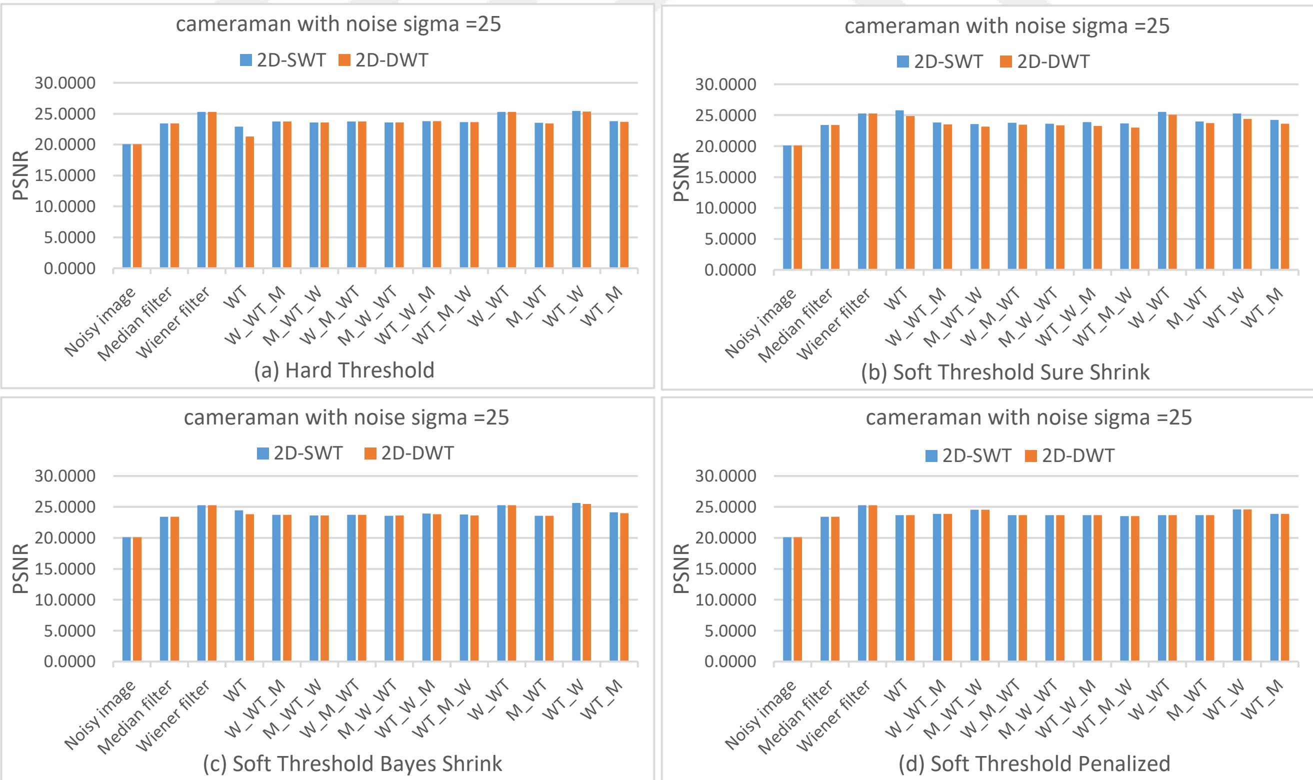

Figure 5.3. PSNR values of the comparison between process steps with (a) Hard, (b) Sure Shrink, (c) Bayes Shrink, and (d) Penalized threshold technics used, for Cameraman image, with noise σ=25.

(I) Original image.

(II) Noisy image.

(III) Denoised by Hard Threshold in DWT.

(IV) Denoised by Hard Threshold in SWT.

(V) Denoised by Sure Shrink in DWT.

(VI) Denoised Sure Shrink in SWT.

(VII) Denoised by Bayes Shrink in DWT.

(VIII) Denoised by Bayes Shrink in SWT.

(IX) Denoised by Penalized in DWT.

(X) Denoised by Penalized in SWT.

(XI) Denoised by Median Filter.

(XII) Denoised by Wiener Filter.

Figure 5.4. Cameraman image with noise ratio σ =10.

(I) Original image.

(II) Noisy image.

(III) Denoised by Hard Threshold in DWT-W.

(IV) Denoised by Hard Threshold in SWT-W..

(V) Denoised by Sure Shrink in DWT.

(VI) Denoised Sure Shrink in SWT.

(VII) Denoised by Bayes Shrink in DWT-W.

(VIII) Denoised by Bayes Shrink in SWT.

(IX) Denoised by Penalized in DWT.

(X) Denoised by Penalized in SWT.

(XI) Denoised by Median Filter.

(XII) Denoised by Wiener Filter.

Figure 5.5. Cameraman image with noise ratio σ =15.

(I) Original image.

(II) Noisy image.

(III) Denoised by Hard Threshold in DWT-W.

(IV) Denoised by Hard Threshold in SWT-W.

(V) Denoised by Sure Shrink in DWT.

(VI) Denoised Sure Shrink in SWT.

(VII) Denoised by Bayes Shrink in DWT-W.

(VIII) Denoised by Bayes Shrink in SWT-W.

(IX) Denoised by Penalized in DWT-W.

(X) Denoised by Penalized in SWT-W.

(XI) Denoised by Median Filter.

(XII) Denoised by Wiener Filter.

Figure 5.6. Cameraman image with noise ratio σ =25.

5.1.2. Implementation and Results Analysis of Lena Image

The experimental performance results are shown in Table 5.2 after applying the proposed algorithm methods' process steps on the Lena image. The three noise ratio levels (σ=10, σ=15, and σ=25) were added to the input image (original). Found that at σ=10, the PSNR value of the noisy image equal to 28.6040, the PSNR value with Median filter equal to 27.7612, and the PSNR value outcome with Wiener filter equal to 29.2112. While at σ=15, the PSNR value of the noisy image is equivalent to 24.0875, the PSNR value with Median filter is 26.6700, and the PSNR value resulting from the Wiener filter formula 28.0880. Finally, at σ=25, the outcome of the PSNR value of the noisy image is equivalent to 19.6911, PSNR value with Median filter equal to 24.7255, and PSNR value with Wiener filter equal to 26.2223.

When using 2D-SWT with selected Coiflets Wavelet Filters Families (coif1), the best process steps resulting from the Lena image is observed by using the Sure Shrink threshold technique referred to in the Figure 4.4 diagram of chapter four (Methodology of Proposed System), which has a better PSNR value than the other cases (process steps) at the noise ratio =10.

While by using a noise ratio of σ=15 and applying 2D-SWT adopting the Sure Shrink threshold technique with selected Haar, Biorthogonal, and Reverse biorthogonal Wavelet Families, the improved result of this image is obtained in the Figure 4.4 scheme (db1, bior1.1, and rbio1.1). In contrast, the more accurate and efficient result value of PSNR is indicated compared to other cases with noise ratio σ = 25 when applying Wiener filter after using 2D-SWT dependent on the Bayes Shrink threshold technique referred to in the Figure 4.6 diagram with selected Reverse biorthogonal Wavelet Filters (rbio6.8).

The charts in Figures 5.7, 5.8, and 5.9 show the comparison of all cases (process steps) between the PSNR value of the noisy image (degraded) and the denoising image of each threshold technique function and noise ratio separately based on Table 5.2. While Figures 5.10, 5.11, and 5.12 show outcome images for each case.

Table 5.2. The best PSNR values of the Lena image for image denoising process steps with all the used threshold cases, for noise ratios σ = 10, σ = 15 and = 25.

Noise Ratio	Threshold Cases	PSNR	2D-WT	W-WT-M	M-WT-W	W-M-WT	M-W-WT	WT-W-M	WT-M-W	W-WT	M-WT	WT-W	WT-M
σ=10	Hard	2D-SWT	29.2483	26.9728	26.4992	26.9728	26.4924	26.9828	26.5003	29.2113	27.7792	29.2230	27.7812
		2D-DWT	28.6462	26.9727	26.4931	26.9727	26.4923	26.9783	26.5001	29.2113	27.7634	29.2168	27.7819
σ=10	Sure Shrink	2D-SWT	**31.8136**	27.0433	26.4462	26.9697	26.4985	27.0068	26.6049	29.2269	27.9007	28.8536	28.1855
		2D-DWT	30.2428	26.5019	25.9284	26.4809	26.0239	26.2910	25.9038	28.4413	27.1322	27.7744	27.1731
σ=10	Bayes Shrink	2D-SWT	30.2991	26.9728	26.4925	26.9727	26.4924	27.0131	26.5411	29.2113	27.7764	29.2094	27.9832
		2D-DWT	29.5979	26.9722	26.4639	26.9727	26.4923	26.9017	26.4283	29.2108	27.7693	29.0844	27.8025
σ=10	Penalized	2D-SWT	30.2110	28.1963	28.3987	30.2110	30.2110	26.9598	26.6187	30.2110	30.2110	28.3998	28.1963
		2D-DWT	30.2110	28.1963	28.3987	30.2110	30.2110	26.9598	26.6187	30.2110	30.2110	28.3998	28.1963
σ=15	Hard	2D-SWT	26.4646	26.5462	26.1133	26.5458	26.0963	26.5813	26.1319	28.0888	26.7338	28.1597	26.8829
		2D-DWT	24.8000	26.5459	26.0994	26.5458	26.0962	26.5691	26.1301	28.0884	26.6799	28.1226	26.8610
σ=15	Sure Shrink	2D-SWT	**29.2087**	26.6424	26.0643	26.5547	26.1154	26.6905	26.3817	28.2194	27.0592	27.8434	27.5327
		2D-DWT	28.0506	26.1246	25.4724	26.0991	25.6589	25.7833	25.4867	27.5688	26.4679	26.7481	26.6781
σ=15	Bayes Shrink	2D-SWT	28.1867	26.5457	26.0986	26.5457	26.0962	26.6827	26.2972	28.0884	26.7392	28.2057	27.3974
		2D-DWT	27.2681	26.5422	26.0706	26.5459	26.0962	26.5142	26.1085	28.0855	26.7384	28.0314	27.1468
σ=15	Penalized	2D-SWT	27.2324	27.3475	27.2861	27.2324	27.2324	26.5490	26.3142	27.2324	27.2324	27.2857	27.3475
		2D-DWT	27.2324	27.3476	27.2861	27.2324	27.2324	26.5490	26.3141	27.2324	27.2324	27.2857	27.3476
σ=25	Hard	2D-SWT	23.4398	25.6286	25.3205	25.6263	25.2987	25.7402	25.4027	26.2315	24.8947	26.3917	25.5142
		2D-DWT	21.6185	25.6279	25.3025	25.6258	25.2984	25.6809	25.3698	26.2245	24.7459	26.3047	25.3158
σ=25	Sure Shrink	2D-SWT	26.6922	25.7535	25.2938	25.6502	25.3378	25.8948	25.7143	26.5287	25.6019	26.3790	26.1579
		2D-DWT	25.9444	25.2331	24.6815	25.1452	24.8948	24.9172	24.7665	25.9600	25.2597	25.3233	25.5499
σ=25	Bayes Shrink	2D-SWT	25.5255	25.6289	25.3102	25.6256	25.2984	25.9382	25.6908	26.2438	24.8858	**26.6966**	25.9988
		2D-DWT	24.9855	25.6290	25.2893	25.6274	25.3032	25.7110	25.4249	26.2390	24.9881	26.4309	25.8833
σ=25	Penalized	2D-SWT	24.3895	25.7781	26.1465	24.3895	24.3895	25.8235	25.6700	24.3895	24.3895	26.1480	25.7781
		2D-DWT	24.3895	25.7781	26.1465	24.3895	24.3895	25.8235	25.6700	24.3895	24.3895	26.1481	25.7781

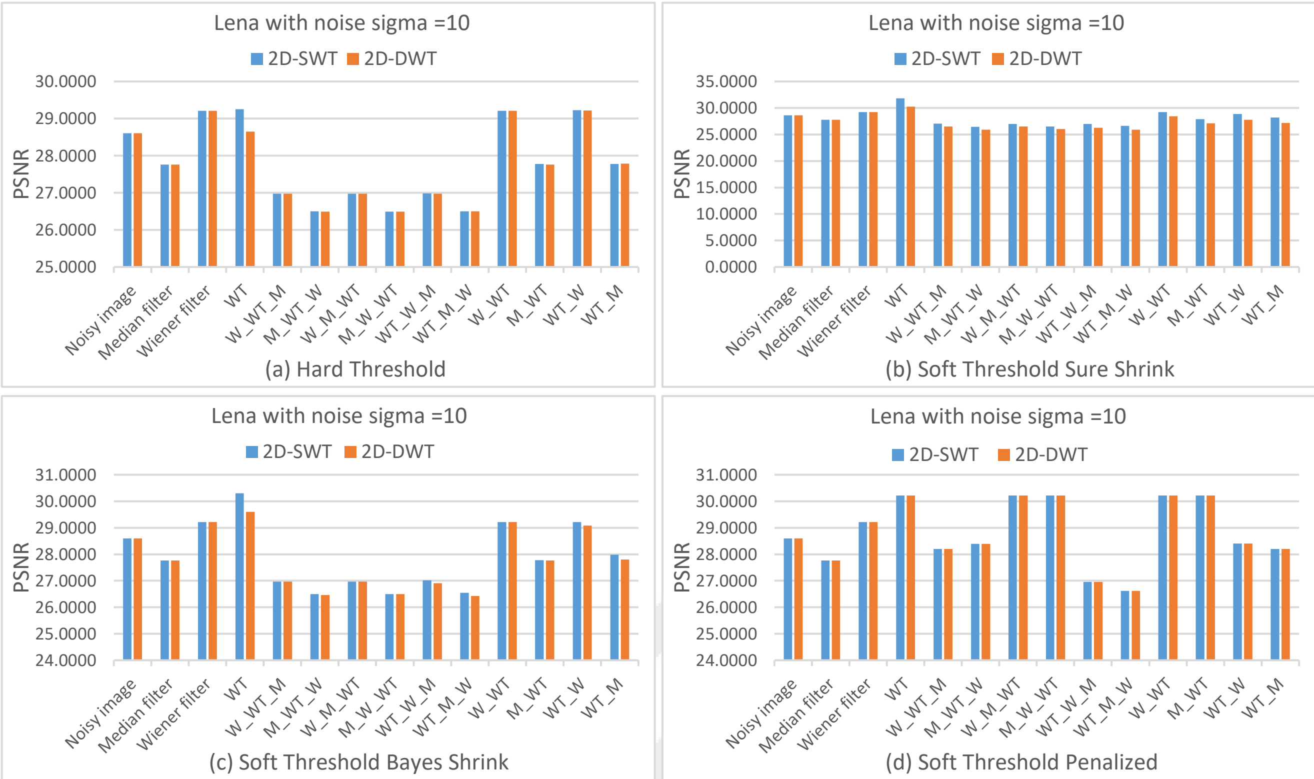

Figure 5.7. PSNR values of the comparison between process steps with (a) Hard, (b) Sure Shrink, (c) Bayes Shrink, and (d) Penalized threshold technics used, for Lena image, with noise σ=10.

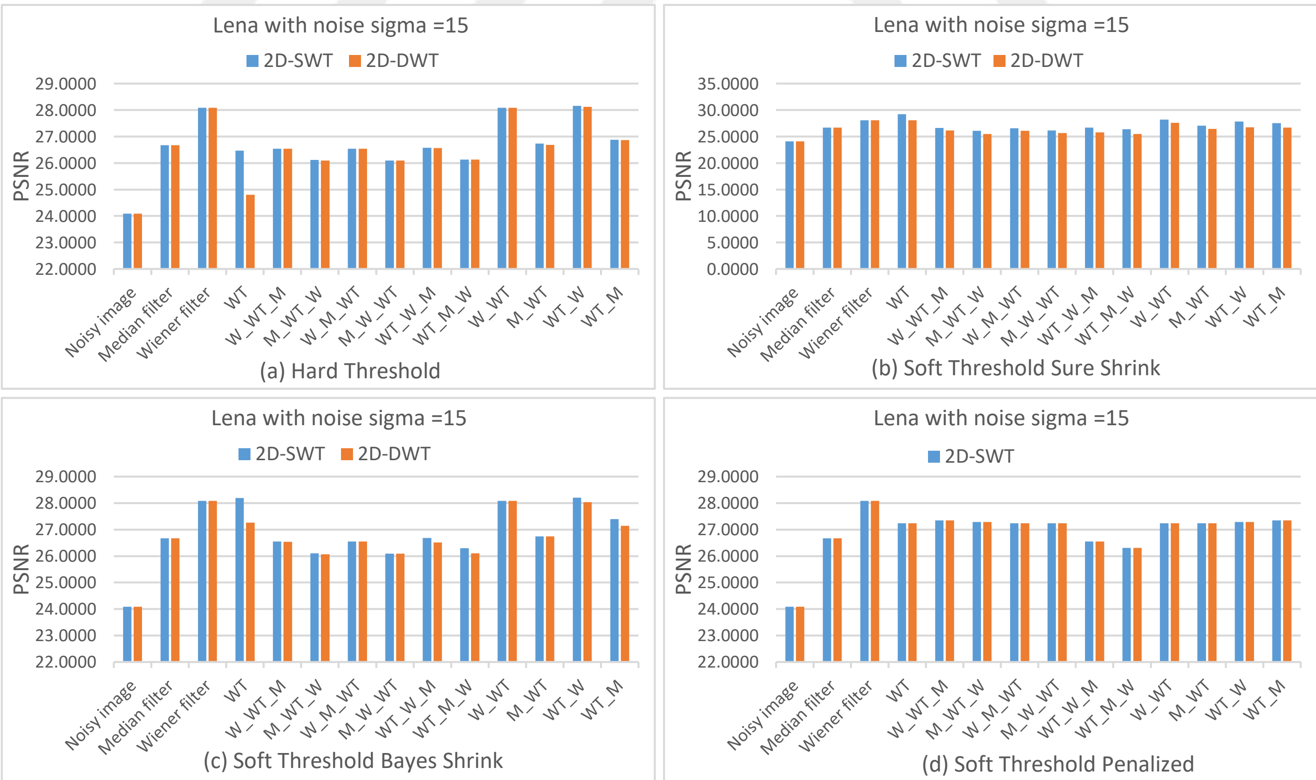

Figure 5.8. PSNR values of the comparison between process steps with (a) Hard, (b) Sure Shrink, (c) Bayes Shrink, and (d) Penalized threshold technics used, for Lena image, with noise σ=15.

Figure 5.9. PSNR values of the comparison between process steps with (a) Hard, (b) Sure Shrink, (c) Bayes Shrink, and (d) Penalized threshold technics used, for Lena image, with noise σ=25.

(I) Original image.

(II) Noisy image.

(III) Denoised by Hard Threshold in DWT-W.

(IV) Denoised by Hard Threshold in SWT.

(V) Denoised by Sure Shrink in DWT.

(VI) Denoised Sure Shrink in SWT.

(VII) Denoised by Bayes Shrink in DWT.

(VIII) Denoised by Bayes Shrink in SWT.

(IX) Denoised by Penalized in DWT.

(X) Denoised by Penalized in SWT.

(XI) Denoised by Median Filter.

(XII) Denoised by Wiener Filter.

Figure 5.10. Lena image with noise ratio σ =10.


(I) Original image.


(II) Noisy image.


(III) Denoised by Hard Threshold in DWT-W.


(IV) Denoised by Hard Threshold in SWT-W.


(V) Denoised by Sure Shrink in DWT.


(VI) Denoised Sure Shrink in SWT.


(VII) Denoised by Bayes Shrink in DWT-W.


(VIII) Denoised by Bayes Shrink in SWT-W.


(IX) Denoised by Penalized in DWT-M.


(X) Denoised by Penalized in SWT-M.


(XI) Denoised by Median Filter.


(XII) Denoised by Wiener Filter.

Figure 5.11. Lena image with noise ratio σ =15.

(I) Original image.

(II) Noisy image.

(III) Denoised by Hard Threshold in DWT-W.

(IV) Denoised by Hard Threshold in SWT-W.

(V) Denoised by Sure Shrink in W-DWT.

(VI) Denoised Sure Shrink in SWT.

(VII) Denoised by Bayes Shrink in DWT-W.

(VIII) Denoised by Bayes Shrink in SWT-W.

(IX) Denoised by Penalized in DWT-M.

(X) Denoised by Penalized in SWT-M.

(XI) Denoised by Median Filter.

(XII) Denoised by Wiener Filter.

Figure 5.12. Lena image with noise ratio σ =25.

5.1.3. Implementation and Results Analysis of Butterfly Image

Denoising images are applied while using WT in three-level to decompose, and the experimental performance results are shown in Table 5.3 to the Butterfly image after the proposed algorithm method process steps are applied to obtain the best result. After the process steps were implemented on Butterfly image for all cases, the original image becomes a noisy image after adding noise depending on three levels of noise ratios (σ=10, σ=15, and σ=25), at σ=10, the PSNR value of the noisy image equal to 28.6637, the PSNR value with Median filter equal to 23.9223, and the PSNR value outcome with Wiener filter equal to 27.2021. While at σ=15, the PSNR value of the noisy image is equivalent to 24.1719, the PSNR value with Median filter formula 23.3827, and the PSNR value resulting from the Wiener filter is 26.2778. While, at σ=25, the outcome of the PSNR value of the noisy image is equivalent to 19.7456, PSNR value with Median filter equal to 22.1911, and PSNR value with Wiener filter = 24.5263.

The more accurate and efficient result in removing noise from the noisy image is observed according to the Butterfly image of all process steps and each noise ratio (σ=10, σ=15, and σ=15). At the noise ratio, σ=10 is detected the best PSNR value compared to the other cases (process steps) when applying 2D-SWT based on the Sure Shrink threshold technique referred to in the Figure 4.4 diagram of chapter four (Methodology of Proposed System) with selected Reverse biorthogonal Wavelet Filters (bior2.2). At the noise ratio σ=15, the best accurate result of denoising images according to the process steps is determined by applying 2D-SWT depending on the Sure Shrink threshold technique with a biorthogonal wavelet Filters (bior1.1).

While the best PSNR result of this image is indicated when applying 2D-SWT with Sure Shrink threshold technique based on Wavelet Filters Families Haar, Biorthogonal, and Reverse biorthogonal (db1, bior1.1, and rbio1.1) compared with the other process steps at the noise ratio σ=25.

The charts in Figures 5.13, 5.14, and 5.15 illustrate the comparison of all cases (process steps) between the PSNR value of the degraded image (noisy) and the denoising image of each threshold technique function and noise ratio separately based on Table 5.3. While Figures 5.16, 5.17, and 5.18 show outcome images for each case.

Table 5.3. The best PSNR values of the Butterfly image for image denoising process steps with all the used threshold cases, for noise ratios $\sigma = 10$, $\sigma = 15$ and $= 25$.

Noise Ratio	Threshold Cases	PSNR	2D-WT	W-WT-M	M-WT-W	W-M-WT	M-W-WT	WT-W-M	WT-M-W	W-WT	M-WT	WT-W	WT-M
σ=10	Hard	2D-SWT	29.0893	22.9561	22.5919	22.9561	22.5911	22.9591	22.5947	27.2023	23.9275	27.2055	23.9334
		2D-DWT	28.7031	22.9561	22.5913	22.9561	22.5911	22.9587	22.5949	27.2022	23.9231	27.2055	23.9295
σ=10	Sure Shrink	2D-SWT	**31.1761**	23.0083	22.5533	22.9408	22.5828	23.0243	22.7409	27.1448	23.9694	26.6166	24.2185
		2D-DWT	28.6518	22.4702	22.0023	22.5258	22.2559	22.1322	21.8975	26.0443	23.3811	25.0514	23.2213
σ=10	Bayes Shrink	2D-SWT	30.4237	22.9561	22.5911	22.9561	22.5911	22.9930	22.6354	27.2022	23.9317	27.1963	24.0309
		2D-DWT	29.6162	22.9442	22.5560	22.9507	22.5836	22.8647	22.5128	27.1806	23.9130	26.9808	23.8985
σ=10	Penalized	2D-SWT	29.0593	24.2900	26.1163	29.0593	29.0593	23.0066	22.7851	29.0593	29.0593	26.1175	24.2905
		2D-DWT	29.0593	24.2902	26.1163	29.0593	29.0593	23.0066	22.7851	29.0593	29.0593	26.1175	24.2905
σ=15	Hard	2D-SWT	25.6052	22.6909	22.3687	22.6904	22.3673	22.7097	22.3868	26.2798	23.4049	26.3012	23.4543
		2D-DWT	24.5812	22.6902	22.3685	22.6902	22.3673	22.7051	22.3821	26.2779	23.3855	26.2926	23.4221
σ=15	Sure Shrink	2D-SWT	**28.2307**	22.7703	22.3166	22.6797	22.3585	22.8414	22.5749	26.2494	23.5154	25.7683	23.8451
		2D-DWT	25.9561	22.1167	21.5049	22.2225	21.9850	21.7342	21.5457	25.2061	22.6476	23.9764	22.7242
σ=15	Bayes Shrink	2D-SWT	27.3001	22.6902	22.3678	22.6902	22.3673	22.7967	22.4811	26.2779	23.4193	26.3121	23.7313
		2D-DWT	26.6914	22.6687	22.3197	22.6766	22.3571	22.5875	22.2874	26.2512	23.3932	26.0052	23.4842
σ=15	Penalized	2D-SWT	25.7858	23.7084	24.7644	25.7858	25.7858	22.6806	22.5015	25.7858	25.7858	24.7594	23.7084
		2D-DWT	25.7858	23.7084	24.7644	25.7858	25.7858	22.6806	22.5015	25.7858	25.7858	24.7594	23.7084
σ=25	Hard	2D-SWT	22.4821	22.1295	21.8761	22.1283	21.8742	22.1785	21.9255	24.5273	22.2599	24.6358	22.4179
		2D-DWT	21.1398	22.1281	21.8759	22.1281	21.8742	22.1708	21.9341	24.5264	22.2008	24.5742	22.3360
σ=25	Sure Shrink	2D-SWT	**25.1847**	22.2429	21.8847	22.1292	21.8712	22.3974	22.2272	24.6441	22.5892	24.2086	23.1205
		2D-DWT	23.2819	21.6058	21.0004	21.5189	21.3780	20.9937	20.8247	23.7808	21.8679	22.3170	21.7340
σ=25	Bayes Shrink	2D-SWT	24.2849	22.1299	21.8760	22.1281	21.8742	22.4095	22.1846	24.5266	22.2947	24.8376	22.9116
		2D-DWT	23.7873	22.0897	21.8044	22.1073	21.8620	22.0632	21.8349	24.4922	22.2847	24.3260	22.6688
σ=25	Penalized	2D-SWT	23.0156	22.7361	23.4784	23.0156	23.0156	22.1235	22.0184	23.0156	23.0156	23.4693	22.7361
		2D-DWT	23.0156	22.7361	23.4784	23.0156	23.0156	22.1235	22.0184	23.0156	23.0156	23.4693	22.7361

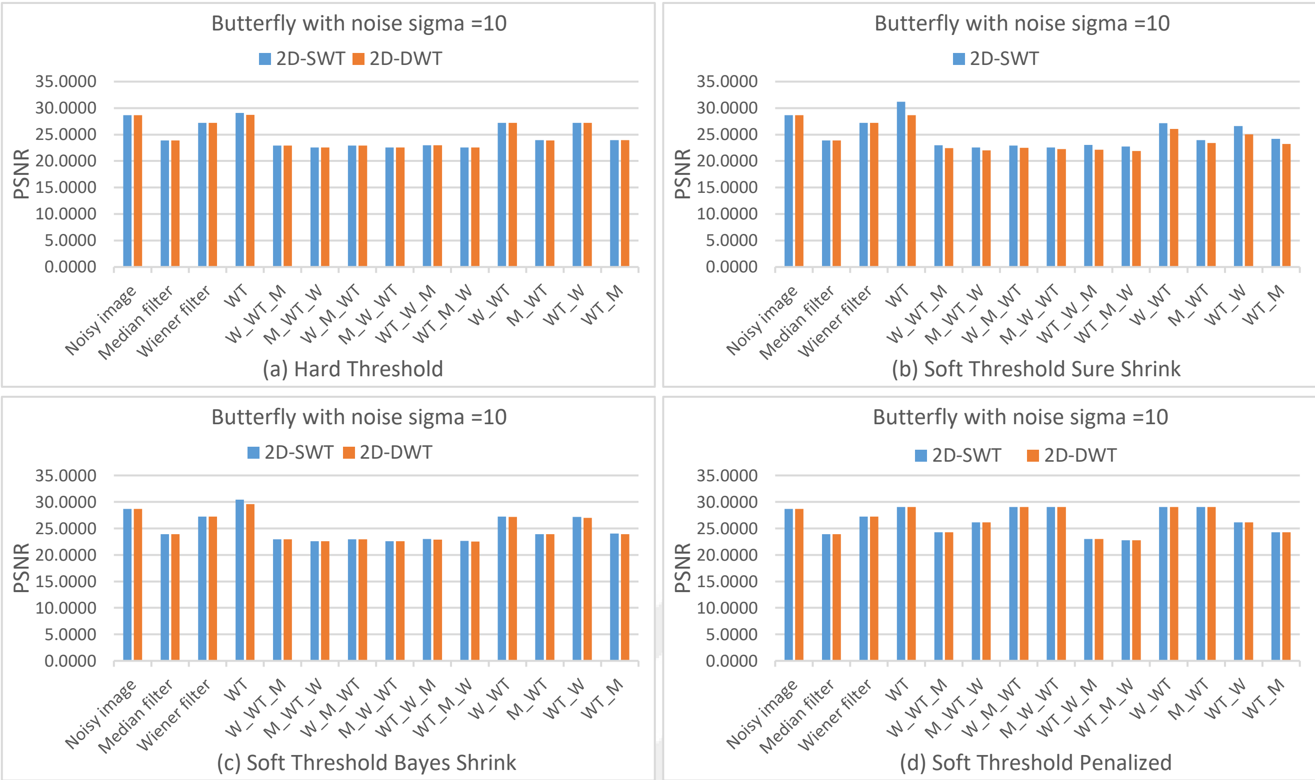

Figure 5.13. PSNR values of the comparison between process steps with (a) Hard, (b) Sure Shrink, (c) Bayes Shrink, and (d) Penalized threshold technics used, for Butterfly image, with noise σ=10.

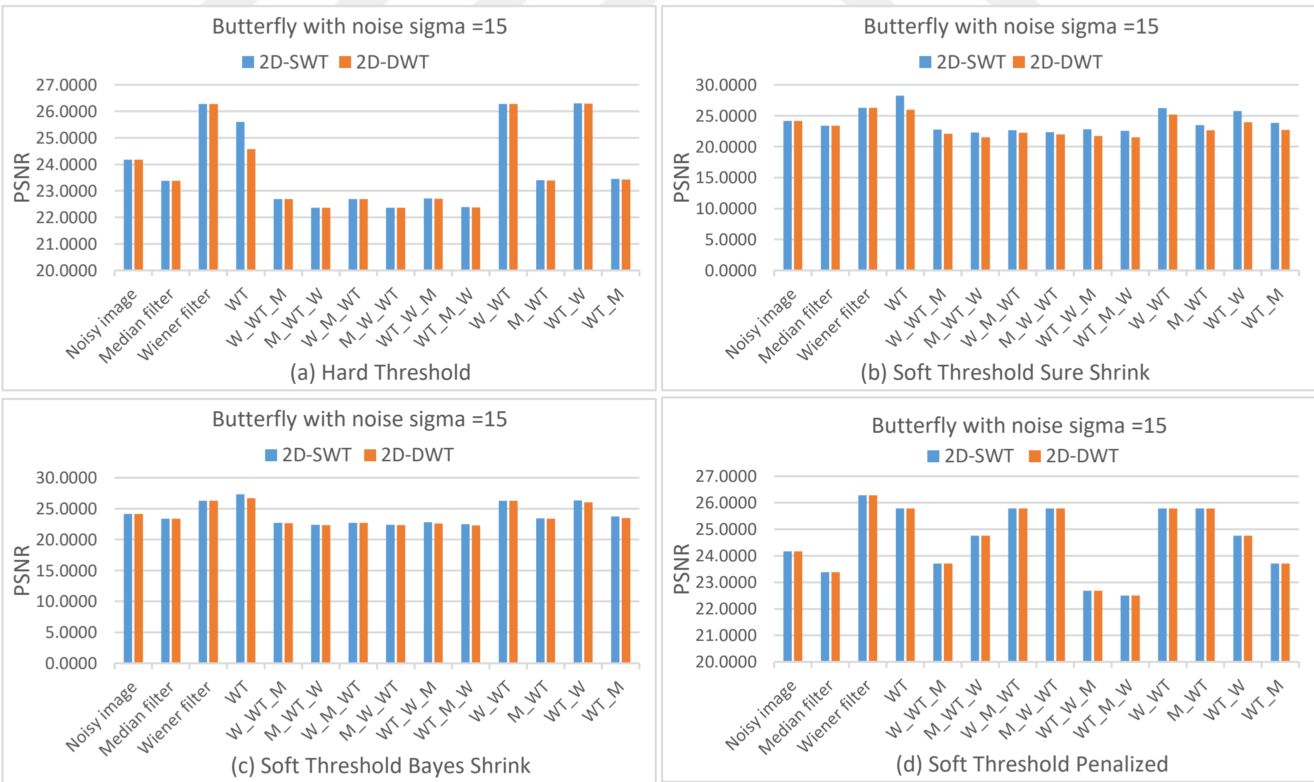

Figure 5.14. PSNR values of the comparison between process steps with (a) Hard, (b) Sure Shrink, (c) Bayes Shrink, and (d) Penalized threshold technics used, for Butterfly image, with noise σ=15.

(a) Hard Threshold

(b) Soft Threshold Sure Shrink

(c) Soft Threshold Bayes Shrink

(d) Soft Threshold Penalized

Figure 5.15. PSNR values of the comparison between process steps with (a) Hard, (b) Sure Shrink, (c) Bayes Shrink, and (d) Penalized threshold technics used, for Butterfly image, with noise σ=25.


(I) Original image.


(II) Noisy image.


(III) Denoised by Hard Threshold in DWT.


(IV) Denoised by Hard Threshold in SWT.


(V) Denoised by Sure Shrink in DWT.


(VI) Denoised Sure Shrink in SWT.


(VII) Denoised by Bayes Shrink in DWT.


(VIII) Denoised by Bayes Shrink in SWT.


(IX) Denoised by Penalized in DWT.


(X) Denoised by Penalized in SWT.


(XI) Denoised by Median Filter.


(XII) Denoised by Wiener Filter.

Figure 5.16. Butterfly image with noise ratio σ =10.


(I) Original image.


(II) Noisy image.


(III) Denoised by Hard Threshold in DWT-W.


(IV) Denoised by Hard Threshold in SWT-W.


(V) Denoised by Sure Shrink in DWT.


(VI) Denoised Sure Shrink in SWT.


(VII) Denoised by Bayes Shrink in DWT.


(VIII) Denoised by Bayes Shrink in SWT.


(IX) Denoised by Penalized in DWT.


(X) Denoised by Penalized in SWT.


(XI) Denoised by Median Filter.


(XII) Denoised by Wiener Filter.

Figure 5.17. Butterfly image with noise ratio σ =15.


(I) Original image.


(II) Noisy image.


(III) Denoised by Hard Threshold in DWT-W.


(IV) Denoised by Hard Threshold in SWT-W.


(V) Denoised by Sure Shrink in W-DWT.


(VI) Denoised Sure Shrink in SWT.


(VII) Denoised by Bayes Shrink in DWT-W.


(VIII) Denoised by Bayes Shrink in SWT-W.


(IX) Denoised by Penalized in M-DWT-W.


(X) Denoised by Penalized in M-SWT-W.


(XI) Denoised by Median Filter.


(XII) Denoised by Wiener Filter.

Figure 5.18. Butterfly image with noise ratio σ =25.

5.1.4. Implementation and Results Analysis of Peppers Image

The experimental output results for the proposed algorithm methods after applying the process steps on the Peppers image are shown in Table 5.4 based on three levels of noise ratio were added to the original image (=10, =15, and =25). At =10, the PSNR value of the noisy image is 28.6044, the PSNR value with the Median filter is 30.1248, and the PSNR value outcome with the Wiener filter is 30.6874. At =15, the PSNR value of the noisy image is 24.1666, the PSNR value with the Median filter is 28.4685, and the PSNR value with the Wiener filter is 29.3833. Finally, at =25, the PSNR value of the noisy image is 19.7744, the PSNR value with the Median filter is 25.7033, and the PSNR value with the Wiener filter is 27.1252.

Following the application of all proposed method process steps to achieve the best outcome for three levels of noise ratios ($\sigma = 10$, $\sigma = 15$, $\sigma = 25$), the most accurate and efficient result of noise removal from the noisy image is calculated according to the Peppers image. Firstly, at the noise ratio, σ=10 is detected the best PSNR value than the other process steps when applying threshold-based 2D-SWT with the Sure Shrink technique referred to the Figure 4.4 diagram in chapter four (Methodology of Proposed System) depending on selected Reverse biorthogonal Wavelet Filters (rbio2.4). Secondly, at the noise ratio σ=15, the best accurate result and best-proposed method of denoising images also according to the process steps are determined by applying 2D-SWT depending on the Sure Shrink threshold technique with the Fejer-Korovkin wavelets Filters (fk4). Finally, while the best PSNR result of the Peppers image is indicated when applying the Wiener filter after using 2D-SWT dependent on the Bayes Shrink threshold technique referred to in the Figure 4.6 diagram with selected Biorthogonal Wavelet Filters (bior1.5) compared with the other process steps at the noise ratio σ=25.

The charts in Figures 5.19, 5.20, and 5.21 illustrate the comparison of all cases (process steps) between the PSNR value of the noisy image and the denoising image of each threshold technique function and noise ratio separately based on Table 5.4. While Figures 5.22, 5.23, and 5.24 show outcome images for each case.

Table 5.4. The best PSNR values of the Peppers image for image denoising process steps with all the used threshold cases, for noise ratios σ = 10, σ = 15 and = 25.

Noise Ratio	Threshold Cases	PSNR	2D-WT	W-WT-M	M-WT-W	W-M-WT	M-W-WT	WT-W-M	WT-M-W	W-WT	M-WT	WT-W	WT-M
σ=10	Hard	2D-SWT	29.1402	29.0280	28.5987	29.0275	28.5942	29.0681	28.6210	30.6884	30.1710	30.7226	30.2037
		2D-DWT	28.6637	29.0275	28.5967	29.0275	28.5941	29.0358	28.6100	30.6875	30.1310	30.6993	30.1438
σ=10	Sure Shrink	2D-SWT	**32.5460**	29.0822	28.5191	29.0338	28.6028	28.8722	28.5724	30.7828	30.4267	30.3507	30.4792
		2D-DWT	30.1612	28.0932	27.5496	28.1929	27.7918	27.4359	27.2181	29.4317	29.3040	28.4026	28.8202
σ=10	Bayes Shrink	2D-SWT	30.2130	29.0275	28.5947	29.0275	28.5941	29.0458	28.6339	30.6875	30.1584	30.7150	30.3539
		2D-DWT	29.4730	29.0273	28.5581	29.0275	28.5941	28.9439	28.5144	30.6873	30.1443	30.5817	30.1950
σ=10	Penalized	2D-SWT	31.0601	30.4430	30.2449	31.0601	31.0601	28.9280	28.6425	31.0601	31.0601	30.2495	30.4430
		2D-DWT	31.0601	30.4430	30.2449	31.0601	31.0601	28.9280	28.6425	31.0601	31.0601	30.2495	30.4430
σ=15	Hard	2D-SWT	26.2946	28.4066	28.0202	28.4052	28.0068	28.4698	28.0664	29.3846	28.5851	29.4889	28.8631
		2D-DWT	24.7556	28.4052	28.0102	28.4051	28.0068	28.4283	28.0398	29.3835	28.4825	29.4285	28.7366
σ=15	Sure Shrink	2D-SWT	**29.9717**	28.4847	27.9417	28.4263	28.0273	28.2557	28.0454	29.6633	29.0697	29.2706	29.3916
		2D-DWT	28.2774	27.4678	26.8507	27.5353	27.1967	26.8981	26.6796	28.3988	28.0489	27.5461	27.9595
σ=15	Bayes Shrink	2D-SWT	28.6675	28.4051	28.0074	28.4051	28.0068	28.4906	28.1458	29.3834	28.5729	29.6080	29.3560
		2D-DWT	27.5182	28.4016	27.9611	28.4051	28.0074	28.3536	27.9836	29.3804	28.5737	29.3990	29.0741
σ=15	Penalized	2D-SWT	28.2220	29.0022	28.9961	28.2220	28.2220	28.2183	27.9960	28.2220	28.2220	28.9945	29.0022
		2D-DWT	28.2220	29.0022	28.9961	28.2220	28.2220	28.2183	27.9960	28.2220	28.2220	28.9945	29.0022
σ=25	Hard	2D-SWT	23.7148	27.0219	26.7357	27.0203	26.7212	27.1919	26.8802	27.1320	25.9334	27.3894	26.8581
		2D-DWT	21.7539	27.0200	26.7278	27.0196	26.7212	27.0787	26.8027	27.1259	25.7290	27.2317	26.5627
σ=25	Sure Shrink	2D-SWT	27.4052	27.1063	26.6861	27.0505	26.7581	26.8415	26.7010	27.6033	26.9848	27.2518	27.2277
		2D-DWT	25.9568	26.2803	25.6065	26.3401	26.1372	25.4663	25.2630	26.6993	26.2102	25.5910	25.8621
σ=25	Bayes Shrink	2D-SWT	25.7444	27.0195	26.7322	27.0194	26.7211	27.2947	27.0460	27.1532	25.8885	**27.6841**	27.2106
		2D-DWT	24.9360	27.0151	26.7146	27.0174	26.7255	27.0600	26.8134	27.1326	26.0173	27.4437	27.0129
σ=25	Penalized	2D-SWT	24.9405	26.7125	27.3979	24.9405	24.9405	27.1120	26.9396	24.9405	24.9405	27.4008	26.7125
		2D-DWT	24.9405	26.7125	27.3979	24.9405	24.9405	27.1120	26.9396	24.9405	24.9405	27.4008	26.7125

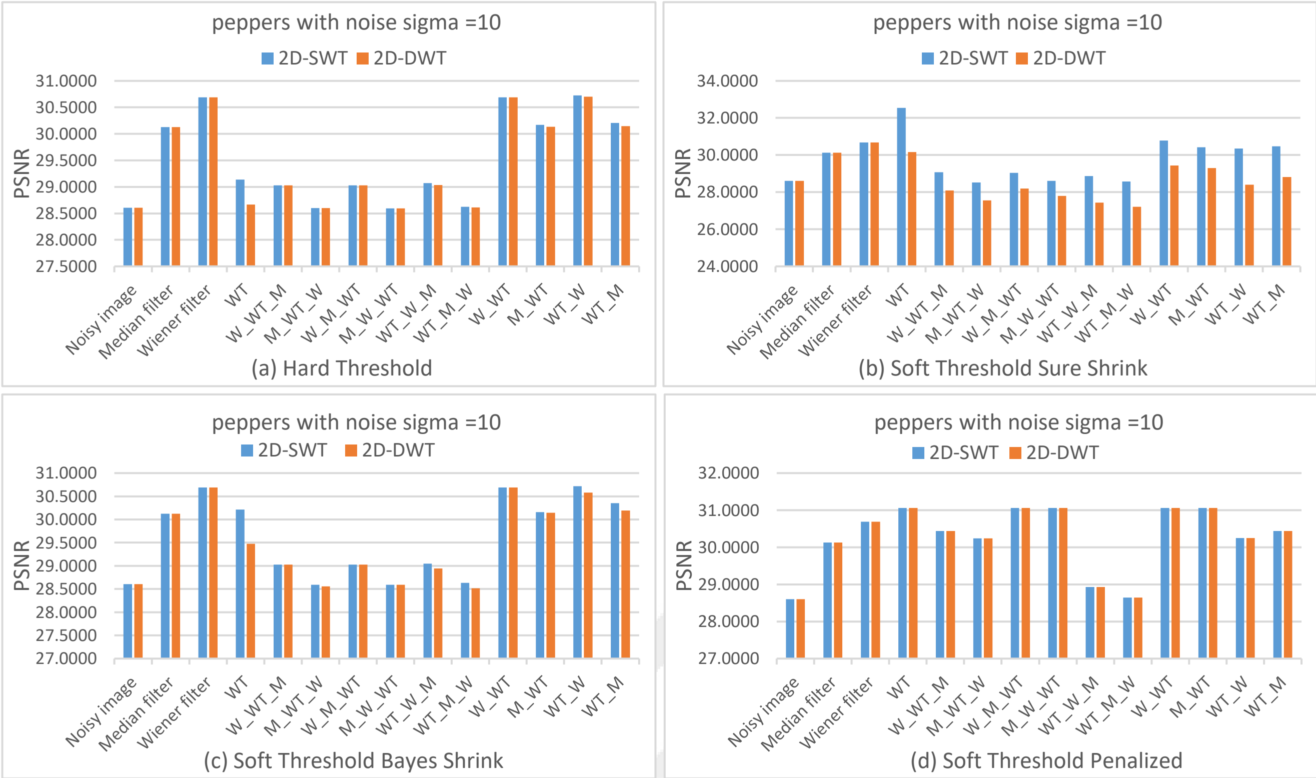

Figure 5.19. PSNR values of the comparison between process steps with (a) Hard, (b) Sure Shrink, (c) Bayes Shrink, and (d) Penalized threshold technics used, for Peppers image, with noise σ=10.

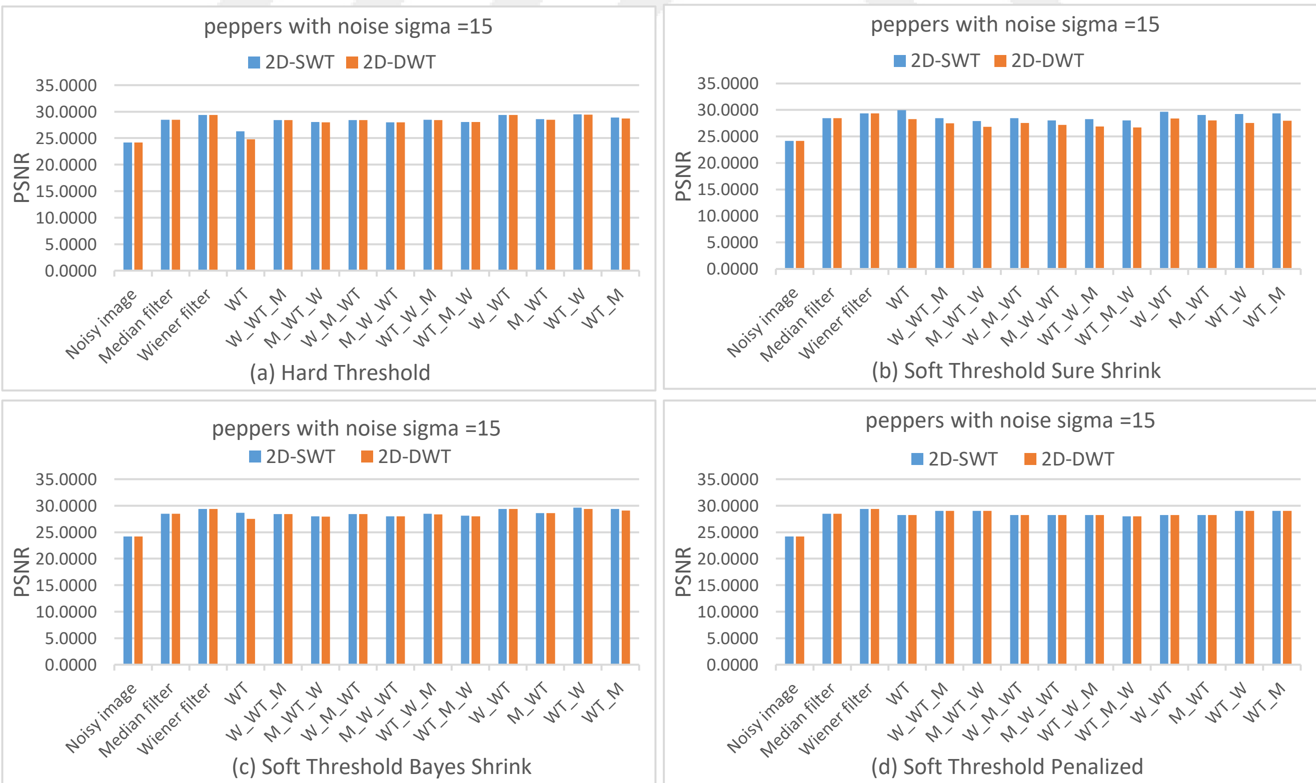

Figure 5.20. PSNR values of the comparison between process steps with (a) Hard, (b) Sure Shrink, (c) Bayes Shrink, and (d) Penalized threshold technics used, for Peppers image, with noise σ=15.

Figure 5.21. PSNR values of the comparison between process steps with (a) Hard, (b) Sure Shrink, (c) Bayes Shrink, and (d) Penalized threshold technics used, for Peppers image, with noise σ=25.

(I) Original image.

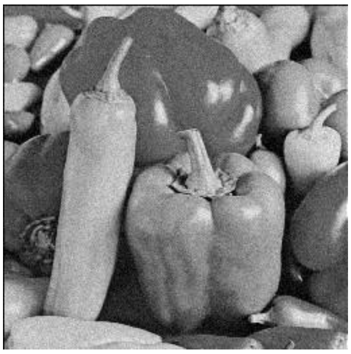

(II) Noisy image.

(III) Denoised by Hard Threshold in DWT-W.

(IV) Denoised by Hard Threshold in SWT-W.

(V) Denoised by Sure Shrink in DWT.

(VI) Denoised Sure Shrink in SWT.

(VII) Denoised by Bayes Shrink in DWT-W.

(VIII) Denoised by Bayes Shrink in SWT-W.

(IX) Denoised by Penalized in W-DWT.

(X) Denoised by Penalized in W-SWT.

(XI) Denoised by Median Filter.

(XII) Denoised by Wiener Filter.

Figure 5.22. Peppers image with noise ratio σ =10.

(I) Original image.

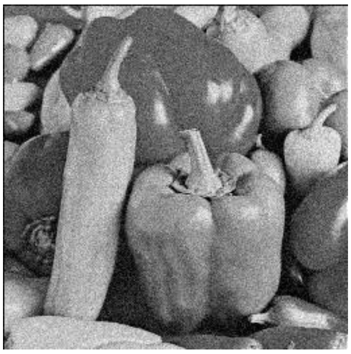

(II) Noisy image.

(III) Denoised by Hard Threshold in DWT-W.

(IV) Denoised by Hard Threshold in SWT-W.

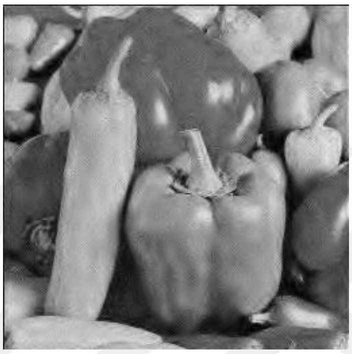

(V) Denoised by Sure Shrink in DWT.

(VI) Denoised Sure Shrink in SWT.

(VII) Denoised by Bayes Shrink in DWT-W.

(VIII) Denoised by Bayes Shrink in SWT-W.

(IX) Denoised by Penalized in W-DWT-M.

(X) Denoised by Penalized in W-SWT-M.

(XI) Denoised by Median Filter.

(XII) Denoised by Wiener Filter.

Figure 5.23. Peppers image with noise ratio σ =15.

(I) Original image.

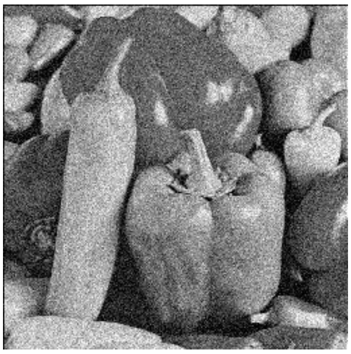

(II) Noisy image.

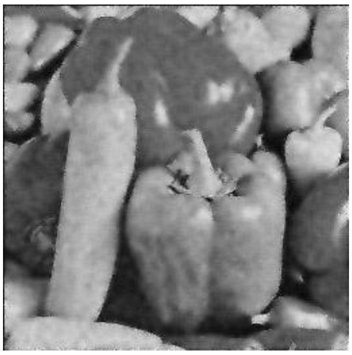

(III) Denoised by Hard Threshold in DWT-W.

(IV) Denoised by Hard Threshold in SWT-W.

(V) Denoised by Sure Shrink in W-DWT.

(VI) Denoised Sure Shrink in W-SWT.

(VII) Denoised by Bayes Shrink in DWT-W.

(VIII) Denoised by Bayes Shrink in SWT-W.

(IX) Denoised by Penalized in DWT-W.

(X) Denoised by Penalized in SWT-W.

(XI) Denoised by Median Filter.

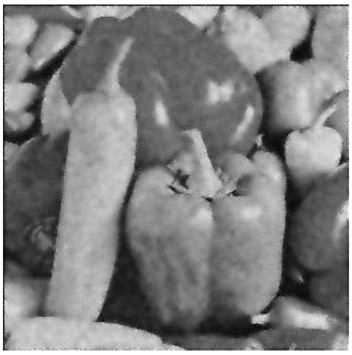

(XII) Denoised by Wiener Filter.

Figure 5.24. Peppers image with noise ratio σ =25.

5.1.5. Implementation and Results Analysis of Fruits Image

The most accurate and efficient result of noise removal from the noisy image is determined according to the fruit image after the proposed method process steps have been applied to achieve the best outcome for three levels of noise ratios (σ = 10, σ = 15, and σ = 25) were added to the input image (original), at σ=10, the PSNR value of the noisy image equals 28.6601, the PSNR value with Median filter equals 26.9869, and the PSNR value outcome with Wiener filter equals 29.5596. While at σ=15, the PSNR value of the noisy image is equivalent to 24.2402, the PSNR value with Median filter is 26.1325, and the PSNR value resulting from the Wiener filter formula 26.1325. Finally, at σ=25, the outcome of the PSNR value of the noisy image is equivalent to 19.8861, the PSNR value with Median filter equals 24.2848, and the PSNR value with Wiener filter equals 26.6765.

According to the information in Table 5.5, the best accurate result and best-proposed method of denoising images of Fruits image is found when applying 2D-SWT based on the Sure Shrink threshold technique referred to in the Figure 4.4 scheme of chapter four (Methodology of Proposed System) with selected Haar, Biorthogonal, and Reverse biorthogonal Wavelet Filters Families (db1, bior1.1, and rbio1.1), which has a better PSNR value compared to the other cases (process steps) according to the process steps at noise ratio σ=10, which mean that the PSNR value of denoising image, in this case, is better than in other cases for this image. However, at noise ratio σ=15, the best result of the same image (Fruits image) is also found by applying 2D-SWT based on the Sure Shrink threshold technique with selected Haar, Biorthogonal, and Reverse biorthogonal Wavelet Filters Families (db1, bior1.1, and rbio1.1). While the more accurate and efficient result value of PSNR is indicated in comparison with other process steps with noise ratio σ = 25 when applying 2D-SWT based on the Sure Shrink threshold technique, but with selected various wavelets which is Biorthogonal Wavelet Filters (bior1.5)

The charts in Figures 5.25, 5.26, and 5.27 show the comparison of all cases (process steps) between the PSNR value of the noisy image and the denoising image of each threshold technique function and noise ratio separately based on Table 5.5. While Figures 5.28, 5.29, and 5.30 show outcome images for each case.

Table 5.5. The best PSNR values of the Fruits image for image denoising process steps with all the used threshold cases, for noise ratios σ = 10, σ = 15 and = 25.

Noise Ratio	Threshold Cases	PSNR	2D-WT	W-WT-M	M-WT-W	W-M-WT	M-W-WT	WT-W-M	WT-M-W	W-WT	M-WT	WT-W	WT-M
σ=10	Hard	2D-SWT	29.2560	26.4652	26.1589	26.4651	26.1583	26.4706	26.1634	29.5597	26.9951	29.5661	27.0044
		2D-DWT	28.7043	26.4652	26.1588	26.4651	26.1583	26.4697	26.1620	29.5596	26.9875	29.5620	26.9979
σ=10	Sure Shrink	2D-SWT	**31.9359**	26.5363	26.1312	26.4688	26.1620	26.5043	26.2689	29.5878	27.1082	29.1177	27.3361
		2D-DWT	29.7469	25.9820	25.5485	26.0568	25.6886	25.7205	25.4721	28.6089	26.3728	27.8212	26.3257
σ=10	Bayes Shrink	2D-SWT	30.3782	26.4654	26.1596	26.4651	26.1583	26.4939	26.1944	29.5597	27.0189	29.5575	27.2053
		2D-DWT	29.6556	26.4651	26.1380	26.4652	26.1583	26.4180	26.1122	29.5597	26.9991	29.4601	27.0444
σ=10	Penalized	2D-SWT	30.1106	27.3460	28.7920	30.1106	30.1106	26.4846	26.2690	30.1106	30.1106	28.7930	27.3460
		2D-DWT	30.1106	27.3460	28.7920	30.1106	30.1106	26.4846	26.2690	30.1106	30.1106	28.7930	27.3460
σ=15	Hard	2D-SWT	26.4000	26.1507	25.8757	26.1506	25.8749	26.1627	25.8885	28.4959	26.1804	28.5299	26.3098
		2D-DWT	24.7632	26.1505	25.8760	26.1505	25.8749	26.1628	25.8933	28.4958	26.1365	28.5170	26.2629
σ=15	Sure Shrink	2D-SWT	**29.2377**	26.2279	25.8506	26.1558	25.8831	26.2052	25.9976	28.6004	26.4962	28.1461	26.8231
		2D-DWT	27.5521	25.6255	25.2186	25.7244	25.3614	25.2755	25.0702	27.7054	25.8483	26.8082	25.7799
σ=15	Bayes Shrink	2D-SWT	28.2139	26.1516	25.8816	26.1505	25.8749	26.2495	25.9861	28.4991	26.2128	28.5816	26.7222
		2D-DWT	27.2589	26.1507	25.8538	26.1505	25.8749	26.1285	25.8641	28.4965	26.1990	28.4601	26.5090
σ=15	Penalized	2D-SWT	27.1739	26.5592	27.4424	27.1739	27.1739	26.0567	25.8996	27.1739	27.1739	27.4390	26.5592
		2D-DWT	27.1739	26.5592	27.4424	27.1739	27.1739	26.0567	25.8996	27.1739	27.1739	27.4390	26.5592
σ=25	Hard	2D-SWT	23.4208	25.3539	25.1583	25.3529	25.1569	25.4034	25.2175	26.6777	24.4314	26.8057	25.0507
		2D-DWT	21.6944	25.3528	25.1582	25.3528	25.1569	25.3962	25.2024	26.6766	24.3020	26.7286	24.8964
σ=25	Sure Shrink	2D-SWT	26.7127	25.4623	25.1564	25.3729	25.1812	25.4862	25.3658	26.9574	25.2243	26.5536	25.6931
		2D-DWT	25.4403	24.8860	24.5936	24.9093	24.7377	24.4009	24.3151	26.2199	24.7232	25.1127	24.6542
σ=25	Bayes Shrink	2D-SWT	25.4736	25.3576	25.1724	25.3528	25.1569	25.5855	25.4252	26.6972	24.4521	**27.0317**	25.4413
		2D-DWT	24.8254	25.3522	25.1591	25.3537	25.1633	25.4340	25.2622	26.6883	24.5276	26.8670	25.3531
σ=25	Penalized	2D-SWT	24.1711	25.0956	25.9694	24.1711	24.1711	25.2837	25.2001	24.1711	24.1711	25.9664	25.0956
		2D-DWT	24.1711	25.0956	25.9694	24.1711	24.1711	25.2837	25.2001	24.1711	24.1711	25.9664	25.0956

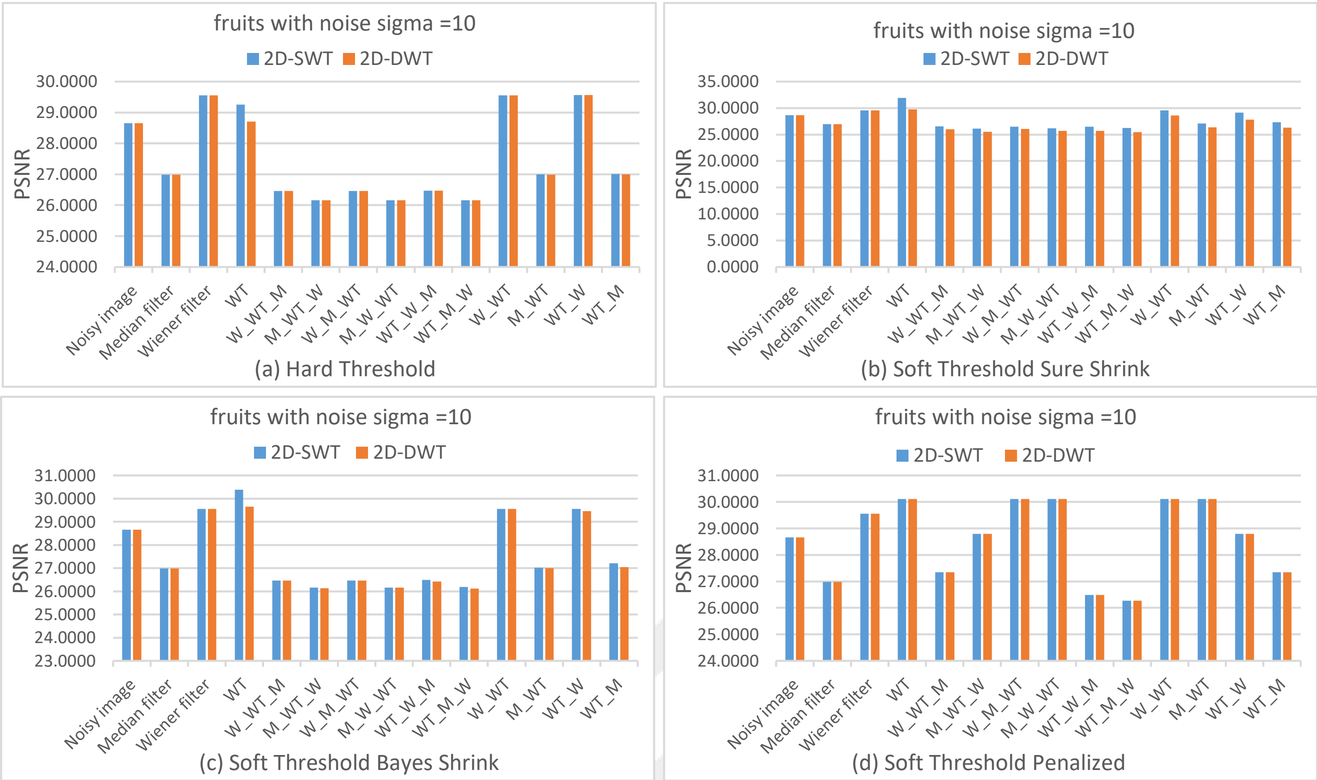

Figure 5.25. PSNR values of the comparison between process steps with (a) Hard, (b) Sure Shrink, (c) Bayes Shrink, and (d) Penalized threshold technics used, for fruits image, with noise σ=10.

Figure 5.26. PSNR values of the comparison between process steps with (a) Hard, (b) Sure Shrink, (c) Bayes Shrink, and (d) Penalized threshold technics used, for fruits image, with noise σ=15.

Figure 5.27. PSNR values of the comparison between process steps with (a) Hard, (b) Sure Shrink, (c) Bayes Shrink, and (d) Penalized threshold technics used, for fruits image, with noise σ=25.

(I) Original image.

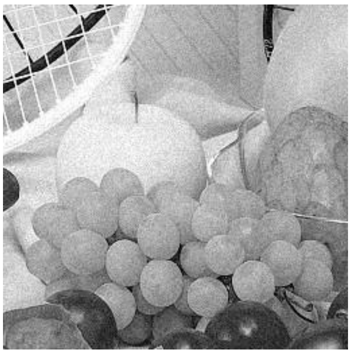

(II) Noisy image.

(III) Denoised by Hard Threshold in DWT-W.

(IV) Denoised by Hard Threshold in SWT-W.

(V) Denoised by Sure Shrink in DWT.

(VI) Denoised Sure Shrink in SWT.

(VII) Denoised by Bayes Shrink in DWT.

(VIII) Denoised by Bayes Shrink in SWT.

(IX) Denoised by Penalized in DWT.

(X) Denoised by Penalized in SWT.

(XI) Denoised by Median Filter.

(XII) Denoised by Wiener Filter.

Figure 5.28. Fruits image with noise ratio σ =10.

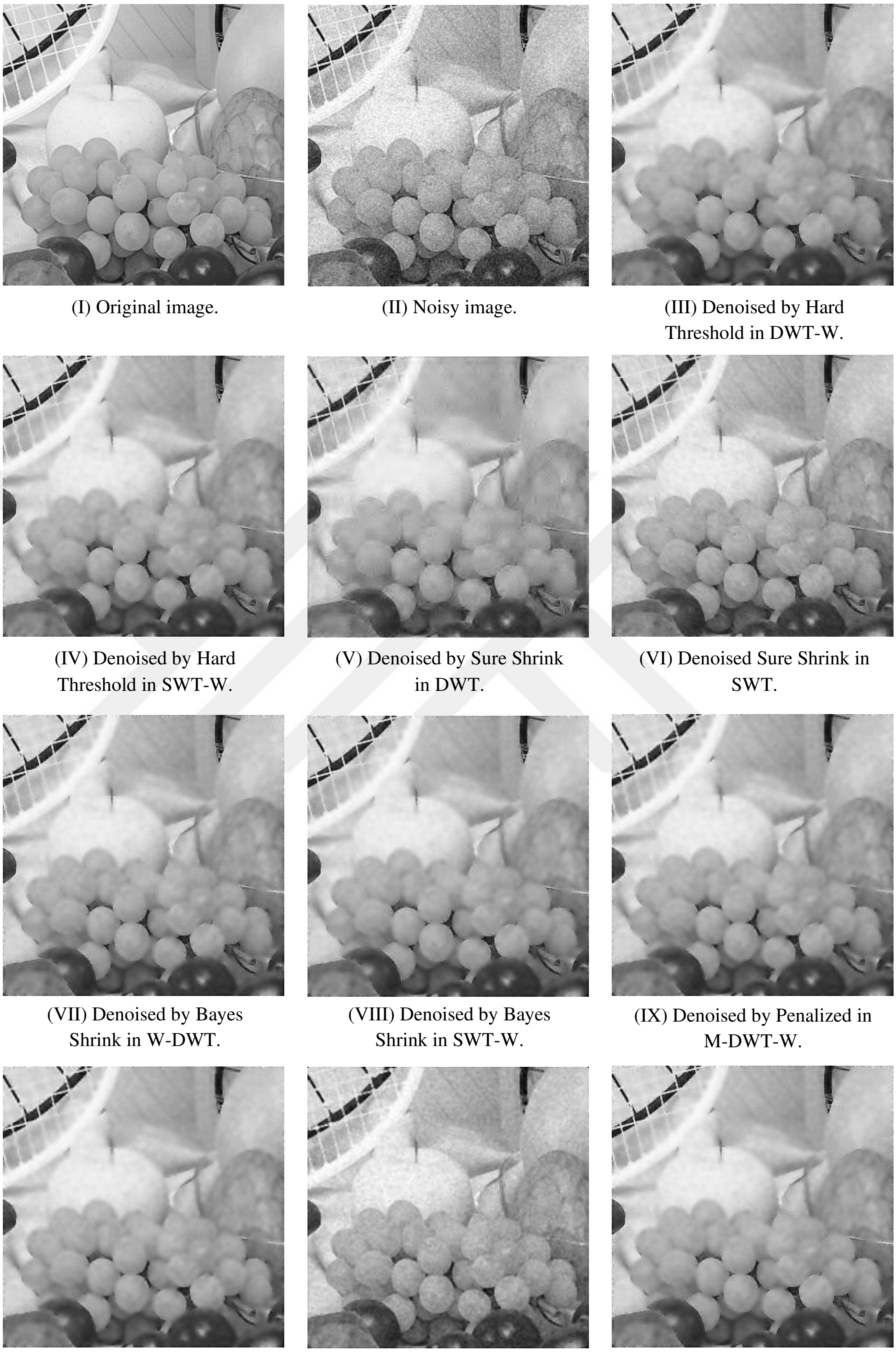

(I) Original image.

(II) Noisy image.

(III) Denoised by Hard Threshold in DWT-W.

(IV) Denoised by Hard Threshold in SWT-W.

(V) Denoised by Sure Shrink in DWT.

(VI) Denoised Sure Shrink in SWT.

(VII) Denoised by Bayes Shrink in W-DWT.

(VIII) Denoised by Bayes Shrink in SWT-W.

(IX) Denoised by Penalized in M-DWT-W.

(X) Denoised by Penalized in M-SWT-W.

(XI) Denoised by Median Filter.

(XII) Denoised by Wiener Filter.

Figure 5.29. Fruits image with noise ratio σ =15.

(I) Original image.

(II) Noisy image.

(III) Denoised by Hard Threshold in DWT-W.

(IV) Denoised by Hard Threshold in SWT-W.

(V) Denoised by Sure Shrink in W-DWT.

(VI) Denoised Sure Shrink in W-SWT.

(VII) Denoised by Bayes Shrink in DWT-W.

(VIII) Denoised by Bayes Shrink in SWT-W.

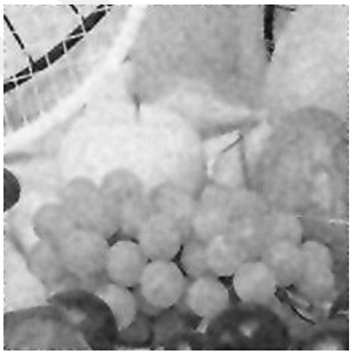

(IX) Denoised by Penalized in M-DWT-W.

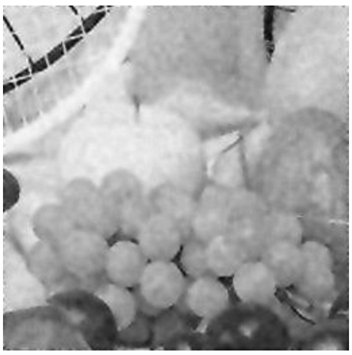

(X) Denoised by Penalized in M-SWT-W.

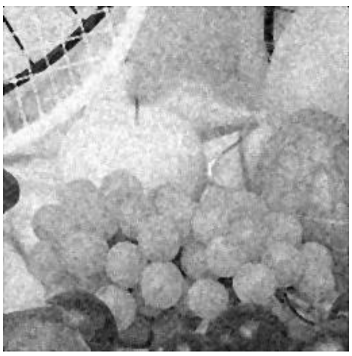

(XI) Denoised by Median Filter.

(XII) Denoised by Wiener Filter.

Figure 5.30. Fruits image with noise ratio σ =15.

5.2. The Evaluation of Proposed Method

Considering the basic comparative requirements, this section analyses and evaluates the obtained results by the proposed methods depending on the specific comparison criteria: PSNR value measurement metrics for five grayscale images of the same size will take into consideration as an original image named (Cameraman, Lena, Butterfly, Peppers, and Fruits) in all process steps referred to in the Tables 5.1, 5.2, 5.3, 5.4 and 5.5 depending on the best PSNR values. Table 5.6 represents this evaluation focusing on the different five grayscale images with three levels of noise ratios (σ=10, σ=15, and σ=25). Furthermore, Table 5.6 shows that the best value of PSNR result and best-proposed method of denoising images are repeated frequently when applying 2D-SWT based on the Sure Shrink threshold technique with selected Haar, Biorthogonal, and Reverse biorthogonal Wavelet Filters Families (db1, bior1.1, and rbio1.1), which has a better PSNR value compared to the other cases (process steps) according to the process steps at each noise ratios (σ=10, σ=15 and σ=25), which mean that the PSNR value of denoising image, in these cases, are better than in other cases. While the best PSNR value at all over-tested cases for all images with all noise ratios equal is (32.5460). As a result, it can have concluded that it is better to use both of Sure Shrink threshold technique and the Reverse biorthogonal filter together to achieve more suitable results.

Table 5.6. The evaluation of the proposed method depending on the best PSNR values.

Image	Noise Ratio	PSNR	Case	Threshold Technique	Wavelet filter
Cameraman	σ=10	31.6320	2D-SWT	Sure Shrink	db1, bior1.1, rbio1.1
	σ=15	28.6777	2D-SWT	Sure Shrink	db1, bior1.1, rbio1.1
	σ=25	25.7784	2D-SWT	Sure Shrink	db1, bior1.1, rbio1.1
Lena	σ=10	31.8136	2D-SWT	Sure Shrink	coif1
	σ=15	29.2087	2D-SWT	Sure Shrink	db1, bior1.1, rbio1.1
	σ=25	26.6966	2D-SWT_WF	Bayes Shrink	rbio6.8
Butterfly	σ=10	31.1761	2D-SWT	Sure Shrink	bior2.2
	σ=15	28.2307	2D-SWT	Sure Shrink	bior1.1
	σ=25	25.1847	2D-SWT	Sure Shrink	db1, bior1.1, rbio1.1
Peppers	σ=10	32.5460	2D-SWT	Sure Shrink	rbio2.4
	σ=15	29.9717	2D-SWT	Sure Shrink	fk4
	σ=25	27.6841	2D-SWT_WF	Bayes Shrink	bior1.5
Fruits	σ=10	31.9359	2D-SWT	Sure Shrink	db1, bior1.1, rbio1.1
	σ=15	29.2377	2D-SWT	Sure Shrink	db1, bior1.1, rbio1.1
	σ=25	27.0317	2D-SWT_WF	Bayes Shrink	bior1.5

These results were selected as the best result of denoising images in the proposed process based on two important properties to obtain this better outcome: the wavelet filters and threshold technique, which had an effective role in obtaining these results and conclusions.

5.3. Comparison of the proposed method with results of related works

This section is related to a detailed comparison between the obtained results of the proposed method in one side and three of the explained references presented at related work in chapter two which are reference [12], [27], and [38] in other side. The proposed method only compared with three of these references because only these references work with the same image and same noise ratio depending on PSNR measurement quality. The results of the comparison operation among the proposed cases of process steps in this work and the results for the related works represented by the references [38], [27], and [12], referred to as Related_1, Related_2, and Related_3, respectively.

5.3.1. Comparison of the proposed method with related works for Cameraman image

The comparison results are shown in Table 5.7 and given in Figure 5.31 with noise values (10,15, and 25). There is one proposed case that refers to the type of threshold technique which is named as proposed for 2D-SWT based on the Sure Shrink threshold with selected Wavelet Filters (db1, bior1.1, and rbio1.1). According to comparison results, the PSNR values for the Cameraman image of three levels of noise ratio (10, 15, and 25) indicate that the proposed case of process steps has better PSNR values than those of the related works.

Table 5.7. PSNR values of the comparison between proposed cases of process steps and related works for the Cameraman image with noise ratios σ=10, σ=15, and σ=25.

Image	Noise Ratio	Author	PSNR	Case	Threshold Technique	Wavelet filter
Cameraman	σ=10	Related_1	----	----	----	----
		Related_2	----	----	----	----
		Related_3	29.7910	2D-DWT	Hard	rbio3.7
		Proposed	31.6320	2D-SWT	Sure Shrink	db1, bior1.1, rbio1.1
Cameraman	σ=15	Related_1	27.1889	WF_2D-DWT	Penalized	bior3.9
		Related_2	25.1232	MF_2D-DWT	Hard	rbio
		Related_3	27.1640	2D-DWT	Hard	sym5
		Proposed	28.6777	2D-SWT	Sure Shrink	db1, bior1.1, rbio1.1
Cameraman	σ=25	Related_1	25.4744	2D-DWT_WF	Bayes Shrink	bior1.3
		Related_2	23.6200	2D-DWT_MF	Hard	db
		Related_3	24.8630	2D-DWT	Hard	sym5
		Proposed	25.7784	2D-SWT	Sure Shrink	db1, bior1.1, rbio1.1

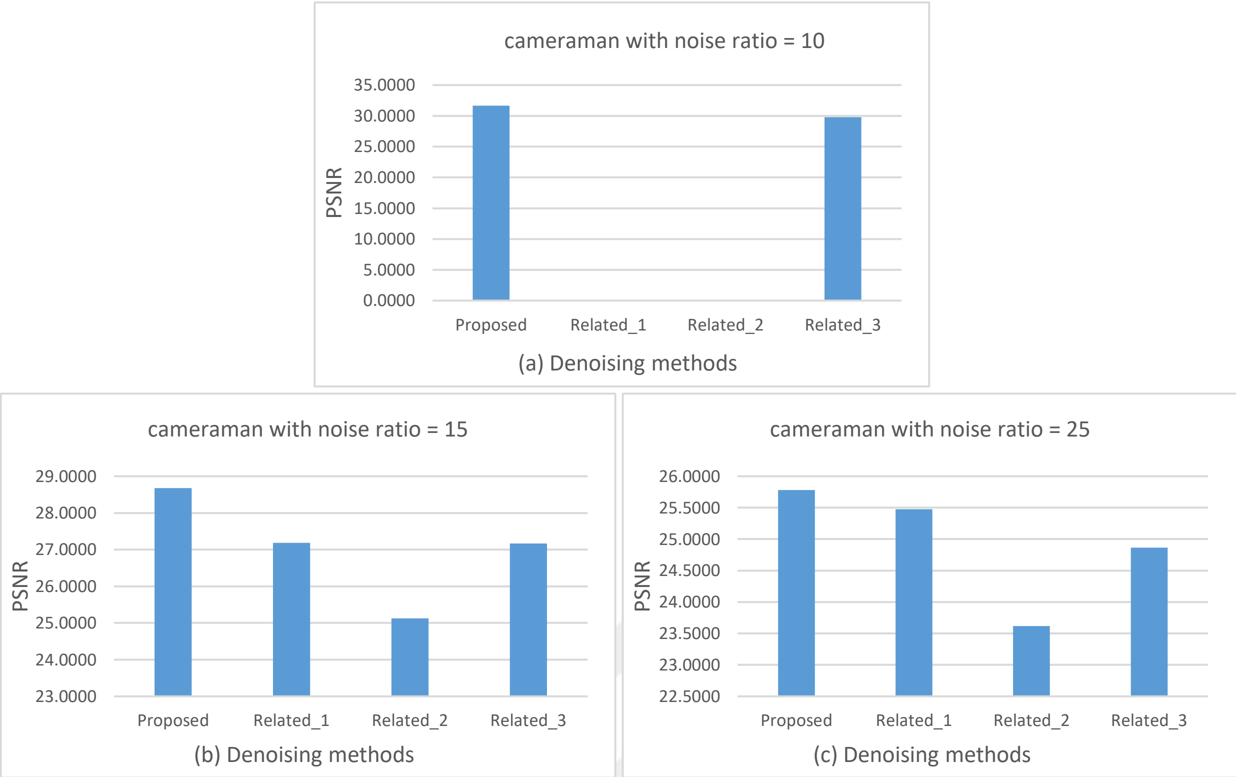

Figure 5.31. PSNR values of the comparison between proposed cases of process steps and related works for the Cameraman image with noise ratios (a) σ=10, (b) σ=15, and (c) σ=25.

Comparing with related_1 and related_2 has a mechanism of applying hybrid denoising method by mixing a 2D-DWT with median filter in the process of images denoising, it can be concluded that the Winer filter is more appropriate to be used with 2D-DWT in the hybrid denoising process than the median filter with 2D-DWT for the type AWGN noise. Compared to our proposed, by mixing 2D-SWT with spatial domain, it is observed that the proposed method is better in removing noise and increasing the quality of images compared to other related works and methods. While Related_3, which depends only on removing noise in the wavelet domain, it is observed that the proposed method is a better intern of increasing the quality of images by removing the noise in both domains (spatial and wavelet). Experimental evaluation showed that the results of the proposed cases of process steps gave an improvement in the denoising operation with about 18.9% comparing with the results of the related works.

5.3.2. Comparison of the proposed method with related works for Lena image

The comparison results are shown in Table 5.8 and given in Figure 5.32 with noise values (10,15, and 25). There is two proposed case refer to the type of threshold technique which is named as proposed for 2D-SWT based on the Sure Shrink threshold with selected Wavelet Filters (db1, bior1.1, rbio1.1, and coif1), as well as Wiener filter after using 2D-SWT dependent on the Bayes Shrink threshold technique with selected Reverse biorthogonal Wavelet Filters (rbio6.8). According to comparison results, the PSNR values for the Lena image of three levels of noise ratio (10,15 and 25) indicate that the two proposed case of process steps has better PSNR values than those of the related works.

Table 5.8. PSNR values of the comparison between proposed cases of process steps and related works for Lena image with noise ratios σ=10, σ=15, and σ=25.

Image	Noise Ratio	Author	PSNR	Case	Threshold Technique	Wavelet filter
Lena	σ=10	Related_1	----	----	----	----
		Related_2	----	----	----	----
		Related_3	29.9320	2D-DWT	Hard	bior5.5
		Proposed	31.8136	2D-SWT	Sure Shrink	coif1
Lena	σ=15	Related_1	----	----	----	----
		Related_2	26.7990	2D-DWT_MF	Hard	db
		Related_3	28.2200	2D-DWT	Hard	sym4
		Proposed	29.2087	2D-SWT	Sure Shrink	db1, bior1.1, rbio1.1
Lena	σ=25	Related_1	----	----	----	----
		Related_2	25.2960	2D-DWT_MF	Hard	rbio
		Related_3	25.1730	2D-DWT	Hard	sym5
		Proposed	26.6965	2D-SWT_WF	Bayes Shrink	rbio6.8

Comparing with related_1 and related_2 has a mechanism of applying hybrid denoising method by mixing a 2D-DWT with median filter in the process of images denoising, it can be concluded that the Winer filter is more appropriate to be used with 2D-DWT in the hybrid denoising process than the median filter with 2D-DWT for the type AWGN noise. Compared to our proposed, by mixing 2D-SWT with spatial domain, it is observed that the proposed method is better in removing noise and increasing the quality of images compared to other related works and methods. While Related_3, which depends only on removing noise in the wavelet domain, it is observed that the proposed method is a better intern of increasing the quality of images by removing the noise in both domains (spatial and wavelet). Experimental evaluation showed that the results of the proposed cases of process steps gave an improvement in the denoising operation with about 18.2% comparing with the results of the related works.

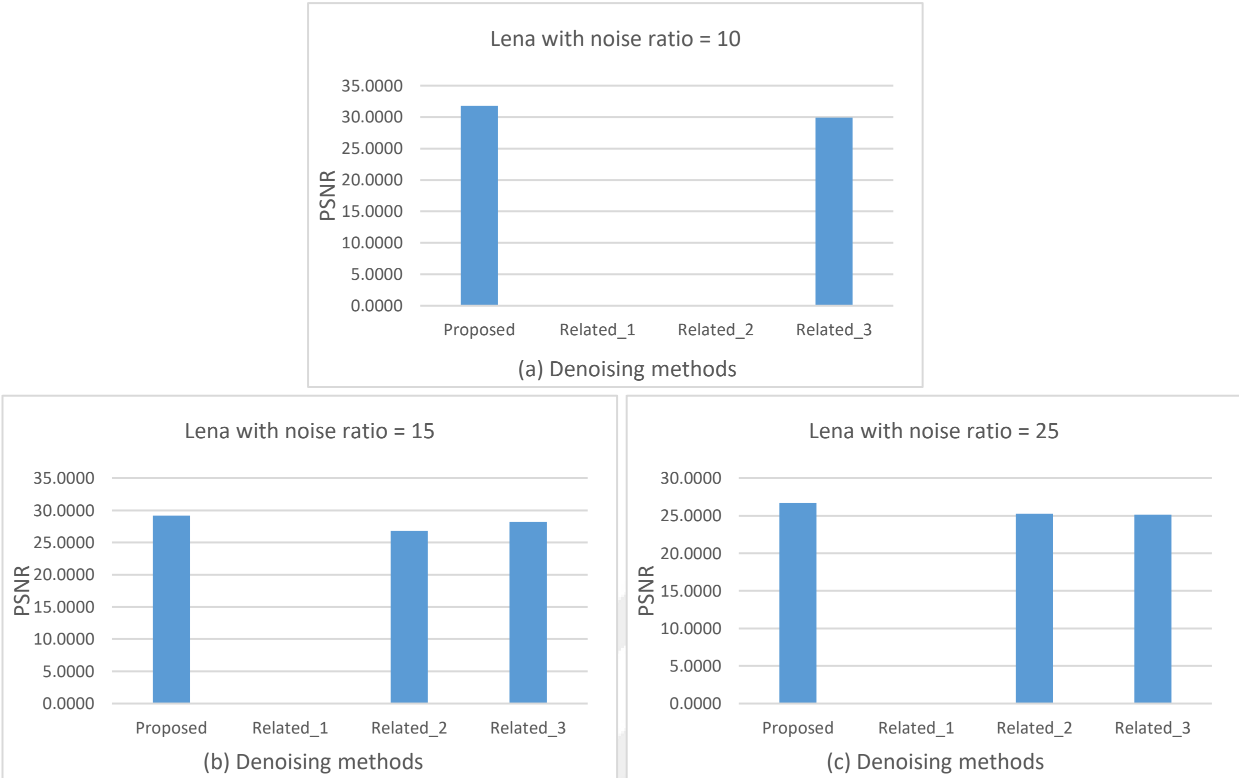

Figure 5.32. PSNR values of the comparison between proposed cases of process steps and related works for Lena image with noise ratios (a) σ=10, (b) σ=15, and (c) σ=25.

5.3.3. Comparison of the proposed method with related works for Butterfly image

The comparison results are shown in Table 5.9 and given in Figure 5.33 with noise values (10,15, and 25). There is two proposed case refer to the type of threshold technique which is named as proposed for Wiener filter after using 2D-SWT dependent on the Bayes Shrink threshold technique with selected Reverse biorthogonal Wavelet Filters (rbio6.8), and 2D-SWT based on the Sure Shrink threshold with selected Wavelet Filters (db1, bior1.1, and rbio1.1). According to comparison results, the PSNR values for the Butterfly image of three levels of noise ratio (10, 15, and 25) indicate that the two proposed case of process steps has better PSNR values than those of the related works.

Table 5.9. PSNR values of the comparison between proposed cases of process steps and related works for Butterfly image with noise ratios σ=10, σ=15, and σ=25.

Image	Noise Ratio	Author	PSNR	Case	Threshold Technique	Wavelet filter
Butterfly	σ=10	Related_1	----	----	----	----
		Related_2	----	----	----	----
		Related_3	----	----	----	----
		Proposed	31.1761	2D-SWT	Sure Shrink	rbio2.2
Butterfly	σ=15	Related_1	26.4665	2D-DWT	Bayes Shrink	rbio2.4
		Related_2	24.7068	MF_2D-DWT	Hard	coif
		Related_3	----	----	----	----
		Proposed	28.2307	2D-SWT_WF	Bayes Shrink	bior1.3
Butterfly	σ=25	Related_1	24.6412	WF_2D-DWT	Penalized	bior3.9
		Related_2	23.6200	MF_2D-DWT	Hard	sym
		Related_3	----	----	----	----
		Proposed	25.1847	2D-SWT	Sure Shrink	db1, bior1.1, rbio1.1

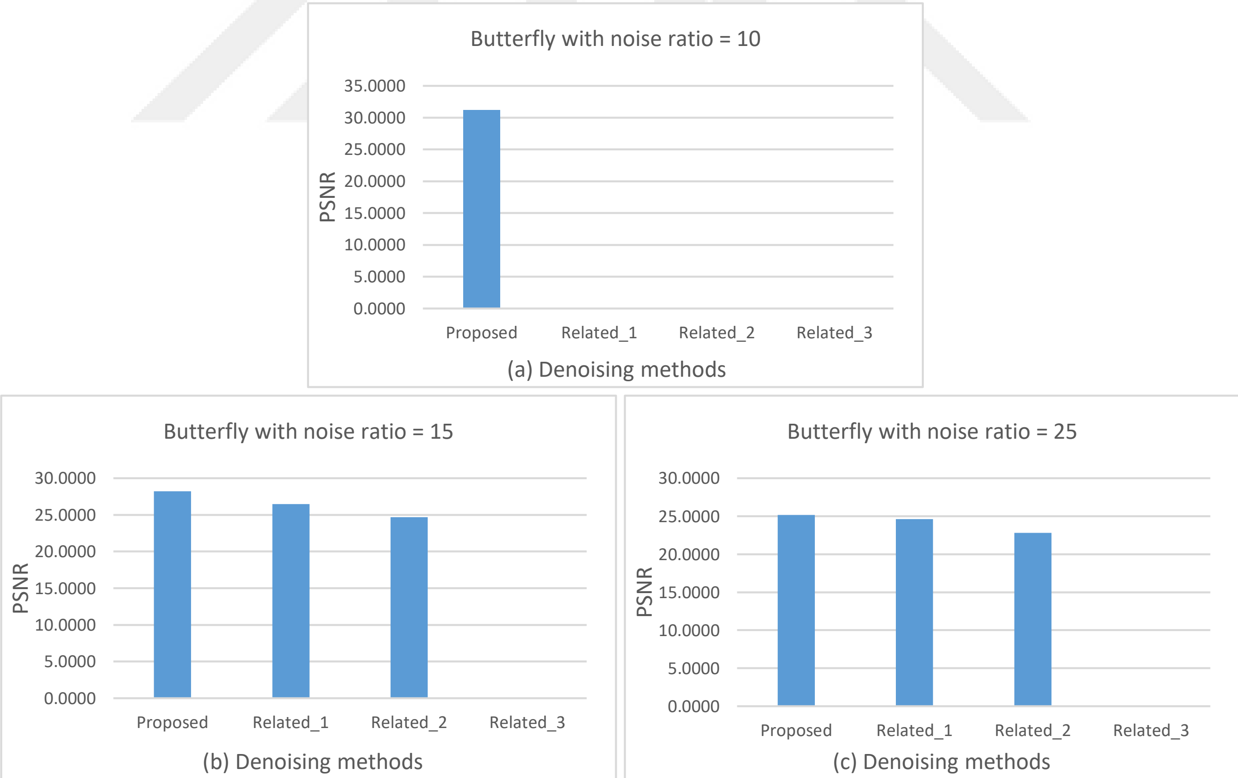

Figure 5.33. PSNR values of the comparison between proposed cases of process steps and related works for Butterfly image with noise ratios (a) σ=10, (b) σ=15, and (c) σ=25.

Comparing with related_1 and related_2 has a mechanism of applying hybrid denoising method by mixing a 2D-DWT with median filter in the process of images denoising, it can be concluded that the Winer filter is more appropriate to be used with 2D-DWT in the hybrid denoising process than the median filter with 2D-DWT for the type AWGN noise. Compared to our proposed, by mixing 2D-SWT with spatial domain, it is observed that the proposed method is better in removing noise and increasing the quality of images compared to other related works and methods. While Related_3, which depends only on removing noise in the wavelet domain, it is observed that the proposed method is a better intern of increasing the quality of images by removing the noise in both domains (spatial and wavelet). Experimental evaluation showed that the results of the proposed cases of process steps gave an improvement in the denoising operation with about 14.7% comparing with the results of the related works.

5.3.4. Comparison of the proposed method with related works for Peppers image

The comparison results are shown in Table 5.10 and given in Figure 5.34 with noise values (10,15, and 25). There is two proposed case refer to the type of threshold technique which is named as proposed for 2D-SWT dependent on the Sure Shrink threshold with selected Wavelet Filters (rbio2.4, fk4), and Wiener filter after using 2D-SWT with Bayes Shrink threshold technique based on the selected Biorthogonal Wavelet Filters (bior1.5). According to comparison results, the PSNR values for the Peppers image of three levels of noise ratio (10,15 and 25) indicate that the two proposed case of process steps has better PSNR values than those of the related works.

Table 5.10. PSNR values of the comparison between proposed cases of process steps and related works for peppers image with noise ratios σ=10, σ=15, and σ=25.

Image	Noise Ratio	Author	PSNR	Case	Threshold Technique	Wavelet filter
Peppers	σ=10	Related_1	----	----	----	----
		Related_2	----	----	----	----
		Related_3	30.1010	2D-DWT	Hard	rbio3.7
		Proposed	32.5459	2D-SWT	Sure Shrink	rbio2.4
Peppers	σ=15	Related_1	29.1246	WF_2D-DWT	Penalized	bior2.8
		Related_2	----	----	----	----
		Related_3	27.6360	2D-DWT	Hard	db4
		Proposed	29.9716	2D-SWT	Sure Shrink	fk4
Peppers	σ=25	Related_1	27.1144	WF_2D-DWT	Penalized	db10
		Related_2	----	----	----	----
		Related_3	25.0020	2D-DWT	Hard	db4
		Proposed	27.6840	2D-SWT_WF	Bayes Shrink	bior1.5

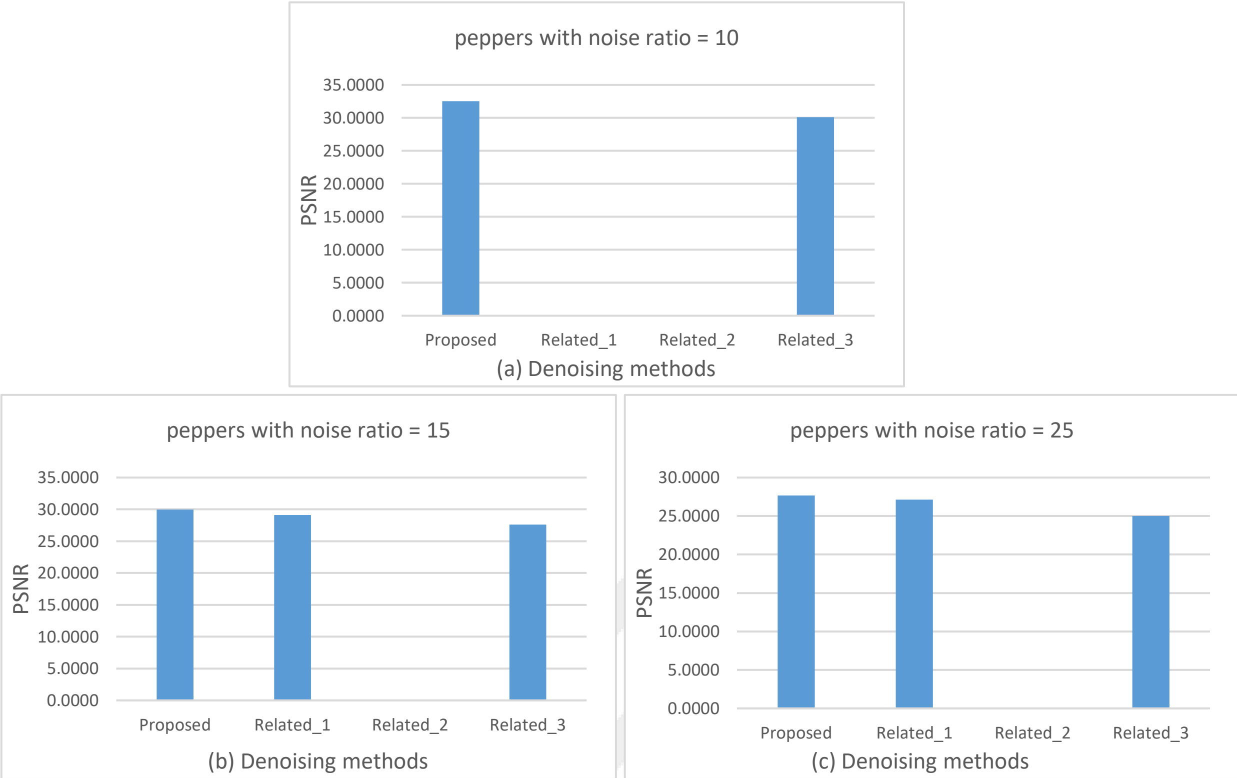

Figure 5.34. PSNR values of the comparison between proposed cases of process steps and related works for peppers image with noise ratios (a) σ=10, (b) σ=15, and (c) σ=25.

Comparing with related_1 and related_2 has a mechanism of applying hybrid denoising method by mixing a 2D-DWT with median filter in the process of images denoising, it can be concluded that the Winer filter is more appropriate to be used with 2D-DWT in the hybrid denoising process than the median filter with 2D-DWT for the type AWGN noise. Compared to our proposed, by mixing 2D-SWT with spatial domain, it is observed that the proposed method is better in removing noise and increasing the quality of images compared to other related works and methods. While Related_3, which depends only on removing noise in the wavelet domain, it is observed that the proposed method is a better intern of increasing the quality of images by removing the noise in both domains (spatial and wavelet). Experimental evaluation showed that the results of the proposed cases of process steps gave an improvement in the denoising operation with about 19.9% comparing with the results of the related works.

5.3.5. Comparison of the proposed method with related works for Fruits image

The comparison results are shown in Table 5.11 and given in Figure 5.35 with noise values (10,15, and 25). There is two proposed case refer to the type of threshold technique which is named as proposed for 2D-SWT with Sure Shrink threshold based on the selected Wavelet Filters (db1, bior1.1, rbio1.1), and Wiener filter after using 2D-SWT depending on Bayes Shrink threshold technique with selected Biorthogonal Wavelet Filters (bior1.5). According to comparison results, the PSNR values for Fruits image of three levels of noise ratio (10,15 and 25) indicate that the two proposed case of process steps has better PSNR values than those of the related works.

Table 5.11. PSNR values of the comparison between proposed cases of process steps and related works for Fruits image with noise ratios σ=10, σ=15, and σ=25.

Image	Noise Ratio	Author	PSNR	Case	Threshold Technique	Wavelet filter
Fruits	σ=10	Related_1	----	----	----	----
		Related_2	----	----	----	----
		Related_3	----	----	----	----
		Proposed	31.9358	2D-SWT	Sure Shrink	db1, bior1.1, rbio1.1
Fruits	σ=15	Related_1	28.2649	WF_2D-DWT	Penalized	bior3.9
		Related_2	25.9091	MF_2D-DWT	Hard	bior
		Related_3	----	----	----	----
		Proposed	29.2376	2D-SWT	Sure Shrink	db1, bior1.1, rbio1.1
Fruits	σ=25	Related_1	26.6877	WF_2D-DWT	Penalized	bior1.5
		Related_2	24.5582	MF_2D-DWT	Hard	rbio
		Related_3	----	----	----	----
		Proposed	27.0316	2D-SWT_WF	Bayes Shrink	bior1.5

Comparing with related_1 and related_2 has a mechanism of applying hybrid denoising method by mixing a 2D-DWT with median filter in the process of images denoising, it can be concluded that the Winer filter is more appropriate to be used with 2D-DWT in the hybrid denoising process than the median filter with 2D-DWT for the type AWGN noise. Compared to our proposed, by mixing 2D-SWT with spatial domain, it is observed that the proposed method is better in removing noise and increasing the quality of images compared to other related works and methods. While Related_3, which depends only on removing noise in the wavelet domain, it is observed that the proposed method is a better intern of increasing the quality of images by removing the noise in both domains (spatial and wavelet). Experimental evaluation showed that the results of the proposed cases of process steps gave an improvement in the denoising operation with about 13.4% comparing with the results of the related works.

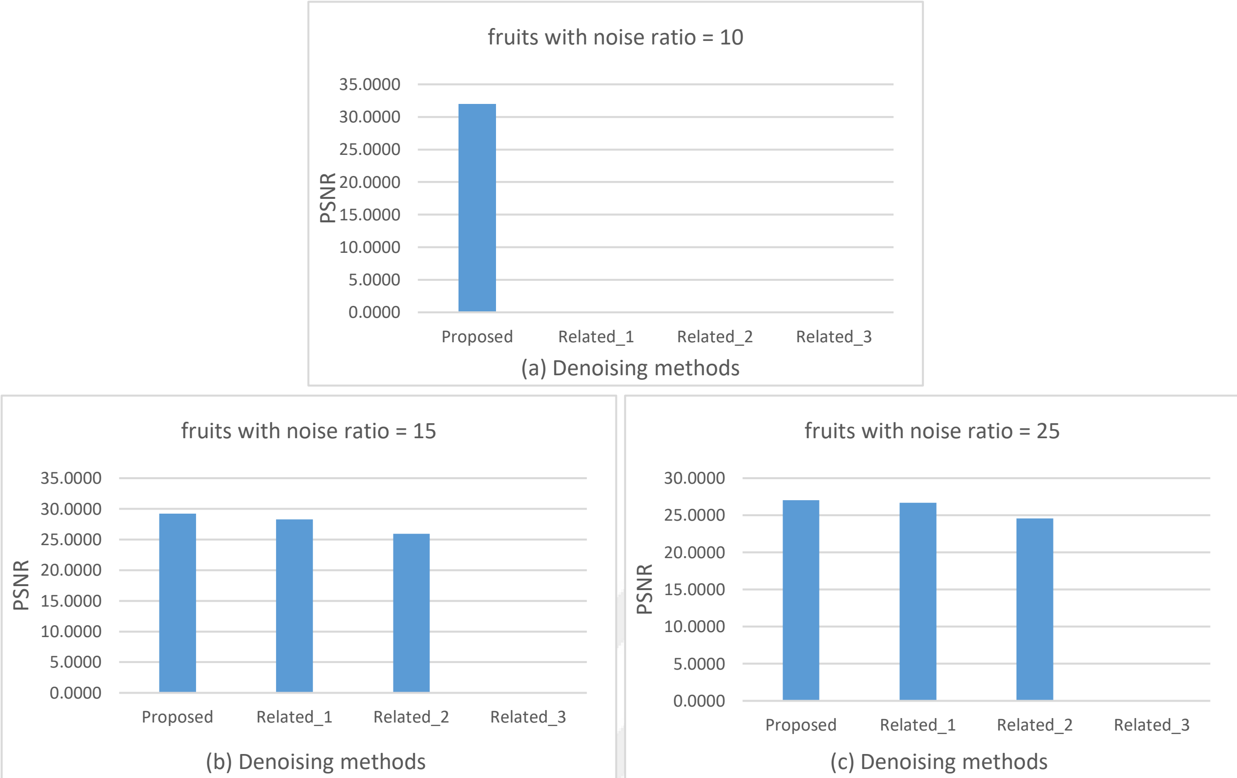

Figure 5.35. PSNR values of the comparison between proposed cases of process steps and related works for fruits image with noise ratios (a) σ=10, (b) σ=15 and (c) σ=25

6. CONCLUSIONS

Through this work, the main aim was to remove noise from digital images affected by Additive White Gaussian Noise (AWGN) with three ratios of the noise sigma as 10, 15, and 25. A new approach is designed and implemented as a noise removal system based on evaluating the effect of implementing the proposed methods, which are designed to be hybrid methods by mix the work of the spatial domain filters with the work of the multiresolution wavelet domain threshold value.

The system has been built by using the Matlab programming environment with several kinds of the wavelet transform, and threshold techniques have been tested on five images to achieve improved results of the image noise reduction process by distinguishing and removing the noise from the affected pixel units, and the wavelet decomposition is applied with a three-levels of analysis.

Finally, the performance metrics Peak Signal to Noise Ratio (PSNR) are calculated to estimate the evaluation of the suggested method. Experimental evaluation outcomes of the proposed method reveal a better improvement of image quality concerning minimizing noise and edge preservation than the results of the related works instead of using a threshold-based WT domain or spatial domain filters separately.

All the results recorded directly from Matlab on Excel files, and by analyzing the results then the following points can be concluded:

- The use of the WT analysis of three levels gave supplementary amendment to this effectiveness in eliminating noise as it decreases a greater quantity of noise during this analysis, and this was exhibited by the results obtained for the criteria used in the performance evaluation of PSNR.
- By increasing the level of the analysis phase in 2D-DWT, the increase of the image enhancement has been noticed. This enhancement will be limit through the limited number of analysis levels because there will be no improvement due to the saturation of the denoising operation. The saturation of the denoising operation means that the number of points in the data is minimal and will not affect the result at all.
- During applying the cases of this work, the wavelet transform has been used in two forms: DWT and SWT. And, through the total results, the SWT provided the best improvement to the PSNR of the work cases.
- The results improved by using the SWT because in this form of the wavelet transformation all the points were used, and there is no down-sampling for the points. Without a down-

sample will let the algorithm deals with all the points which contain the information and remove as much as possible of the noise.

- The SWT increased the improvement ratio of the PSNR results, but the cost was the processing time, which increased because there is no down-sampling in SWT, and all the points were used.
- The method of applying the threshold technique in the wavelength domain has shown effectiveness and efficiency in removing the noise of AWGN type by dealing adaptively with each frequency band and the corresponding threshold value.
- In this work and for all cases that belong to the DWT and SWT of the wavelet transform, four methods of the threshold have been used which are (Hard Threshold, Soft Threshold Sure Shrink, Soft Threshold Bayes shrink, and Soft Threshold Penalized). The results showed that for all images and cases with SWT, the improved PSNR values were by 80% with the Soft Threshold Sure Shrink, and 20% with the Soft Threshold Bayes Shrink only. While for all images and cases with DWT, the improved PSNR values were by 20% with the Hard Threshold, 26.66% with the Soft Threshold Sure Shrink, 40% with the Soft Threshold Bayes shrink, and 13.34% with the Soft Threshold Penalized.
- Through the results of all the cases applied in this work, the largest percentage of the best results (about 87%) was obtained when using filters belongs to the families (Daubechies, Biorthogonal, and Reverse biorthogonal) of the wavelet transform filter families. This indicates the effectiveness of these filter families to be applied in noise reduction applications in digital images. The best results were by using the following filters with the cases of this work: (db1, bior1.1, bior1.3, bior1.5, rbio1.1, rbio2.4, rbio6.8, coif1, and fk4).
- The results provided strong indicators that the hybrid method process by combining the denoising technique in the spatial domain filters with the WT domain based on threshold function produces improved results compared to either method alone.
- The results of the comparison operation between the proposed cases in this work and the results for the related works represented by the references [12], [27] and [38] (referred to as Related_1 Related_2, and Related_3, respectively) indicate that the proposed cases are presented better PSNR values than the related works for all noise values 10,15 and 25. The improvement in PSNR results was about 8.45%.

RECOMMANDATIONS

- As a suggestion for continuing this field of work in the future, it is preferable to design and implement the proposed system in this thesis using Field Programmable Gate Array (FPGA) high-performance devices.
- Additional can be determined performance parameters to investigate the behavior of hybrid methods that achieve a successful balance of noise reduction in various noise reduction fields.
- Apply the proposed denoising system with other types of noise (salt and pepper, poisson, speckle noise, etc.).

REFERENCES

[1] Y. Wu, H.Y. Duan, Y.F. Wen, Study on denoising technology reproduction image detail, Imaging Sci. Photochem. 36 (2018) 187–191.

[2] B.M. Ferzo, F.M. Mustafa, Digital Image Denoising Techniques in Wavelet Domain with another Filter: A review, Acad. J. Nawroz Univ. 9 (2020) 158–176.

[3] P. Koranga, G. Singh, D. Verma, S. Chaube, A. Kumar, S. Pant, Image Denoising Based on Wavelet Transform using Visu Thresholding, (n.d.).

[4] L. Singh, R. Janghel, Image Denoising techniques: a brief survey, Harmon. Search Nat. Inspired Optim. Algorithms. (2019) 731–740.

[5] R. Saluja, A. Boyat, Wavelet based image denoising using weighted highpass filtering coefficients and adaptive wiener filter, in: 2015 Int. Conf. Comput. Commun. Control, IEEE, 2015: pp. 1–6.

[6] R. Dhiman, S. Kumar, An Improved threshold estimation technique for image denoising using Wavelet thresholding techniques, Int. J. Res. Eng. Appl. Sci. 1 (2011).

[7] J. Wang, J. Wu, Z. Wu, J. Jeong, G. Jeon, Wiener filter-based wavelet domain denoising, Displays. 46 (2017) 37–41.

[8] R. Guhathakurta, Denoising of image: A wavelet based approach, in: 2017 8th Annu. Ind. Autom. Electromechanical Eng. Conf., IEEE, 2017: pp. 194–197.

[9] M. Abinaya, J. Amudha, Image denoising and quality measurements using wavelet thresholding, Int. J. Sci. Innov. Eng. Technol.(IJSIET). 2 (2015) 1–6.

[10] A. Dogra, Performance comparison of different wavelet families based on bone vessel fusion, Asian J. Pharm. Free Full Text Artic. from Asian J Pharm. 10 (2017).

[11] S. Thakral, P. Manhas, Image processing by using different types of discrete wavelet transform, in: Int. Conf. Adv. Informatics Comput. Res., Springer, 2018: pp. 499–507.

[12] S.H. Ismael, F.M. Mustafa, I.T. Okümüs, A new approach of image denoising based on discrete wavelet transform, in: 2016 World Symp. Comput. Appl. Res., IEEE, 2016: pp. 36–40.

[13] N.A. Golilarz, H. Demirel, Image de-noising using un-decimated wavelet transform (UWT) with soft thresholding technique, in: 2017 9th Int. Conf. Comput. Intell. Commun. Networks, IEEE, 2017: pp. 16–19.

[14] X. Jianhui, T. Li, Image Denoising Method Based on Improved Wavelet Threshold Transform, in: 2019 IEEE Symp. Ser. Comput. Intell., IEEE, 2019: pp. 1064–1067.

[15] N. Mittal, A. Raj, H. Goyal, Enhancement and Removal of Noise from Medical Images by Wavelet Transform Method, in: 2019 3rd Int. Conf. Electron. Commun. Aerosp. Technol., IEEE, 2019: pp. 1126–1130.

[16] X. Zhang, Image denoising using local Wiener filter and its method noise, Optik (Stuttg). 127 (2016) 6821–6828.

[17] N. Arazm, A. Sahab, M.F. Kazemi, Noise reduction of SEM images using adaptive Wiener filter, in: 2017 IEEE Int. Conf. Cybern. Comput. Intell., IEEE, 2017: pp. 50–55.

[18] R. Devi, P. Sujatha, Enhancement of fingerprint image using wiener filter, Int. J. Eng. Technol. 7 (2018) 206–212.

[19] S. Metri, T. Asha, Patch Based Wiener filter for Image Denoising, in: 2018 Int. Conf. Comput. Tech. Electron. Mech. Syst., IEEE, 2018: pp. 392–396.

[20] S. Zhang, X. Li, C. Zhang, Modified adaptive median filtering, in: 2018 Int. Conf. Intell. Transp. Big Data Smart City, IEEE, 2018: pp. 262–265.

[21] J. Tang, Y. Wang, W. Cao, J. Yang, Improved adaptive median filtering for structured light image denoising, in: 2019 7th Int. Conf. Information, Commun. Networks, IEEE, 2019: pp. 146–149.

[22] U. Erkan, L. Gökrem, S. Enginoğlu, Adaptive Right Median Filter for Salt-and-Pepper Noise Removal, Uluslararası Mühendislik Araştırma ve Geliştirme Derg. 11 (2019) 542–550.

[23] P.A. Lyakhov, A.R. Orazaev, N.I. Chervyakov, D.I. Kaplun, A new method for adaptive median filtering of images, in: 2019 IEEE Conf. Russ. Young Res. Electr. Electron. Eng., IEEE, 2019: pp. 1197–1201.

[24] S. Mridula, P. Mohanan, Speckle noise reduction in images using Wiener filtering and adaptive Wavelet thresholding, in: 2016 IEEE Reg. 10 Conf., IEEE, 2016: pp. 2860–2863.

[25] M. Diwakar, M. Kumar, Edge preservation based CT image denoising using Wiener filtering and thresholding in wavelet domain, in: 2016 Fourth Int. Conf. Parallel, Distrib. Grid Comput., IEEE, 2016: pp. 332–336.

[26] K. Chithra, T. Santhanam, Hybrid denoising technique for suppressing Gaussian noise in medical images, in: 2017 IEEE Int. Conf. Power, Control. Signals Instrum. Eng., IEEE, 2017: pp. 1460–1463.

[27] A. Ramadhan, F. Mahmood, A. Elci, Image denoising by median filter in wavelet domain, ArXiv Prepr. ArXiv1703.06499. (2017).

[28] M. Longkumer, H. Gupta, Denoising of Images Using Wavelet Transform, Weiner Filter and Soft Thresholding, Int. Res. J. Eng. Technol. 5 (2018).

[29] A. Aghabalaei, Y. Amerian, H. Ebadi, Y. Maghsoudi, Speckle noise reduction of time series SAR images based on wavelet transform and Kalman filter, in: IGARSS 2018-2018 IEEE Int. Geosci. Remote Sens. Symp., IEEE, 2018: pp. 625–628.

[30] H. Choi, J. Jeong, Despeckling images using a preprocessing filter and discrete wavelet transform-based noise reduction techniques, IEEE Sens. J. 18 (2018) 3131–3139.

[31] R. Dass, Speckle noise reduction of ultrasound images using BFO cascaded with wiener filter and discrete wavelet transform in homomorphic region, Procedia Comput. Sci. 132 (2018) 1543–1551.

[32] P.M. Tayade, S.P. Bhosale, Medical Image Denoising and Enhancement using DTCWT and Wiener filter, Int. J. Adv. Res. Ideas Innov. Technol. 4 (2018).

[33] P. Luo, X. Qu, X. Qing, J. Gu, CT image denoising using double density dual tree complex wavelet with modified thresholding, in: 2018 2nd Int. Conf. Data Sci. Bus. Anal., IEEE, 2018: pp. 287–290.

[34] Y. Qian, Image denoising algorithm based on improved wavelet threshold function and median filter, in: 2018 IEEE 18th Int. Conf. Commun. Technol., IEEE, 2018: pp. 1197–1202.

[35] Y. Qian, Removing of Salt-and-pepper Noise in Images Based on Adaptive Median Filtering and Improved Threshold Function, in: 2019 Chinese Control Decis. Conf., IEEE, 2019: pp. 1431–1436.

[36] I.Z. Nishu, M.F. Tanjim, A.S.M. Badrudduza, M. Al Mamun, A New Image Despeckling Method by SRAD Filter and Wavelet Transform Using Bayesian Threshold, in: 2019 Int. Conf. Electr. Comput. Commun. Eng., IEEE, 2019: pp. 1–6.

[37] W. Fan, W. Xiao, Image denoising based on wavelet thresholding and Wiener filtering in the wavelet domain, J. Eng. 2019 (2019) 6012–6015.
[38] B.M. Ferzo, F.M. Mustafa, Image Denoising in Wavelet Domain Based on Thresholding with Applying Wiener Filter, in: 2020 Int. Conf. Comput. Sci. Softw. Eng., IEEE, 2020: pp. 106–111.
[39] P.M. Ingale, The importance of Digital Image Processing and its applications, Int. J. Sci. Res. Comput. Sci. Eng. 6 (2018) 31–32.
[40] E.R. Dougherty, Digital image processing methods, CRC Press, 2020.
[41] I. Singh, N. Neeru, Performance comparison of various image denoising filters under spatial domain, Int. J. Comput. Appl. 96 (2014) 21–30.
[42] P. Bhargava, S. Choubey, R.K. Bhujade, N. Jain, Image Denoising Using Discrete Wavelet Transform: A Theoretical Framework, Int. J. Eng. Technol. 7 (2018) 120–124.
[43] D. Gupta, M. Ahmad, Brain MR image denoising based on wavelet transform, Int. J. Adv. Technol. Eng. Explor. 5 (2018) 11–16.
[44] R. Verma, J. Ali, A comparative study of various types of image noise and efficient noise removal techniques, Int. J. Adv. Res. Comput. Sci. Softw. Eng. 3 (2013).
[45] S. Kaur, Noise types and various removal techniques, Int. J. Adv. Res. Electron. Commun. Eng. 4 (2015) 226–230.
[46] M. M. Puranik, S.V.Halse, A Review Paper: Study of Various Types of Noises in Digital Images, Int. J. Eng. Trends Technol. 57 (2018) 40–43. https://doi.org/10.14445/22315381/ijett-v57p208.
[47] R. Swaminathan, Application of Spatial Domain Filters on Noisy Images using MATLAB, Int. J. Comput. Appl. 134 (2016) 27–30.
[48] R. Rajni, A. Anutam, Image denoising techniques-an overview, Int. J. Comput. Appl. 86 (2014) 13–17.
[49] J.S. Owotogbe, T.S. Ibiyemi, B.A. Adu, A Comprehensive Review on various types of noises in Image Processing, Int. J. Sci. Eng. Res. ISSN. (n.d.) 2229–5518.
[50] A.K. Boyat, B.K. Joshi, A review paper: noise models in digital image processing, ArXiv Prepr. ArXiv1505.03489. (2015).
[51] P B Alisha, K.G. Sheela, Image Denoising Techniques-An Overview, IOSR J. Electron. Commun. Eng. 11 (2016) 78–84.
[52] A. Pandey, K.K. Singh, Analysis of noise models in digital image processing, Int J Sci Technol Manag. 4 (2015) 1537–2394.
[53] M.P. Charde, A Review on Image Denoising Using Wavelet Transform and Median Filter over AWGN Channel, Int. J. Technol. Enhanc. Emerg. Eng. Res. 1 (2013).
[54] M.D. Sontakke, M.S. Kulkarni, Different types of noises in images and noise removing technique, Int. J. Adv. Technol. Eng. Sci. 3 (2015) 102–115.
[55] L. Fan, F. Zhang, H. Fan, C. Zhang, Brief review of image denoising techniques, Vis. Comput. Ind. Biomed. Art. 2 (2019) 1–12.
[56] G. Wang, Z. Wang, J. Liu, A new image denoising method based on adaptive multiscale morphological edge detection, Math. Probl. Eng. 2017 (2017).
[57] S. Somashekhar, K. P.K, A Basic Overview On Image Denoising Techniques, Int. Res. J. Eng.

Technol. 7 (2020) 850–857.

[58] H. Om, M. Biswas, A generalized image denoising method using neighbouring wavelet coefficients, Signal, Image Video Process. 9 (2015) 191–200.

[59] S. Shenbagavadivu, M.R. Devi, An investigation of noise removing techniques used in spatial domain image processing, Int. J. Comput. Sci. Mob. Comput. 2 (2013) 378–384.

[60] A. Maity, R. Chatterjee, Impulsive noise in images: a brief review, (2018).

[61] V. Kumar, A. Kumar, P. Pal, Image denoising using hybrid filter, Int. J. Data Netw. Secur. 1 (2012).

[62] M.C. Arya, A. Semwal, Comparison on Average, Median and Wiener Filter using Lung Images, Image (IN). 1 (2017) 3–45.

[63] Y. Zhu, C. Huang, An improved median filtering algorithm for image noise reduction, Phys. Procedia. 25 (2012) 609–616.

[64] MARAPAREDDY. R, Restoratıon of Blurred Images Using Wiener Filtering, Int. J. Electr. Electron. Data Commun. 5 (2017) 45–49.

[65] K. Jaspreet, K. Rajneet, Biomedical Image denoising using Symlet wavelet with Wiener filter, Int. J. Eng. Res. Appl. 3 (2013) 548–550.

[66] D.S. khudayer Jadwa, Wiener Filter based Medical Image De-noising, Int. J. Sci. Eng. Appl. 7 (2018) 318–323. https://doi.org/10.7753/IJSEA0709.1014.

[67] S. Kumar, P. Kumar, M. Gupta, A.K. Nagawat, Performance comparison of median and wiener filter in image de-noising, Int. J. Comput. Appl. 12 (2010) 27–31.

[68] V.J. Umapathi, V.S. Narayanan, Medical image denoising based on Gaussian filter and Dwt Swt based enhancement technique, Int. J. Soft Comput. Artif. Intell. 2 (2014).

[69] S. Bonny, Y.J. Chanu, Denoising of Image by Wiener Filtering in Wavelet Domain, (n.d.).

[70] P. Kumar, S.K. Agarwal, A Color Image Denoising By Hybrid Filter for Mixed Noise, Int. J. Curr. Eng. Technol. 5 (2015).

[71] B. Toufik, N. Mokhtar, The wavelet transform for image processing applications, Adv. Wavelet Theory Their Appl. Eng. Phys. Technol. 17 (2012) 395–422.

[72] E.W. Weisstein, Fast fourier transform, Https//Mathworld. Wolfram. Com/. (2015).

[73] Wim van Drongelen, Signal Processing for Neuroscientists (Second Edition) Continuous, Discrete, and Fast Fourier Transform, Elsevier. (2013) 103–118.

[74] M. Sifuzzaman, M.R. Islam, M.Z. Ali, Application of wavelet transform and its advantages compared to Fourier transform, (2009).

[75] C. da Costa, M. Kashiwagi, M.H. Mathias, Rotor failure detection of induction motors by wavelet transform and Fourier transform in non-stationary condition, Case Stud. Mech. Syst. Signal Process. 1 (2015) 15–26. https://doi.org/10.1016/j.csmssp.2015.05.001.

[76] R.X. Gao, R. Yan, Wavelets: Theory and applications for manufacturing, Springer Science & Business Media, 2010.

[77] A. Vyas, J. Paik, Review of the Application of Wavelet Theory to Image Processing, IEIE Trans. Smart Process. Comput. 5 (2016) 403–417.

[78] P. Sleziak, K. Hlavcova, J. Szolgay, Advantages of a time series analysis using wavelet transform as compared with a fourier analysis, Slovak J. Civ. Eng. 23 (2015) 30.

[79] S. Dyllon, P. Xiao, Wavelet transform for educational network data traffic analysis, Wavelet Theory Its Appl. Ed. by Radhakrishnan, S., Intechopen, London, UK. (2018) 155–172.

[80] Y. Bao, H. Krim, Discrete Multi-Scale Transforms in Signal Processing, in: Acad. Press Libr. Signal Process., Elsevier, 2014: pp. 467–560.

[81] P. Bhirud, N. Prabhu, Performance Evaluation of Filters of Discrete Wavelet Transforms for Biometrics, Int. J. Informatics Commun. Technol. 3 (2014) 97. https://doi.org/10.11591/ijict.v3i2.pp97-102.

[82] W. Liu, L. Wu, X. Zhang, A. Wang, Wavelet-based noise reduction in power analysis attack, in: 2014 Tenth Int. Conf. Comput. Intell. Secur., IEEE, 2014: pp. 405–409.

[83] K.A. Bozed, N.L.M. Hweesa, Image De-noising Signal Based on Discrete Wavelet Transforms, (n.d.).

[84] Q. Song, L. Ma, J. Cao, X. Han, Image denoising based on mean filter and wavelet transform, in: 2015 4th Int. Conf. Adv. Inf. Technol. Sens. Appl., IEEE, 2015: pp. 39–42.

[85] M. Sonka, V. Hlavac, R. Boyle, Image processing, analysis, and machine vision, Cengage Learning, 2014.

[86] K. Sumathi, C. Hima Bindu, Image Denoising in Wavelet Domain with Filtering and Thresholding, Int. J. Eng. Technol. 7 (2018) 327. https://doi.org/10.14419/ijet.v7i3.34.19218.

[87] G. Strang, T. Nguyen, Wavelets and filter banks, SIAM, 1996.

[88] C. Sidney Burrus, R.A. Gopinath, H. Guo, Introduction to wavelets and wavelet transforms, A Prim. Prentice Hall Up. Saddle River, NJ, USA. (1998).

[89] D. Ravichandran, R. Nimmatoori, M. Gulam Ahamad, Mathematical representations of 1D, 2D and 3D wavelet transform for image coding, Int. J. Adv. Comput. Theory Eng. 5 (2016) 1–8.

[90] A. Shahbahrami, Algorithms and architectures for 2D discrete wavelet transform, J. Supercomput. 62 (2012) 1045–1064.

[91] D. Zhang, Wavelet transform, in: Fundam. Image Data Min., Springer, 2019: pp. 35–44.

[92] M. Merah, T.A. Abdelmalik, B.H. Larbi, R-peaks detection based on stationary wavelet transform, Comput. Methods Programs Biomed. 121 (2015) 149–160.

[93] P.B. Srinivas, B. Venkatesh, Comparative Analysis of DWT SWT DWT & SWT and DT-CWT-Based Satellite Image Resolution Enhancement, Int. J. Electron. Commun. Technol. 5 (2014) 137–141.

[94] T. Bhattacharya, S. Hore, S.R.B. Chaudhuri, A semi-fragile blind digital watermarking technique for medical image file authentication using stationary wavelet transformation, Int. J. Comput. Appl. 104 (2014).

[95] D.S. Candra, DENOISING OF HIGH RESOLUTION REMOTE SENSING DATA USING STATIONARY WAVELET TRANSFORM, J. Penginderaan Jauh Dan Pengolah. Data Citra Digit. 5 (2010).

[96] C. Qin, X. Gu, An Image Denoising Method Based on Improved Wavelet Thresholding, in: IOP Conf. Ser. Mater. Sci. Eng., IOP Publishing, 2018: p. 42199.

[97] P. Hedaoo, S.S. Godbole, Wavelet thresholding approach for image denoising, Int. J. Netw. Secur. Its Appl. 3 (2011) 16–21.

[98] M. Srivastava, C.L. Anderson, J.H. Freed, A new wavelet denoising method for selecting decomposition levels and noise thresholds, Ieee Access. 4 (2016) 3862–3877.

[99] L. Feng, L. Lin, Image Denoising Methods Based on Wavelet Transform and Threshold Functions., J. Multim. Process. Technol. 8 (2017) 1–10.

[100] A.G. Al-Azzawi, Image denoising based using hybrid techniques mixed between (hard and soft threshold) with multiwavelet transform and multi-stage vector quantization, Diyala J. Pure Sci. 8 (2012) 45–67.

[101] P. Koranga, G. Singh, D. Verma, S. Chaube, A. Kumar, S. Pant, Image denoising based on wavelet transform using Visu thresholding technique, Int. J. Math. Eng. Manag. Sci. 3 (2018) 444–449.

[102] M. Saha, M.K. Naskar, B.N. Chatterji, Soft, hard and block thresholding techniques for denoising of mammogram images, IETE J. Res. 61 (2015) 186–191.

[103] R.K. Rai, J. Asnani, T.R. Sontakke, Review of shrinkage techniques for image denoising, Int. J. Comput. Appl. 42 (2012) 13–16.

[104] K. Moghtased-Azar, M. Gholamnia, Effect of using different types of threshold schemes (in wavelet space) on noise reduction over GPS times series, J. Geomatics Sci. Technol. 4 (2014) 51–66.

[105] S.-H. Wang, Y.-D. Zhang, Z. Dong, P. Phillips, Wavelet Families and Variants, in: 2018: pp. 85–104. https://doi.org/10.1007/978-981-10-4026-9_6.

[106] N. Bajaj, R. Kashyap, Extension of wavelet family in fractional fourier domain, in: 2012 1st Int. Conf. Emerg. Technol. Trends Electron. Commun. Netw., IEEE, 2012: pp. 1–4.

[107] R. Reisenhofer, S. Bosse, G. Kutyniok, T. Wiegand, A Haar wavelet-based perceptual similarity index for image quality assessment, Signal Process. Image Commun. 61 (2018) 33–43. https://doi.org/10.1016/j.image.2017.11.001.

[108] Mathworks, Introduction to Wavelet Families, (n.d.). https://www.mathworks.com/help/wavelet/gs/introduction-to-the-wavelet-families.html.

[109] L. Li, K. Shi, Research and realization of transient disturbance detection algorithm based coiflet wavelets and FPGA, Int. J. Futur. Gener. Commun. Netw. 9 (2016) 133–142.

[110] Y.-D. Zhang, Z.-J. Yang, H.-M. Lu, X.-X. Zhou, P. Phillips, Q.-M. Liu, S.-H. Wang, Facial emotion recognition based on biorthogonal wavelet entropy, fuzzy support vector machine, and stratified cross validation, IEEE Access. 4 (2016) 8375–8385.

[111] S.-H. Wang, T.-M. Zhan, Y. Chen, Y. Zhang, M. Yang, H.-M. Lu, H.-N. Wang, B. Liu, P. Phillips, Multiple sclerosis detection based on biorthogonal wavelet transform, RBF kernel principal component analysis, and logistic regression, IEEE Access. 4 (2016) 7567–7576.

[112] S. Lal, S. Kumar, M. Chandra, Removal of high density salt & pepper noise through super mean filter for natural images, Int. J. Comput. Sci. Issues. 9 (2012) 303.

[113] R. Marudhachalam, G. Ilango, Fuzzy hybrid filtering techniques for removal of random noise from medical images, Int. J. Comput. Appl. 38 (2012) 15–18.

[114] Mathworks, Compute peak signal-to-noise ratio (PSNR) between images, (n.d.). https://www.mathworks.com/help/vision/ref/psnr.html.

APPENDICES

APPENDIX- 1: SWT AND DWT PSNR VALUE RESULTS

https://drive.google.com/file/d/1E6mCBXNTtHkyLT-IxYYUdHntFq_SGRny/view?usp=sharing

APPENDIX- 2: SWT AND DWT IMAGE RESULTS

https://drive.google.com/file/d/1XC-7kpzEozLc8u4CrmEP-MWf5PSI1__N/view?usp=sharing

CURRICULUM VITAE

Ahmed Abdulmaged ISMAEL

[redacted]

[redacted]

[redacted]

RESEARCH EXPERIENCES

- ✓ Laboratory Instruments you use, such as test systems, etc. you know
- ✓ Computer Programming languages available (MATLAB, Java, PHP, Python)
- ✓ Computer programs you can use (MATLAB, GNS3, Cisco Packet Tracer, Computer Networking, Architecture, Hardware, Graph and Security, Microsoft Office)

WORK EXPERIENCE

[redacted]